EINDHOVEN UNIVERSITY OF TECHNOLOGY

Plasma needle : exploring biomedical applications of non-thermal plasmas

Citation for published version (APA):
Kieft, I. E. (2005). *Plasma needle : exploring biomedical applications of non-thermal plasmas*. [Phd Thesis 1 (Research TU/e / Graduation TU/e), Biomedical Engineering]. Technische Universiteit Eindhoven. https://doi.org/10.6100/IR594662

DOI:
10.6100/IR594662

Document status and date:
Published: 01/01/2005

Document Version:
Publisher's PDF, also known as Version of Record (includes final page, issue and volume numbers)

Please check the document version of this publication:

• A submitted manuscript is the version of the article upon submission and before peer-review. There can be important differences between the submitted version and the official published version of record. People interested in the research are advised to contact the author for the final version of the publication, or visit the DOI to the publisher's website.
• The final author version and the galley proof are versions of the publication after peer review.
• The final published version features the final layout of the paper including the volume, issue and page numbers.

Link to publication

General rights
Copyright and moral rights for the publications made accessible in the public portal are retained by the authors and/or other copyright owners and it is a condition of accessing publications that users recognise and abide by the legal requirements associated with these rights.

• Users may download and print one copy of any publication from the public portal for the purpose of private study or research.
• You may not further distribute the material or use it for any profit-making activity or commercial gain
• You may freely distribute the URL identifying the publication in the public portal.

If the publication is distributed under the terms of Article 25fa of the Dutch Copyright Act, indicated by the "Taverne" license above, please follow below link for the End User Agreement:

www.tue.nl/taverne

Take down policy
If you believe that this document breaches copyright please contact us at:

openaccess@tue.nl

providing details and we will investigate your claim.

Download date: 15. Jul. 2025

Plasma needle: exploring biomedical applications of non-thermal plasmas

PROEFSCHRIFT

ter verkrijging van de graad van doctor
aan de Technische Universiteit Eindhoven,
op gezag van de Rector Magnificus, prof.dr.ir. C.J. van Duijn,
voor een commissie aangewezen door het College voor Promoties
in het openbaar te verdedigen
op woensdag 28 september 2005 om 16.00 uur

door

Ingrid Elisabeth Kieft

geboren te Wageningen

Dit proefschrift is goedgekeurd door de promotoren:

prof.dr. D.W. Slaaf
en
prof.dr.ir. G.M.W. Kroesen

Copromotor:
dr.ir. E. Stoffels-Adamowicz

This research was sponsored by the Netherlands Organization for Scientific Research (NWO).

CIP-DATA LIBRARY TECHNISCHE UNIVERSITEIT EINDHOVEN

Kieft, Ingrid E.

Plasma needle: exploring biomedical applications of non-thermal plasmas / by Ingrid E. Kieft. - Eindhoven : Technische Universiteit Eindhoven, 2005.
Proefschrift. - ISBN 90-386-2737-8
NUR 954
Subject headings: atmospheric pressure plasma / plasma needle / plasma diagnostics / fluorescent probes / ultraviolet irradiation / cell adhesion / carotid artery

Copyright ©2005 I.E. Kieft

All rights reserved. No part of this book may be reproduced, stored in a database or retrieval system, or published, in any form or in any way, electronically, mechanically, by print, photoprint, microfilm or any other means without prior written permission of the author.

Printed by Printservice Technische Universiteit Eindhoven, Eindhoven, The Netherlands
Cover design by Ingrid Kieft

Contents

1 General introduction **1**

2 Plasmas in biomedical applications: an overview **5**

2.1 Introduction 6

2.1.1 Non-thermal plasmas 6

2.1.2 Cells and tissues 9

2.1.3 A "bio-compatible" plasma source: safety issues 12

2.2 Established surgical plasma equipment 18

2.2.1 Electrosurgery 19

2.2.2 Plasma coagulation 19

2.2.3 Spark erosion 21

2.3 Goal of the plasma needle 22

2.3.1 *In vivo* plasma disinfection 23

2.3.2 Plasma interactions with living objects 24

3 Electrical and optical characterization of the plasma needle **29**

3.1 Introduction 30

3.2 Method 31

3.2.1 Plasma needle 31

3.2.2 Impedance measurements 32

3.2.3 Light emission 35

3.3 Result and discussion 35

3.3.1 Impedance measurements 35

3.3.2 Light emission 40

3.3.3 Influence of helium flow speed 42

3.4 Conclusions 44

3.5 Acknowledgments 45

4 Radicals of plasma needle detected with fluorescent probe **47**

4.1 Introduction 48

4.2 Experimental . . . 49
4.2.1 Plasma needle . . . 49
4.2.2 Raman scattering . . . 50
4.2.3 Fluorescent probe . . . 51
4.2.4 Calibration with NO radicals . . . 52
4.2.5 Plasma treatment . . . 54
4.3 Results and discussion . . . 54
4.3.1 Raman scattering . . . 54
4.3.2 The fluorescent probe measurements . . . 55
4.4 Conclusions . . . 60

5 Electric Discharge Plasmas Influence Attachment of Cultured Cells 65
5.1 Introduction . . . 66
5.1.1 Plasma Application . . . 66
5.2 Experimental methods . . . 67
5.2.1 Principle of Plasma Operation . . . 67
5.2.2 Electric Apparatus . . . 68
5.2.3 Plasma Chamber . . . 69
5.2.4 Cell Culture . . . 69
5.2.5 Plasma Treatment . . . 70
5.2.6 Visualization . . . 70
5.2.7 Apoptosis detection . . . 71
5.2.8 Temperature Measurements . . . 71
5.3 Results and discussion . . . 72
5.3.1 Thermal Properties of the Plasma Needle . . . 72
5.3.2 Cell Responses . . . 73
5.3.3 Apoptosis . . . 77
5.4 Conclusions . . . 78

6 Plasma treatment of mammalian vascular cells: a quantitative description 81
6.1 Introduction . . . 82
6.2 Experimental . . . 83
6.2.1 Plasma Needle . . . 83
6.2.2 Cells . . . 84
6.2.3 Stains . . . 84
6.2.4 Exposure procedures . . . 85
6.3 Results . . . 85
6.3.1 Penetration depth . . . 85

6.3.2 Effect of exposure time 87
6.3.3 Effect of applied voltage 88
6.4 Discussion 90
6.5 Conclusions 91

7 A comparison of UV irradiation and gas plasma treatment of cells and bacteria 93
7.1 Introduction 94
7.2 The Experimental Setup 95
7.2.1 Cell culture preparation 95
7.2.2 Bacterial sample preparation 95
7.2.3 Ultraviolet radiation sources 96
7.2.4 Low-temperature plasma 97
7.2.5 Sample treatment 98
7.2.6 Observation 100
7.3 Results and Discussion 100
7.4 Conclusions 106
7.5 Acknowledgment 108

8 Plasma treatment of *ex vivo* arteries: preliminary results 111
8.1 Introduction 112
8.2 Experimental 113
8.2.1 Plasma treatment 113
8.2.2 Temperature measurements 114
8.2.3 Tissue preparation 114
8.2.4 Plasma treatment 115
8.2.5 Microscopy 115
8.2.6 Staining procedure 116
8.3 Results and discussion 116
8.3.1 Temperature measurements 116
8.3.2 Plasma irradiation of arteries in dry environment 118
8.3.3 Dehydration and helium flow 119
8.3.4 Staining procedure 121
8.3.5 Plasma irradiation of artery under thin liquid layer 121
8.4 Conclusions 122

9 General discussion 125
9.1 Introduction 126
9.2 Plasma needle working range 126

9.3 Active plasma ingredient 129
9.4 Detachment mechanism 131
9.5 Conclusion and future directions 132

Summary **135**

Samenvatting **137**

Publications **141**

Dankwoord **145**

Curriculum Vitae **147**

Chapter 1

General introduction

The work described in this thesis is part of a project that investigates possible medical applications of the plasma needle. To this end, effects of the plasma needle treatment on both bacteria and biological cells and tissues are examined.

A plasma is an ionized gas that contains ions, radicals, and electrons. It usually emits UV light. The temperature of the electrons is normally above 10,000 K; the temperature of the neutral particles and ions is strongly dependent on the type of plasma and can vary from room temperature to 10^7 K. It is sometimes referred to as the fourth state of matter. A well known example of a plasma is the sun. Sometimes the flame of a candle is also considered a plasma, but the concentration of ions is very low. One of the characteristics of a plasma is its chemical activity. Inside the plasma radicals and other species are formed that are highly reactive [1–3].
Plasmas can also be created on earth, in a laboratory: in most cases this is done inside a vacuum vessel at low pressure. This type of plasmas is used e.g., for activating the surface of polymers, growing solar cells and etching materials [4, 5].

The plasma needle, the subject of my research, is a plasma at atmospheric pressure. The advantage of this is that it can be operated in open air, outside a vessel. The plasma that is generated with the plasma needle setup is small (about one millimeter) and non-thermal, the temperature of the neutral particles and ions is about room temperature. This gives us the opportunity to use this type of plasma in the biomedical field. Future applications may be for example treatment of cancer or skin ailments.
This study focusses on the possibilities for the application of a plasma on biological tissue without causing inflammation reactions. For a reliable study of the biological effects it is necessary to have a stable and reproducible plasma. Thus, the design of the plasma is part of the study. The research into the biological implications consists of a study of the effects on cultured cells and preliminary experiments on arteries. Effects of the plasma on the cells are expected from the reactive species that were mentioned before and of UV light emission by the plasma.

In the first part of the thesis focus is on the physics of the plasma needle and the characterization of its properties. In the second half the effect of the plasma on cells will be discussed. A literature overview of the work that has been performed on plasmas with biomedical applications is given in **Chapter 2**. Existing *in vivo* applied plasma tools are described.
In **Chapter 3** the plasma needle is characterized both electrically and optically. For the application of the plasma on biological material, it is important to know the emitted radicals that actually reach the surface that is to be treated. Thus, a fluorescent probe dissolved in liquid was used for the detection. The results are given in **Chapter 4**. From

a calibration against NO radicals, the concentration of plasma radicals was assessed to be in the μM range. Basic effects of the plasma treatment on cultured cells are described in **Chapter 5** and quantified in **Chapter 6**. The main effect was found to be cell detachment. When little liquid covered the cells, this resulted in a large working area. Most likely this is caused by a small penetration depth of the radicals. However, using small amounts of liquid increases dehydration. To understand the importance of the UV that is emitted by the plasma needle, a comparison between plasma treatment and UV radiation is made in **Chapter 7**. In **Chapter 8** pilot experiments performed on arterial walls are described. The thesis ends with the general discussion in **Chapter 9** which will give an overview of the findings and the current status of the plasma needle research. Publications associated with this thesis can be found on page 141.

References

[1] Y. P. Raizer. *Gas discharge physics.* Springer, Berlin, 1991.

[2] T. J. M. Boyd and J. J. Sanderson. *The physics of plasmas.* Cambridge University press, Cambridge, 2003.

[3] Y. P. Raizer, M. N. Schneider, and N. A. Yatsenko. *Radio-Frequency Capacitive Discharges.* CRC Press, Boca Raton, Florida, 1995.

[4] R. Hippler, S. Pfau, and M. Schmidt. *Low temperature plasma physics: fundamental aspects and applications.* Wiley VCH, Berlin, 2001.

[5] J. Reece Roth. *Industrial Plasma Engineering, vol 2: Applications to nonthermal plasma processing.* IOP Publishing Ltd, Cornwall, UK, 2001.

Chapter 2

Plasmas in biomedical applications: an overview

A plasma is a (partly) ionized gas, which contains free charge carriers (electrons and ions), active radicals and excited molecules. So-called non-thermal plasmas are particularly interesting, because they operate at relatively low temperatures and do not inflict thermal damage to nearby objects. In the past two decades non-thermal plasmas have made a revolutionary appearance in solid state processing technology. The recent trends focus on using plasmas in the health care for "processing" of medical equipment and even living tissues. The major goal of tissue treatment with plasmas is non-destructive surgery: controlled, high-precision removal of diseased sections with minimum damage to the organism. Furthermore, plasmas allow fast and efficient bacterial inactivation, which makes them suitable for sterilization of surgical tools and local disinfecting of tissues. Much research effort must be undertaken before these techniques will become common in medicine, but it is expected that a novel approach to surgery will emerge from plasma science.

Large parts of this chapter were published as E. Stoffels, I.E. Kieft, R.E.J. Sladek, E.P. van der Laan, D.W. Slaaf, Gas plasma treatment: a new approach to surgery?, *Crit. Rev. Biomed. Eng.*, 32(5-6):427-460, 2004.

2.1 Introduction

2.1.1 Non-thermal plasmas

A plasma is an ionized gaseous medium. Its unique properties result from the presence of free charge carriers: electrons and ions. Most of the matter in universe is in ionized state; huge objects like stars or planetary nebulae are nothing else but very dense or very diffuse plasmas. Somewhat smaller specimens are encountered in every day life - fire and lightning are natural plasma phenomena, while neon lamps and plasma TV displays are typical man-made plasmas.

Plasmas can be created in several ways, e.g., by laser beams. Usually, a discharge in gas is induced electrically, by applying voltage to a set of electrodes [1]. In this case only charged species (electrons and ions) can gain energy from the electric field. The plasmas generated by electric fields are divided in [2]:

- direct current (DC) discharges
- pulsed DC discharges
- radio frequency (RF) discharges
- microwave discharges.

The RF discharges can be divided in inductively and capacitively coupled configurations. A general schematic of an RF capacitively coupled discharge is depicted in Figure 2.1. The plasma needle, which is used in this study, is an RF capacitively coupled plasma in a unipolar configuration. The surrounding environment acts as counter-electrode.

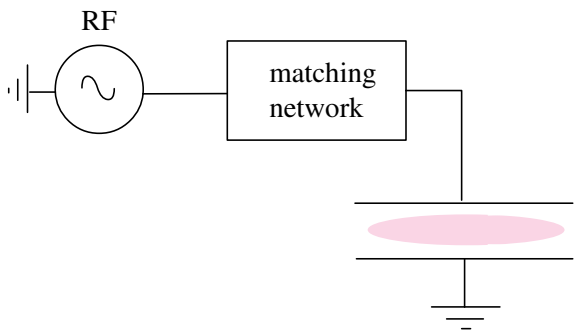

Figure 2.1: *Schematic of an RF capacitively coupled plasma.*

In common perception, plasmas are hot gases that emit light and conduct electricity. Indeed, plasmas often contain energetic electrons (at 3 eV or higher) that in turn transfer

their energy to neutral molecules and excite radiating transitions. However, not all plasmas are hot. Small and light electrons cannot heat the large and heavy molecules very efficiently, so in many cases the background gas remains at or close to room temperature. In such non-equilibrium systems (often called non-thermal plasmas), the complex plasma chemistry is driven by electrons. They perform ionization, necessary to sustain the plasma; in addition, they are responsible for atomic/molecular excitation, dissociation and production of "exotic" species. The result is an active gaseous medium that can be safely used without thermal damage to the surrounding. Such exceptional non-equilibrium chemistry is the base of plasma applications in lighting technology [3], exhaust gas treatment [4] and material processing [5].

There are several methods to generate non-thermal plasmas. When charged particles are in minority, heating of neutral molecules is limited. Thus, diffuse plasmas where the fraction of ionized species is below 0.1%, are usually non-thermal. This situation is readily achieved under reduced pressures, in the range of 10 to 1000 Pa. The effect of low pressure is double: in a rarefied gas ionization events are scarce, which keeps the charge density low. Moreover, the frequency of elastic collisions between electrons and atoms/molecules is low, so electrons do not have much chance to convey their energy to the gas.
Low-pressure plasmas are of great value in fundamental research as well as plasma technology, but they have many serious drawbacks. These plasmas must be confined in massive vacuum reactors, their operation is costly, and the access for observation or sample treatment is limited. Therefore, one of the recent trends focuses on developing new plasma sources, which operate at atmospheric pressure, but retain the properties of low-pressure media. Non-thermal atmospheric plasmas may be created using one or more of the following principles:

- Transient plasmas. The frequency of energy transfer in collisions between electrons and gas is given by: $\nu[s^{-1}] = (m_e/m_a)2n_a\sigma_{ea}v_e$
  where m_e/m_a is electron to atom(molecule) mass ratio, σ_{ea} is their mutual collision cross-section, n_a is the atom density and v_e is the electron velocity. In atmospheric plasmas n is about 10^8 collisions/s; for efficient gas heating at least 100-1000 collisions are necessary. Thus, if the plasma duration is shorter than $10^{-6} - 10^{-5}$ s, gas heating is limited. Of course, for practical purposes such plasma has to be operated in a repetitive mode, e.g., in trains of microsecond pulses with millisecond intervals.

- Micro-plasmas. Gas heating occurs in the plasma volume, and the energy is carried away by thermal diffusion/convection to the outside. If the plasma has a small volume and a relatively large surface, gas heating is limited. This situation can be

also achieved for a spherical plasma glow. In case of the plasma needle, its typical dimension should not exceed 1 mm [6].

- Dielectric barrier discharges (DBD's) [7, 8]. These plasmas are typically created between flat parallel metal plates, which are covered by a thin layer of dielectric or highly resistive material. Usually they are driven by a high frequency electric current (in the kHz range), but it is also possible to obtain a DBD by simple transformation of 50 Hz/220 V network voltage to about 1 kV. The dielectric layer plays an important role in suppressing the current: the cathode/anode layer is charged by incoming positive ions/electrons, which reduces the electric field and hinders charge transport towards the electrode. DBD's have typically low ionization degrees (ion densities of $10^{19} - 10^{20}$ m^{-3}) and currents in the order of mA. Besides, the electrode plates are quite large (10 cm) and the distance between them usually does not exceed a few millimetres. Thus, DBD has a large surface-to-volume ratio, which promotes diffusion losses and maintains a low gas temperature (at most a few tens of degrees above the ambient). The only serious drawback of a DBD is its limited flexibility. Since the distance between the plates must be kept small, treatment of large and irregular samples is impossible.

In the last decades, non-thermal plasmas have made a fast career in surface processing technology. At present, virtually any surface treatment can be performed in a plasma reactor: etching (fabrication of semiconductor elements); deposition of amorphous silicon layers for solar cells; deposition of various thin coatings: hard/protective layers (diamond), nano-structured composite films, cleaning/ashing, tailoring of surface properties: wettability, surface energy, adhesion. The versatility of plasma interactions with various surfaces was the inspiration for a completely new application: plasma-surface treatment in medical care.

Several biomedical applications of plasmas have been already identified, e.g., bacterial decontamination of medical equipment, air, biological warfare [7, 9], coating of implants with bio-compatible layers [10], and surface modification of substrates for cell culture [11, 12]. These *ex vivo* techniques are subject of extensive studies, which are beyond the scope of this chapter. Here we shall concentrate on the most recent development, which is plasma treatment of living tissues. The aim of this treatment is controlled tissue removal, devitalization, and hemostasis. Since modern plasma sources have become quite friendly and "bio-compatible", the area of applications is expanding rapidly and many novel medical techniques are under preparation. It is expected that plasmas will be used for *in vivo* tissue disinfection and induction of specific reactions at the cellular level (proliferation stop, apoptosis). All these applications will be addressed.

2.1.2 Cells and tissues

The ultimate goal of our plasma needle research is to develop it into a surgical tool. This tool can then be used to treat several types of human pathological tissue. Tissues are complex materials that usually consists of several cell types with connecting extracellular matrix (ECM). The direct application of plasma to tissues of any kind will lead to complicated chains of reactions. For research purposes, it is thus logical to start using cultured cells as model system.

Cells

Cell biologists have developed ways of dissociating cells from tissues. The various cell types are then separated, which results in a relatively homogenous population of cells. Cell cultures prepared directly from the tissue are called primary cultures. When cells are removed from the culture dish, they can be used to form a large number of secondary cultures; they may be subcultured for weeks or months. The cells in culture are provided with media. Most media used are derived from horse serum or fetal calf serum. However, serum-free chemically defined media also exist. They include amino acids, vitamins, salts, proteins (e.g., growth factors), and some miscellaneous additions. An example of the latter is penicillin, to protect the cells from a bacterial infection [13].

A typical animal cell is 10 to 20 μm in diameter. It is a complex structure of organelles in cytoplasm. Mammalian cells are surrounded by a membrane that shields its contents from the outside environment. The membrane is a continuous sheet of phospholipid molecules in which various proteins are embedded [13]. An important organelle is the nucleus, which has its own membranes surrounding it. It holds the DNA with the genetic information. Furthermore, the cell consists of parts such as the cytoskeleton for structure, and mitochondria for energy conversion.

If the cell is irreversibly injured, this will result in cell death. There are two types of cell death: apoptosis and necrosis.

- Necrosis, or accidental cell death. Necrosis is defined as the consequence of a catastrophic injury to the mechanisms that maintain the integrity of the cell. In necrotic cells the membrane is damaged, and the cytoplasm can leak out. Since the content

of the cell is harmful to the tissue, the organism responds with an inflammatory reaction. In surgery, mechanical, thermal or laser methods always cause severe injury at the cellular level and cell necrosis. The necrotic tissue is eventually removed by the organism, but the inflammation slows down the healing process and may cause complications. The body reacts to inflammation by excessive tissue formation. In arteries it may lead to (re)stenosis, in other places it leaves scar tissue. Surgery without necrosis and inflammation would be surely a great improvement.

- Apoptosis, or programmed cell death. Apoptosis is an internal mechanism of self-destruction, which is activated by cells, which are damaged, dangerous to the tissue, or simply too old and not functional anymore. Thus, apoptosis takes place in developmental morphogenesis, in natural renewal of tissues, in DNA-damaged, virus-infected or cancer cells, etc. Presumably, any moderate yet irreversible cell damage can also activate apoptosis. Known factors are UV exposure, oxidative stress and specific chemicals. The role of radicals and UV has given rise to the hypothesis, that plasma treatment may also induce apoptosis.

The intracellular mechanism of apoptosis is described in detail in textbooks on cell biology [13] and specific articles [14]. The morphological changes in the cell during apoptosis are easy to recognize. In early apoptosis, the DNA in the nucleus undergoes condensation and fragmentation and the cell membrane displays blebs. Later, the cell is fragmented in membrane-bound elements (apoptotic bodies). However, the membrane retains its integrity, so no cytoplasm leakage and no inflammatory reaction occur. The cell vanishes in a neat manner, without damage to the rest of the tissue. The organic material of the cell is "recycled", as the apoptotic bodies are engulfed by macrophages or neighboring cells.
It is clear that in the pursuit of fine surgery apoptosis is the preferred way of cell removal. Selective induction of apoptosis can make a pathological tissue disappear virtually without a trace. Such surgery, performed with a high precision, may be called the least destructive therapeutic intervention. No inflammation, no complications in healing and no scar formation/stenosis is expected.

There are only four basic types of cells: cells of epithelial, connective, muscle, and nervous tissue [15]. Within these basic tissues, there are many subtypes that exhibit different morphologic and functional phenotypes. The cell types used in this study include fibroblasts, endothelial cells and smooth muscle cells. Fibroblasts are part of the connective-tissue family, which means that they are specialized in the secretion of collagenous extracellular matrix. This property makes them important after tissue injury to help isolate and repair the damaged tissue [13].

The epithelial cells that make up the inner surface of blood and lymph vessels are called endothelial cells. The endothelia consist of closely-packed cells arranged in flat sheets. A layer of connective tissue is interposed between the endothelium and the underlying smooth muscle. The contractile properties of the smooth muscle cells vary according to the location of the blood vessel [16].

Standard protocols to detect cell damage include e.g., visual observation, cell counting and (fluorescent) dyes. The dyes are most often used to detect specific proteins or other molecules in cells and tissues. Examples are: calcium markers, metabolic markers and stress markers. Fluorescent dyes are detected with the help of fluorescence microscopy.

Extracellular matrix

The surrounding environment of connective tissue cells is called the extracellular matrix (ECM). This ECM consists of several components. For example, fibroblasts secrete various proteins and polysaccharide chains; these chains then become part of the ECM. The ECM has in total five components that make up a stable complex: collagens, basement membranes, elastic fibers, structural glycoproteins, and proteoglycans [16]. A schematic drawing is given in Figure 2.2. The exact composition of the extracellular matrix depends on the cell type.

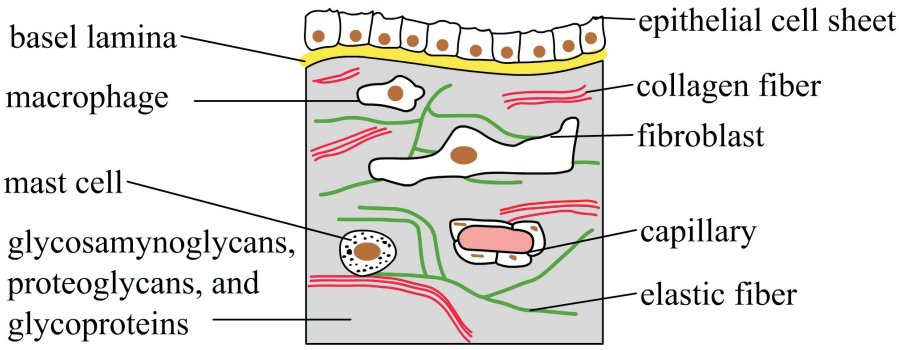

Figure 2.2: *The connective tissue underlying an epithelial cell sheet. It consists largely of extracellular matrix that is secreted by the fibroblasts. Picture after [13].*

The ECM is important because it

- helps to cushion and support the cells,
- participates in signal transduction,

- helps to maintain the cell shape,
- is important for the cell development (migration and cell growth)[15].

The cells interact with the extracellular matrix through the cell adhesion molecules (CAMs), e.g., integrins. They are cell surface receptors that bind to extracellular matrix components. Due to the connection of cells with the ECM, it is expected that the effect of plasma treatment of tissues is different from treatment of cultured cells.

Tissues are usually fixed and sectioned for microscopy, because confocal fluorescence microscopy is not suitable for thicknesses above 50 μm. This is due to loss of resolution and limited penetration depth. Fixation makes cells permeable to staining reagents and cross-links their macromolecules so that they are stabilized and locked in position. Examples of fixation liquids are alcohol and formaldehyde [13]. An alternative for the fixation procedure is rapid freezing. An alternative to these procedures is given by the two photon laser scanning microscope (TPLSM). This method is less limited in penetration depth and can for example be used to image mouse carotid arteries [17].

2.1.3 A "bio-compatible" plasma source: safety issues

What is a "bio-compatible" plasma? It depends very much on what one expects from plasma treatment. But generally, everyone agrees that damage to the living organism should be avoided or at least minimized, and that refined/selective modifications are preferred to non-specific effects. This imposes quite a number of restrictions on the plasma source, in particular on its thermal and electrical properties and its chemical activity (toxicity). Before going into details on the possibilities and consequences of *in vivo* plasma treatment, some basic features of atmospheric plasmas shall be described, and the necessary safety requirements shall be discussed.

Thermal properties of non-equilibrium plasmas

As stated above, non-equilibrium plasmas are often referred to as non-thermal. In such plasmas, the electron temperature can be 100 to 1000 times higher than neutral gas temperature. But is the gas temperature always low enough to fully eliminate thermal damage?

Thermal damage was already of much concern in processing of heat-sensitive (non-living) surfaces, like plastics and fabrics. For living tissues, it becomes even more crucial. Thermal effects were elaborately studied in relation to laser surgery [18]. Temperature elevation

above 43 °C causes in most cases damage to cells and tissues. The extent of this damage depends on the type of cell or tissue, and the duration of the exposure to heat.

For example, a temperature increase of only 2.2 °C in the dental pulp causes not only intense pain, but also partial pulp necrosis [19]. Conversely, tissues like skin can withstand temperature elevation to 60 °C or more for several seconds without substantial damage [20].

Depending on the desired effect of plasma treatment, rigorous control of gas temperature in the plasma, and surface temperature of the exposed tissue may be necessary. In non-specific treatment, like burning and coagulation of wounds (see section 2.2 about *in vivo* treatment), heating of the tissue is a part of the therapy. For this purpose, hot plasmas are used, and the temperature is not so critical as long as there is no carbonization or deep damage. In other applications, like specific treatment without tissue devitalization, temperature is an essential issue. The tissue may be warmed up to at most a few degrees above the ambient temperature, and treatment time must be limited to several minutes.

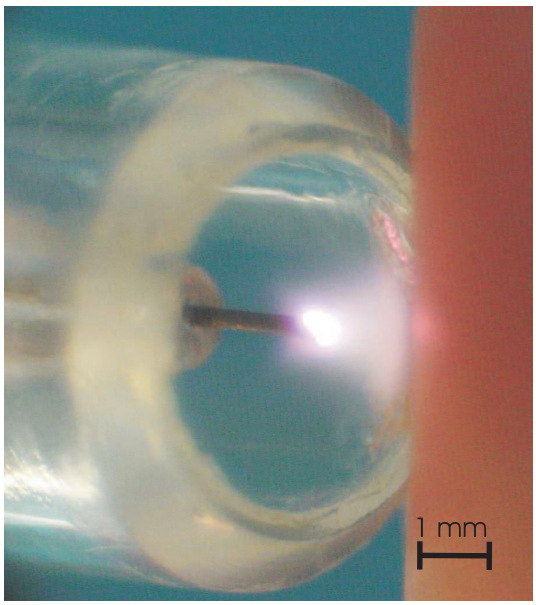

Figure 2.3: *The plasma from the plasma needle expands to skin.*

There are many techniques for the determination of plasma and surface temperature. In most plasma physical works, spectroscopic measurement of relative intensities of rotation bands (rotation temperature) is a popular method to determine the gas temperature. Unfortunately, the accuracy is somewhat limited: at low temperatures (close to room temperature) the error is in the best case of the order of ten degrees. This may be not so critical in plasma physics, but in medicine every degree above the body temperature may

become a problem. In biology (biophysics) and material technology thermocouples are often used. In the present context, thermocouples are more useful as they provide direct information about the thermal flux towards the exposed surface.

Table 2.1: *A selection of atmospheric discharges*

Plasma source	**Type**	**Gas**	**T (K)**	**Ref.**
Atmospheric Pressure Plasma Jet (APPJ)	RF capacitively coupled	Helium, argon	400	Park *et al* [21]
Atmospheric glow	AC/DC glow above water	Air	800-1500	Lu and Laroussi [22]
Cold arc-plasma jet AC	10-40 kHz	Air, N_2, O_2	520	Toshifuji *et al*[23]
Microwave torch	2.45 GHz	Argon + O_2	2200	Moon and Choe[24]
AC plasma	AC	Helium + O_2	800-900	Moon and Choe [24]
DBD	Dielectric barrier	N_2 + O_2 + NO	300	Baeva *et al*[25]
Pulsed DBD	Dielectric barrier	Argon + H_2O	350-450	Motret *et al*[26]
Atmospheric glow	DC glow with micro-hollow cathode electrode	Air	2000	Mohamed *et al*[27]
Plasma needle	RF capacitively coupled, mm size	Helium + N_2	350-700	Stoffels *et al* 2002 [6]
Plasma needle	RF micro-plasma	Helium (+H_2O)	300	Stoffels *et al*[28]

In Table 2.1, a few typical non-thermal plasma sources and their corresponding gas temperatures are listed. Most of these results were obtained using spectroscopic methods: optical emission and coherent antistokes Raman scattering: CARS [25]. Moon and Choe calibrated optical emission spectroscopy against thermocouples [24]. Stoffels *et al* also used both methods for the plasma needle (Figure 2.3) [6, 28]. The table comprises a reasonable selection of atmospheric discharges. One can thus conclude that not many of these plasmas

are suitable for non-thermal processing of organic samples.

Electricity and plasma

Gas discharge and electricity are inevitably coupled. At atmospheric pressure, the breakdown voltages may be quite high: from several hundreds of Volts even to 10 kV, dependent on the type of discharge (DC, RF, microwave), electrode gap and gas composition. Such high electric fields are surely a matter of concern for the health of the patient: they may interact with the nervous system, disturb the heartbeat, and cause damage to individual cells.

Obviously, electricity does pose a danger: lightning is probably its most awesome and frightening manifestation. However, most of the commonly encountered electrical phenomena - sparks in dry air, shocks experienced after touching some surfaces, charging of hair and clothes - are by far not so destructive. Yet the electric voltages that induce such phenomena may be considerably high; for example, sparks are generated when the local field strength is about $3x10^6$ V m^{-1}. The reason for their harmlessness lies in very low electric currents and consequently low power dissipation. Thus, one can tentatively state that damage is related to the (too high) electric power rather than voltage or field strength.

Electrical methods are not unfamiliar in medicine. Electrosurgery may be the most prominent example: substantial electric power is dissipated in a living tissue, with controlled coagulation/cutting as a result. However, not only electrosurgical devices, but also most of the advanced medical equipment involves electricity. With the introduction of new techniques, a thorough study of the effects of electric fields and EM radiation on living beings was undertaken. In particular, much attention was given to alternate (high-frequency) currents passing through the body. For detailed data, the reader should refer to the works of Gabriel *et al* [29] (dielectric properties and conductivity of tissues), Reilly [30] (nerve and muscle stimulation) and Polk [31] (electroporation and other field-induced effects). These studies revealed that the sensitivity of nerves and muscles to electric current decreases with increasing current frequency. The threshold current that causes irritation is only 1 mA at 10 Hz, but as high as 0.1 A at 100 kHz. This result is of major importance for electrosurgery and plasma treatment: it implies that for medical applications high-frequency sources should be employed. The "safety limit" lies around 100 kHz, but to be "on the safe side", most of the equipment operates at 300 kHz or higher.

Nowadays, much attention is given to interactions of electric fields with the cell membrane. Cell death due to membrane rupture is one of the hazards related to electric fields - electroporation is a well known phenomenon, and it may become an undesired side effect

during plasma treatment. The rupture occurs when the potential difference across the cell membrane is 1 V [31]. Since the membrane has a thickness of several nm, the external electric field, which causes this damage, must be of the order of 10^8 V m^{-1}. In man-made plasmas electric fields are typically much lower: in extreme cases (close to the powered electrode) they are about $10^5 - 10^6$ V m^{-1}. Moreover, during plasma treatment only peripheral plasma zones are involved, where the electric fields are practically absent. Thus, one can state that plasma treatment does not inflict electrical damage.

In some cases, the electric field may even become beneficial. Field-induced reversible permeabilization of the membrane is an interesting effect with many potential applications. The effects of transient electric fields on living cells was elaborately studied by Schoenbach and Beebe [32–35]. The duration of the electric pulse was from 60 ns to 100 μs; the electric field strength was 3-15x10^6 V m^{-1}. The authors found conditions in which membrane electroporation is reversible. Furthermore, they reported remarkable modifications to the cell interior. Short electric field pulses are capable of inducing programmed cell death (apoptosis) in cancer cells, so they may be used therapeutically to suppress tumor growth [33].

Toxicity by reactive species

Plasma is a rich source of radicals and other active species. Free radicals have earned a bad name in biology and medicine, because of their capability of causing severe cell damage [36]. Especially the ROS (reactive oxygen species) are well known as evildoers. The ROS family comprises radicals like O, OH and HO_2, peroxide anions O_2^- and HO_2^-, ozone and hydrogen peroxide. These species are easily created in ambient air and water (e.g., due to radiation), and they live long enough to reach the cell and attack the organic matter. When the ROS level in body fluids becomes too high, various types of damage occur, known under a common name of oxidative stress. It is believed that the oxidative stress bears at least partial responsibility for diseases like atherosclerosis, cancer and respiratory problems. Moreover, a high concentration of oxygen radicals accelerates ageing of cells and tissues. On the cellular level, several effects leading to cell injury have been identified:

- lipid peroxidation - the oxidation of unsaturated lipids in the cell membrane (damage to the membrane),

- DNA damage - oxidation of DNA bases, leading to breakage of the DNA strand (on the positive side, this can also induce apoptosis),

- protein oxidation - generally not so harmful, because damaged proteins are efficiently replaced. However, it can temporarily decrease the enzyme activity.

On the other hand, free radicals have various important functions in the body. Small amounts of them are produced by the organism itself. For example, macrophages generate ROS to destroy invading bacteria; endothelial cells produce nitric oxide (NO) to regulate artery dilation. It is not completely clear which radical concentrations are indispensable for the proper functioning of the body, and which are too dangerous. There must be always a compromise between benefit and damage, but the numbers can vary from individual to individual. Radical production by the body during physical exercise can increase the ROS concentration in blood plasma even up to 0.1 mM [37]. However, physical activity is generally considered healthy.

Potential toxicity of plasmas is an issue, which surely must be addressed. In order to determine the radical activity, standard gas-phase plasma characterization is not very relevant. Instead, one has to identify radical species that can "survive" in an aqueous solution, interact with the cell membrane and eventually penetrate into the cell. Biochemists have some standard methods for radical detection. The principle is roughly the same as in plasma diagnostics: laser spectroscopy. A confocal microscope is commonly used to image cells and tissues. It has been developed to detect laser-induced fluorescence (LIF) from biological samples stained with specific fluorescent probes (organic molecules). The probes bind selectively so some target molecules in the cell, and after irradiation by a laser they produce fluorescent light. In the confocal arrangement, the light collected by the detector originates almost exclusively from the focal region of the laser beam. Three-dimensional profiling with a resolution of about 0.3 μm is possible. The variety of available fluorescent probes is virtually endless (see http://www.probes.com), and so is the number of applications. Verification of cell viability and detection of apoptosis are just a few simple examples. Also for detection of free radicals in fluids, a large selection of dyes is available. The derivatives of dihydrofluorescein diacetate are especially useful, because they can penetrate through the cell membrane. Once present in the cytoplasm, they are hydrolysed by esterases and the products of hydrolysis become trapped in the cell interior. These products can react with various radicals and turn into fluorescent species.

Radiation hazard

UV irradiation is a well known factor that induces cell injury [38]. Dependent on the wavelength, UV effects are split into three categories.

- UV-A (315-380 nm) - the least harmful; causes tanning but may also accelerate skin aging.
- UV-B (280-315 nm) - absorbed by the DNA, causes DNA damage; carcinogenic.
- UV-C (100-280 nm) - more aggressive than UV-B, damages DNA, proteins and cellular lipids. However, radiation below 150 nm is blocked by water (absorption coefficient $10^3 - 10^4$ cm^{-1}), so the eventual damage is not so severe.

It is known that UV radiation in the B and C range can efficiently inactivate bacteria [39]. UV (in all ranges) is also an important factor in bacterial sterilization using low-pressure plasmas [40]. However, non-thermal plasmas under atmospheric pressures are generally poor sources of near UV [41]: the irradiated power in the 200-300 nm region is of the order of 1 mW cm^{-2}. It is known that UV exposure can accelerate wound healing [16], probably due to disinfecting and thus reducing the inflammation. A more detailed investigation is needed to decide whether UV treatment can become a competitive technique for wound sterilization. As regards atmospheric plasmas, it seems unlikely that their weak UV radiation can have much effect on cells and bacteria. The specific cell responses are probably induced by other factors, like plasma chemistry.

2.2 Established surgical plasma equipment

The first application of gas discharges in biomedical engineering was their use to make X-rays: a method that was put into practice in the last years of the nineteenth century.
In the past decades, plasmas are more and more often used in the biomedical world. For example for coatings of implants with bio-compatible layers [10, 42], sterilization [43] and surface modification of polymeric biomaterials [44]. However, these techniques are all applied *ex vivo*. The first *in vivo* applied plasma was developed by Erbe med; its application is called argon plasma coagulation (APC)[45]. Using a flexible endoscopic probe, APC has been used to destroy gastric and colon carcinoma among others.

In this section three *in vivo* applications of electricity and plasmas are described: electrosurgery, plasma coagulation and Spark erosion.

2.2.1 Electrosurgery

In the 19th century, the technology of artificial generation of electricity was well developed and ready to seek for more advanced medical applications. In 1893, d'Arsonval discovered that high frequency current passing through the body does not cause nerve and muscle stimulation [46]. Soon after, high-frequency devices were introduced for cutting of tissues, but it took many decades before the technology of producing safe, efficient and compact surgical tools became available.

At present, electrosurgery has a solid, established name in medicine: the electric cutting device replaces the scalpel in virtually any kind of surgery. A detailed list of applications can be found in the database of ERBE (http://www.erbe-med.de), a leading company producing equipment for electric, cryogenic and plasma surgery. The electrosurgical tools manufactured by ERBE are powered by high-frequency generators: either at 330 kHz or at 1 MHz. The reason for using these frequencies has been already explained in the previous section: they are well above 100 kHz, which is the lower-limit for electric safety. The devices can supply reasonably high powers - up to 200 or 450 W, dependent on the type and application. The power can be (automatically) regulated during the operation, to obtain the desired depth of the incision. Various electrode designs and configurations are used: a monopolar high-frequency powered pin (in this case the current is flowing through the patient's body), a bipolar coaxial head, and a tweezers-like design.

The features that make electric devices so successful and desired are: good cutting reproducibility, high precision, good control of depth, and the possibility of local coagulation. The latter is especially important in achieving hemostasis and thus preventing blood loss, formation of thrombus, and contamination of tissues during surgery. Electric coagulation is also used on its own, when no incision is necessary. Current flowing through the tissue induces Ohmic heating that causes fast and superficial coagulation. This method is often used to seal small blood vessels.

2.2.2 Plasma coagulation

Electrosurgical methods discussed above are based on tissue heating due to Ohmic dissipation. Since the electric current is flowing through the body, tissue damage is not strictly

localized and depth effects occur. However, there are also specific applications, which require superficial tissue modification with minimum penetration depth. Plasma offers such a possibility, so the step from electric to plasma surgery is readily made.

Devitalization by heat is a rather unsophisticated effect, which can be achieved by exposure to any heat source. Atmospheric plasma generated by a high-power electric discharge is one of the options. The aim of the treatment is coagulation and stop of the bleeding, and sometimes even total desiccation and devitalization of the tissue.

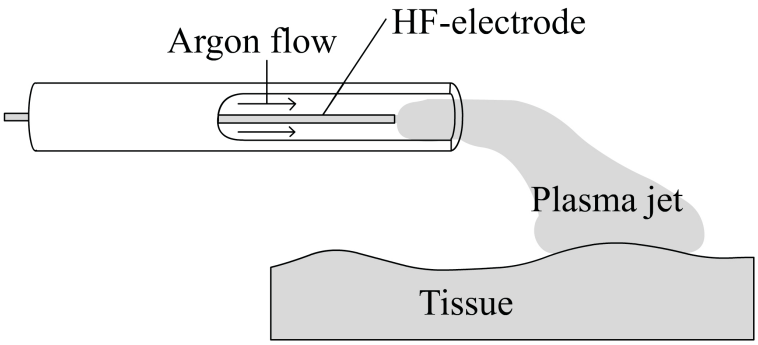

Figure 2.4: *An argon plasma coagulation device, developed by ERBE. Argon flow is blown through the tube, in which the high-frequency electrode is placed. The plasma flame stretches out of the tube. Picture after ERBE (http://www.erbe-med.de)*

An adequate discharge has been developed by ERBE, and the corresponding surgical technique is called argon plasma coagulation (APC), see Figure 2.4. The design of the APC source resembles somewhat the APPJ [21], because in the latter case the plasma is also generated in a tube with flowing argon (flow rate adjustable between 0.1 to 0.9 l min^{-1}). The APC source has not been characterized, but considering the parameters - frequency of 350 kHz, operating voltage of several kV and power input of 50 W, it seems to be a classical AC atmospheric jet. The gas temperature within the plasma can easily reach several hundreds of degrees Celsius.

The powered electrode is placed coaxially inside the tube (monopolar configuration). Like in monopolar electrosurgery, the patient is placed on a conducting sheet and the high-frequency current flows through the body. The APC electrode generates argon plasma, which stretches about 2 to 10 mm from the tip. Since the plasma is electrically conductive, the current can flow to the tissue, but the electrode does not touch it. This is one of the most important advantages of APC: the energy is transferred in a non-contact way, so the problems with tissue sticking to the metal device, heavy burning and tearing can

be avoided. Another unique feature of APC is its self-limiting character. Since the desiccated tissues have a lower electric conductivity than the bleeding ones, the plasma beam will turn away from already coagulated spots toward bleeding or still inadequately coagulated tissue in the area receiving treatment. The argon plasma beam acts not only in a straight line (axially) along the axis of the electrode, but also laterally and radially and "around the corner" as it seeks conductive bleeding surfaces. This automatically results in evenly applied, uniform surface coagulation. The tissues are not subjected to surface carbonization and deep damage, and the penetration depth is at most 3-4 mm. It should be mentioned that the action "around the corner" is typical for all plasmas, but it cannot be achieved in e.g., laser surgery. Capability of superficial scanning of irregular surfaces, small penetration depths and last but not least, low equipment costs, make plasma devices competitive to lasers.

It is not entirely clear what causes the coagulation of the treated tissue. It may be the heat transferred directly from the hot gas as well as the heat generated within the tissue by electric power dissipation (Ohmic heating). However, in the latter case one would expect bulk heating, or at least a higher penetration depth.
May the exact physical mechanism of coagulation be not yet completely resolved, the APC device has been successfully applied in many kinds of surgery. The most obvious application is open surgery: promoting hemostasis in wounds and bleeding ulcers. Treatment of various skin diseases has been discussed by Brand *et al*[47]. Most of the APC applications involve endoscopy. In gastroenterology there are many situations where large bleeding areas must be devitalized [48–50].

2.2.3 Spark erosion

Spark erosion is a special and unconventional application of plasma in surgery. It is remarkable for two reasons: first, as an attempt to treat atherosclerosis, a complex cardiovascular disease that plagues most of the Western world, and second, as an example to show that a quite powerful discharge can be induced in vulnerable places, like blood vessels.

Atherosclerosis is a chronic inflammatory disease, where lipid-rich plaque accumulates in arteries. The consequences are plaque rupture and/or obstruction of the arteries. Atherosclerotic plaque can be formed in all large and medium-sized arteries. Details on the pathogenesis can be found in the overview article by Ross [51]. Treatment of atherosclerosis is in most cases surgical [52]. The plaque must be removed, but in a way that causes least damage to the artery, so as to minimise restenosis. Recently, laser methods have been applied with reasonable success. However, as mentioned earlier, lasers cannot act "around

the corner", which in this case is very essential.

Slager *et al* [53] presented a new concept, which lies between electrosurgery and plasma treatment. This technique, called spark erosion, is based on plaque vaporization by electric heating. The tool developed by Slager is similar to the monopolar device used in APC, but no feed gas is used. Instead, the electrode is immersed directly in the blood stream and directed towards the diseased area. Alternate current (250 kHz) is applied to the electrode tip in a pulsed way, with a pulse duration of 10 ms. The voltages are relatively high - up to 1.2 kV. Under these conditions, the tissue is rapidly heated and vaporized. The produced vapor isolates the electrode from the tissue, so that further treatment is performed in a non-contact way. After vaporization, electric breakdown in the vapor occurs and a small (< 1 mm) spark is formed. Spark erosion allows removing substantial amounts of plaque; produced craters have dimensions of up to 1.7 mm. However, the crater edges are smooth and the coagulation layer does not exceed 0.1-0.2 mm.

It is not yet clear whether spark erosion will become competitive to lasers and mechanical methods in treatment of atherosclerosis. One possible problem is formation of vapor bubbles, which may lead to vascular embolization. Nevertheless, the spark-producing electrode can be used in other operations, where embolization does not pose such a danger. For example, it can be applied in open heart surgery, like treatment of hypertrophic obstructive cardiomyopathy [54]. The cutting performance is similar to electrosurgery, but like in plasma techniques, the treatment is essentially non-contact. Compared to argon plasma coagulation, thermal effects in spark erosion are minor. The spark plasma is much smaller than the argon plasma, so that a) the gas temperature is lower and b) heating is more local. Since there is no gas flow, no heat is transferred by convection. Finally, pulsed operation suppresses the thermal load. Summarizing, spark erosion is still an interesting surgical technique, which combines the advantages of electrosurgery and gas plasma-induced coagulation.

2.3 Goal of the plasma needle

In the medical techniques described above, the action of plasma is not refined: it is based on local burning, vaporization or cutting of the tissue. Using the analogy to material science, electrosurgery, APC and spark erosion can be compared to cutting and welding. However, plasmas are capable of much more sophisticated surface treatment than mere thermal processing. If the analogy to material science holds, it is expected that fine tissue modification can be achieved using non-thermal plasma techniques.

However, the construction of non-thermal and atmospheric plasma source suitable for fine tissue treatment is not trivial. In section 2.1.3 a list of restrictions on the temperature, voltage, chemical activity and radiation has been given. Next to these restrictions, there is one more requirement: the flexibility to act on the tissue. There are not so many sources that can be applied directly and with a high precision to a diseased area. Most plasmas cannot operate in ambient air: they are confined in (partly) closed reactors and direct exposure to the plasma is hindered. Therefore, our research is focused on a flexible and non-destructive microplasma for direct and specific treatment of living tissues.

2.3.1 *In vivo* plasma disinfection

A very important feature of plasma treatment is related to plasma sterilization. Plasma sterilization is a well known effect, demonstrated by many authors and even implemented in practice [7, 9, 55–57]. Various types of discharges (low-pressure or atmospheric) and many gas chemistries were used. The general conclusion is that antibacterial plasma activity is due to the synergy of active plasma radicals and UV photons. Especially in the low-pressure case, the role of (vacuum) UV photons is prominent: since they are not reabsorbed in the gas phase, they can easily reach the bacteria and damage their DNA. In atmospheric plasmas bacterial inactivation is mainly due to the membrane damage as a result of plasma radical (ROS) etching. It has been established that air and oxygen plasmas are more efficient than noble gas discharges. Various types of bacteria (Gram positive and negative) and spores were investigated. Typical D-values (treatment times that lead to deactivation of one decade/90% of bacteria) range from minutes under low-pressure conditions to seconds in atmospheric plasmas.

It is expected that the needle will be applied in dentistry for preparation of dental cavities and/or inactivation of oral plaque [58]. Oral flora consists of several kinds of bacteria; the most important of them is Streptococcus Mutans. These bacteria usually form thick biofilms (dental plaque) or, when enabled to attack the enamel (e.g. at a weak spot, fissure, or in acidic conditions), destroy the dentine and lead to tooth decay (caries). Small cavities, produced this way, need not be filled and often remineralize when the bacteria are gone. In large cavities the decayed matter must be removed and the cavity must be filled. The cavity must be also disinfected prior to filling: typically, two-decades (99%) reduction of bacterial population is sufficient. Recently, plasma disinfection has been proposed as an alternative. As said before, the plasma needle is adapted for treatment of small objects, due to its small size and flexibility in operation. Like all gaseous media, plasma can penetrate into small fissures ("around the corner"), which are difficult to reach in another way.

2.3.2 Plasma interactions with living objects

After reading about existing medical plasma technologies, one might wonder: what is the "refined" organism reaction, which one expects to achieve by non-thermal plasma treatment, a reaction that makes plasma needle operation essentially different from APC and spark erosion? The answer is the manner, in which the cells must be affected: cell damage should be minimal. Cell death should be induced only when necessary, and even then it should fit in the natural pathway, in which the body renews and repairs its tissues. Interactions of non-thermal plasmas with living objects are an entirely new area of research. Of course, the ultimate goal of this research is introducing plasma treatment as a novel medical therapy. However, living organisms are so complicated that one has to begin with a relatively simple and predictable model system, like a culture of cells.

References

[1] Y. P. Raizer. *Gas discharge physics.* Springer, Berlin, 1991.

[2] R. Hippler, S. Pfau, and M. Schmidt. *Low temperature plasma physics: fundamental aspects and applications.* Wiley VCH, Berlin, 2001.

[3] I. S. Marshak. *Pulsed Light Sources.* New York Consultants Bureau, New York, 1984.

[4] E. M. van Veldhuizen. *Electrical discharges for environmental purposes: Fundamentals and applications.* NOVA Science Publishers, Inc., Huntington, New York, 1999.

[5] W. Nicholas and G. Hitchon. *Plasma processes for semiconductor fabrication.* Cambridge University Press, Cambridge; New York, 1999.

[6] E. Stoffels, A. J. Flikweert, W. W. Stoffels, and G. M. W. Kroesen. Plasma needle: a non-destructive atmospheric plasma source for fine surface treatment of (bio)materials. *Plasma Sources Sci. Technol.*, 4:383–388, 2002.

[7] M. Laroussi. Nonthermal decontamination of biological media by atmospheric-pressure plasmas: review, analysis, and prospects. *IEEE Trans. Plasma Sci.*, 30(4):1409–1415, 2002.

[8] I. Radu, R. Bartnikas, and M. R. Wertheimer. Dielectric barrier discharges in helium at atmospheric pressure: experiments and model in the needle-plane geometry. *J. Phys. D: Appl. Phys.*, 36:1284–1291, 2003.

[9] M. Moisan, J. Barbeau, S. Moreau, J. Pelletier, M. Tabrizian, and L. H. Yahia. Low-temperature sterilization using gas plasmas: a review of the experiments and an analysis of the inactivation mechanisms. *Int. J. Pharmac.*, 226(1-2):1–21, 2001.

[10] D. E. MacDonald, F. Betts, M. Stranick, S. Doty, and A. L. Boskey. Physicochemical study of plasma-sprayed hydroxyapatite-coated implants in humans. *J. Biomed. Mater. Res.*, 54:480–490, 2001.

[11] D. Keller, A. Meyer-Plath, A. Ohl, and K. Schroder. Pattern guided cell growth on gas discharge plasma induced chemical microstructured polymer surfaces. In H. Stallforth and P. A. Revell, editors, *Materials for Medical Engineering, Euromat 99*. Wiley-VCH, Weinheim, 2000.

[12] R. Gristina, E. Sardella, L. Detomaso, G. Senesi, P. Favia, and R. d'Agostino. Fibroblast and keratinocyte behaviour on substrates plasma-patterned with fouling and non-fouling domains. *Eur. cell. mater.*, 4(2):94–95, 2002.

[13] B. Alberts, D. Bray, J. Lewis, M. Raff, K. Roberts, and J. D. Watson. *Molecular biology of the cell*. Garland Publishing, 1994.

[14] G. M. Cohen. Caspases: the executioners of apoptosis. *Biochem. J.*, 326:1–16, 1997.

[15] G. M. Fuller and D. Shields. *Molecular Basis of Medical Cell Biology*. Appleton and Lange, Stamford, Connecticut, 1998.

[16] E. Rubin and J. L. Farber. *Pathology*. Lippincot-Raven Publishers, Philadelphia, 1999.

[17] M. v. Zandvoort, W. Engels, K. Douma, L. Beckers, M. oude Egbrink, M. Daemen, and D. W. Slaaf. Two-photon microscopy for imaging of the (atherosclerotic) vascular wall: A proof of concept study. *J. Vasc. Res.*, 41:54–63, 2004.

[18] M. H. Niemz. *Laser-tissue interactions: fundamentals and applications*. Springer, Berlin, 1996.

[19] L. Zach and G. Cohen. Pulp response to externally applied heat. *Oral Surg. Oral Med. Oral Pathol.*, 19:515–530, 1965.

[20] C. R. Behl, G. L. Flynn, T. Kurihara, W. Smith, O. Gatmaitan, W. I. Higuchi, N. F. Ho, and C. L. Pierson. Permeability of thermally damaged skin: I. immediate influences of 60 degrees C scalding on hairless mouse skin. *J. Invest. Dermatol.*, 75(4):340–345, 1980.

[21] J. Park, I. Henins, H. W. Herrmann, G. S. Selwyn, and R. F. Hicks. Discharge phenomena of an atmospheric pressure radio-frequency capacitive plasma source. *J. Appl. Phys.*, 89(1):20–28, 2001.

[22] X. P. Lu and M. Laroussi. Ignition phase and steady-state structures of a non-thermal air plasma. *J. Phys. D: Appl. Phys.*, 36(6):661–665, 2003.

[23] J. Toshifuji, T. Katsumata, H. Takikawa, T. Sakakibara, and I. Shimizu. Cold arc-plasma jet under atmospheric pressure for surface modification. *Surf. Coat. Technol.*, 171(1-3):302–306, 2002.

[24] S. Y. Moon and W. Choe. A comparative study of rotational temperatures using diatomic OH, O2 and N2+ molecular spectra emitted from atmospheric plasmas. *Spectrochimica Acta B - Atomic Spectroscopy*, 58(2):249–257, 2003.

[25] M. Baeva, A. Dogan, J. Ehlbeck, A. Pott, and J. Uhlenbusch. CARS diagnostic and modeling of a dielectric barrier discharge. *Plasma Chem. Plasma Process.*, 19(4):445–466, 1999.

[26] O. Motret, C. Hibert, S. Pellerin, and J. M. Pouvesle. Rotational temperature measurements in atmospheric pulsed dielectric barrier discharge - gas temperature and molecular fraction effects. *J. Phys. D: Appl. Phys.*, 33(12):1493–1498, 2000.

[27] A. A. H. Mohamed, R. Block, and K. H. Schoenbach. Direct current glow discharges in atmospheric air. *IEEE Trans. Plasma Sci.*, 30(1):182–183, 2002.

[28] E. Stoffels, I. E. Kieft, and R. E. J Sladek. Superficial treatment of mammalian cells using plasma needle. *J. Phys. D: Appl. Phys.*, 36:2908–2913, 2003.

[29] S. Gabriel, R. W. Lau, and C. Gabriel. The dielectric properties of biological tissues. 2. measurements in the frequency range 10Hz to 20GHz. *Phys. Med. Biol.*, 41(11):2251–2269, 1996.

[30] J. P. Reilly. *Electrical Stimulation and Electropathology.* Cambridge Univ. Press, Cambridge, 1992.

[31] C. Polk. Biological applications of large electric fields: some history and fundamentals. *IEEE Trans. Plasma Sci.*, 28(0093-3813):6–14, 2000.

[32] J. Deng, K. H. Schoenbach, E. S. Buescher, P. S. Hair, P. M. Fox, and S. J. Beebe. The effects of intense submicrosecond electrical pulses on cells. *Biophys. J.*, 84:2709–2714, 2003.

[33] S. J. Beebe, P. M. Fox, L. J. Rec, K. Somers, R. H. Stark, and K. H. Schoenbach. Nanosecond pulsed electric field (nsPEF) effects on cells and tissues: Apoptosis induction and tumor growth inhibition. *IEEE Trans. Plasma Sci.*, 30(1):286–292, 2002.

[34] K. H. Schoenbach, S. J. Beebe, and E. S. Buescher. Intracellular effect of ultrashort electrical pulses. *Bioelectromagnetics*, 22:440–448, 2001.

[35] R. P. Joshi and K. H. Schoenbach. Mechanism for membrane electroporation irreversibility under high-intensity, ultrashort electrical pulse conditions. *Phys. Rev. E*, 66(5):052901, 2002.

[36] Barry Halliwell and John M. C. Gutteridge. *Free radicals in biology and medicine.* Oxford University Press, New York, 1999.

[37] Stefan A. J. Coolen. *Antipyrine Hydroxylates as Indicators for Oxidative Damage.* PhD thesis, Eindhoven University of Technology, Eindhoven, 2000.

[38] E. Straface, P. Ulderico Giacomoni, and W. Malorni. Cultured cells as a model system for the study of UV-induced cytotoxicity. *J. Photochem. Photobiol. B*, 63(1-3):52–60, 2001.

[39] N. Giese and Darby J. Sensitivity of microorganisms to different wavelengths of UV light: implications on modelling of medium pressure UV systems. *Wat. Res.*, 34:4007–4013, 2000.

[40] N. Philip, B. Saoudi, M-C. Crevier, M. Moisan, J. Barbeau, and J. Pelletier. The respective roles of UV photons and oxygen atoms in plasma sterilization at reduced gas pressure: the case of N2-O2 mixtures. *IEEE Trans. Plasma Sci.*, 30(4):1429–1436, 2002.

[41] M. Laroussi and F. Leipold. Evaluation of the roles of reactive species, heat, and UV radiation in the inactivation of bacterial cells by air plasmas at atmospheric pressure. *Int. J. Mass Spectrom.*, 233(1-3):81–86, 2004.

[42] C. P. Klein, P. Patka, J. G. Wolke, J. M. Blieck-Hogervorst, and K. de Groot. Long-term in vivo study of plasma-sprayed coatings on titanium alloys of tetracalcium phosphate, hydroxyapatite and alpha-tricalcium phosphate. *Biomaterials*, 15(2):146–150, 1994.

[43] M. Laroussi. Sterilization of contaminated matter with an atmospheric pressure plasma. *IEEE Trans. Plasma Sci.*, 24(3):1188–1191, 1996.

[44] K. Schroder, A. Meyer-Plath, D. Keller, W. Besch, G. Babucke, and A. Ohl. Plasma-induced surface functionalization of polymeric biomaterials in ammonia plasma. *Contrib. Plasma Phys.*, 41:562–572, 2001.

[45] K. E. Grund, T Straub, and G Farin. New haemostatic techniques: argon plasma coagulation. *Best. Pract. Res. Clin. Gastroenterol.*, 13:67–84, 1999.

[46] A. D'Arsonval. Action physiologique des courants alternatifs a grand frequence. *Archives Physiol. Norm. Path.*, 5:401–408, 1893.

[47] C. U. Brand, A. Blum, A. Schlegel, G. Farin, and C. Garbe. Application of argon plasma coagulation in skin surgery. *Dermatol.*, 197:152–157, 1998.

[48] J. Waye. Delivery system for argon coagulator offers non-contact method for control of GI bleeding. *Gastroenterol. Endosc. N*, 1997.

[49] P. J. Wahab, C. H. H. Mulder, G. Den Hartog, and J. E. Thies. Argon plasma coagulation in flexible gastrointestinal endoscopy: Pilot experiences. *Endoscopy*, 29:176–181, 1997.

[50] G. Focke, Ch. Seidl, and V. Grouls. Behandlung des wassermelonen-magens (GAVE-syndrom) mit der endoskopischen argon-plasma-koagulation (APC). ein neuer therapieansatz. *Leber-Magen-Darm*, 26:254–259, 1996.

[51] R. Ross. Atherosclerosis - an inflammatory disease. *N. Engl. J. Med.*, 340(2):115–126, 1999.

[52] A. C. Guyton and J. E. Hall. *Textbook of medical physiology.* W.B. Saunders Company, 2000.

[53] C. J. Slager, C. E. Essed, J. C. H. Schuurbiers, N. Bom, P. W. Serruys, and G. T. Meester. Vaporisation of atherosclerotic plaques by spark erosion. *J. Am. Coll. Cardiol.*, 5(6):1382–1386, 1985.

[54] L. P. W. M. Maat, C. J. Slager, L. A. Van Herwerden, J. C. H. Schuurbiers, R. J. Van Suylen, M. J. M. Kofflard, F. J. Ten Cate, and E. Bos. Spark erosion myectomy in hypertrophic obstructive cardiomyopathy. *Ann. Thorac. Surg.*, 58(2):536–540, 1994.

[55] S. Lerouge, M. R. Wertheimer, and L. H. Yahia. Plasma sterilisation: a review of parameters, mechanisms, and limitations. *Plasmas Polym.*, 6:175–188, 2001.

[56] S. J. Fraser, R. B. Gillette, and R. L. Olson. Sterilizing process and apparatus utilizing gas plasma. *U. S. Patent 3*, 948:601, 1976.

[57] I. A. Soloshenko, V. V. Tsiolko, V. A. Khomich, A. I. Shchedrin, A. V. Ryabtsev, V. Yu Bazhenov, and I. L. Mikhno. Sterilization of medical products in low-pressure glow discharges. *Plasma Phys. Rep.*, 26:792–800, 2000.

[58] R. E. J Sladek, E. Stoffels, R. Walraven, P. J. A. Tielbeek, and R. Koolhoven. Plasma treatment of caries: a novel method in dentistry. *IEEE Trans. Plasma Sci.*, 32(4):1540–1543, 2004.

Chapter 3

Electrical and optical characterization of the plasma needle

Abstract
The plasma needle is a source to create a non-thermal radio frequency plasma at atmospheric pressure. To improve the ease of working on biological samples, a flexible plasma probe was designed. In the new configuration, the needle was confined in a plastic tube through which helium flow was supplied. The new setup was characterized by impedance measurements and emission spectroscopy. Impedance measurements were performed by means of an adjustable matching network; the results were modeled. The discharge was found to be entirely resistive; the measured voltage was in the range 140-270 V_{rms} and it was in excellent agreement with model results. From the resistance, the electron density was estimated to be 10^{17} m^{-3}.
Optical measurements showed substantial UV emission in the range 300-400 nm. Active oxygen radicals (O· and OH·) were detected. Furthermore, the influence of helium flow speed was investigated. At low flow speeds, the density of molecular species in the plasma increased.
UV emission and density of active species are important factors that determine the performance of plasma in the treatment of biological materials. Therefore, the new characterization will help to understand and optimize the interactions of atmospheric plasma with cells and tissues.

This chapter was published as I.E.Kieft, E.P.v.d. Laan, E. Stoffels, Electrical and optical characterization of the plasma needle, *New J. Phys.*,6:149, 2004.

3.1 Introduction

The plasma needle is a type of non-thermal atmospheric glow discharge; it has a single-electrode configuration and is operated in helium [1]. Important properties of this type of plasma are that it operates near room temperature, allows treatment of irregular surfaces and has a small penetration depth. These characteristics give the needle great potential for use in the biomedical field. This work is aimed at studying cells and bacteria that are treated with the plasma. The experiments have already shown that the plasma needle is capable of bacterial decontamination [2] and of localized cell removal without causing necrosis to the treated or the neighboring cells [3]. Areas of detached cells were made with a diameter of 0.1 mm, which indicates that the precision of the treatment can be very high. It is believed that plasma particles, such as radicals and ions, and also emitted UV light interact with the cell membranes and cell adhesion molecules and therefore cause the detachment of the cells [3]. The penetration of the plasma radicals in liquid was tested [4], and densities in the μM range were observed.

In this chapter, we characterize a new configuration of the plasma needle, by describing its electrical setup and by studying light emission. The design of the needle was changed to improve the ease of working and to allow treatment of large-sized objects. This was not possible in the former configuration because the needle was enclosed in a box [1], which meant that specimens had to be placed inside. The box had dimensions of 10 x 10 x 10 cm and it was filled with helium after the specimens had been put in, which took 30 s to 1 min. In the new design, this box is replaced by a tube, through which helium flow is directed coaxially with the needle. Near the needle tip, the helium mixes with air. The percentage of air at this point has been determined by Raman scattering to be in the range 0.1-1% [4]. This way, a plasma is created that is at first sight comparable with the high frequency plasma pencil [5] and the plasma-energized jet [6]. However, the micro-plasma generated by the plasma needle has a gas temperature much closer to room temperature than in the other designs and is thus more suitable for the intended tissue treatment.

To electrically characterize the plasma, the voltage at the needle as well as the power dissipated by the plasma were determined. Furthermore, we measured the impedance of both the plasma and the matching network.
The method used to obtain the impedance of the RF discharge that was applied here was based on the transmission line theory: a variable matching network was inserted to match the impedance of the plasma setup to the internal impedance of the power supply [7, 8]. Firstly, the impedance of the matching network was determined and put into a model. The model allowed calculating the impedance of the discharge. The plasma appeared to be entirely resistive: no capacitive component was found. The power dissipated by the

plasma was found to be dependent on the distance between the plasma needle and the treated surface. This property might be used as a measurement tool for automatic control of the position of the needle relative to a surface.

The light emission by the plasma was studied by optical emission spectroscopy. This method is commonly used for plasma analysis [9–11]. The emission spectra are used to investigate possible UV emission and the composition of the plasma. UV emission and radicals are important for the application of plasma to biological samples because both are known to be potentially damaging to cells; they can induce programmed cell death (apoptosis) [12–14].
Emission spectroscopy was also used to investigate the effect of a change in helium flow rate. Under all conditions, UV radiation was mainly emitted in the region between 305 and 390 nm; the species that could be detected were OH·, O·, N_2^+, N_2 and He. An abrupt increase (jump) in the intensity of the light emission was found when the applied voltage was increased while keeping the other parameters constant. This jump could indicate a transition to another plasma mode.

3.2 Method

3.2.1 Plasma needle

The schematic drawing of the plasma needle (Figure 3.1) shows the plasma at the sharp end of a metal-alloy pin (diameter 0.3 mm). The typical size of the plasma glow was 2 mm in diameter (Figure 3.2).

The metal pin was inserted coaxially in a Perspex tube; it protruded from the stainless steel holder by 1.5 cm. The total length of the needle was about 8 cm. To prevent a discharge along the entire pin, it was insulated by glass. Helium flowed through the plastic tube at a rate of 2 l min^{-1} unless stated otherwise. The flow rate was regulated with a mass flow controller from Brooks series 5850E. Because the inner diameter of the Perspex tube was 5.5 mm, this flow rate resulted in a velocity of 1.4 m s^{-1}. The helium flow was mixed with a small amount of air near the tip. Moving the Perspex tube relative to the fixed needle regulated the percentage of air. In the study described here, the end of the tube reached as far as the needle tip.

The RF signal was generated with a waveform generator Hewlett Packard 33120A and amplified by an RF amplifier model 75AP250 by Amplifier Research. From the amplifier, the signal was directed to a home-built matching network, which is described in a later

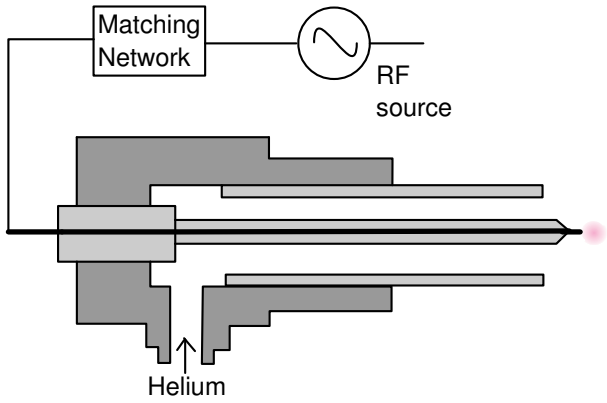

Figure 3.1: *Schematic drawing of the experimental setup. The electrode wire is fixed in a stainless steel holder and insulated by a glass tube, leaving only the tip exposed. The outer Perspex tube surrounding the wire can be moved horizontally.*

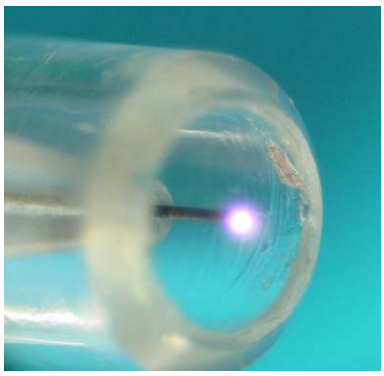

Figure 3.2: *Plasma generated by the plasma needle. The plasma appeared as a pink glow with a diameter of approximately 1 mm at the tip of the needle.*

section.
A bi-directional power meter was placed in-between the amplifier and the matching network to measure forward and reflected power. The meter was the PM 2002 obtained from Amplifier Research with directional couplers also from Amplifier Research. A voltage probe P6150A by Tektronix was attached to the feed-through of the needle when voltage measurements were carried out. The probe was a 1000x attenuator with 100 M
Omega resistance and 3 pF capacitance.

3.2.2 Impedance measurements

In order to measure the impedance of both the metal pin and the discharge, first the impedance of the matching network (Figure 3.3) had to be determined. The matching net-

work had to be characterized carefully, and thus it was necessary to know the components of the network as well as its stray impedances. To determine these stray impedances, the method described by Bakker *et al* [8] was used, which is based on the reflection of power by the matching network. To use this method for our setup, it was necessary to first adapt the matching network: it was made adjustable and more stable.

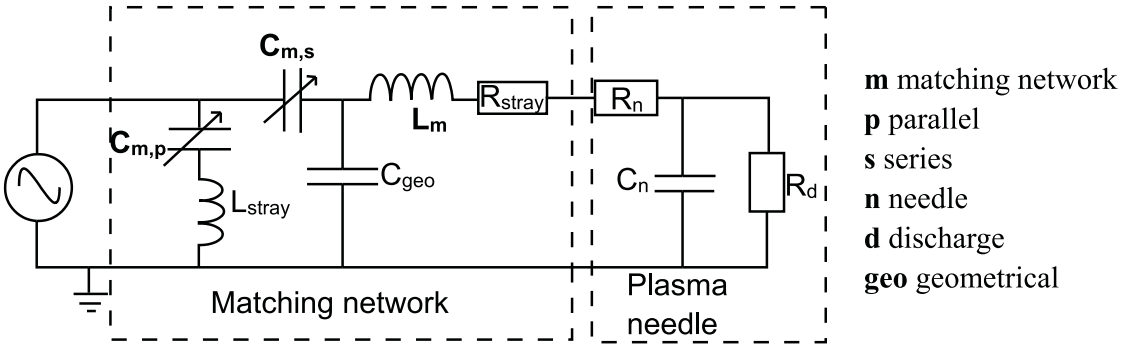

Figure 3.3: *The components of the matching network and of the plasma needle.*

Then a stepwise approach was followed to determine the discharge impedance: (1) the matching network was short-circuited and stray impedances were calculated; (2) the load impedance (the plasma needle) was connected and the network was matched; (3) from the settings, the plasma impedance was calculated. A short-circuit (used in step 1) is a fixed load with zero real and imaginary values and it is independent of voltage and frequency.

For step 1, the components of the matching network were identified with the assumed stray impedances (Figure 3.3). The basic components that were physically put into the network were the coil L_{m} and the capacitances $C_{\mathrm{m,s}}$ and $C_{\mathrm{m,p}}$. These capacitances were Jennings tuning vacuum capacitors with very high quality factors (Q). Therefore, they were assumed not to have any intrinsic stray impedance. The capacitors' impedances were measured when they were fully disconnected; the measured values were then put into the model. Because of the high Q values, the capacitances could be measured at 1 kHz and the obtained values were still reliable for use at 13.56 MHz. The impedances of these capacitances were measured with an automatic RCL meter by Fluke (model 6303A) at 1 kHz. Depending on the plasma load, $C_{\mathrm{m,s}}$ and $C_{\mathrm{m,p}}$ varied between 500 and 520 pF and 290 and 310 pF respectively. The inductance of the coil was determined to be 3.4 μH at 3.2 MHz. However, because the coil did not have a high Q factor, at higher frequencies the inductance deviated from the measured value at 3.2 MHz and thus the latter could only be used as an indication for the model.

Besides the impedances of the basic components, stray impedances were taken into account. These were called L_{stray} and R_{stray}. The impedance L_{stray} originated from the wires that were connected to the capacitor $C_{\text{m,p}}$, because these wires had a small inductance. Since the wires were very flat, the resistive skin effect was neglected. The stray inductance from the wires that connected $C_{\text{m,s}}$ and L_{m} was included in L_{m} in the model. In the model of the matching network, a capacitance C_{geo} had to be added because $C_{\text{m,s}}$ was located very close to the grounded case and this gave an extra capacitive impedance.

To determine the stray impedance values, we used Equation 3.1, which stated that the reflection of power is a function of the impedance.

$$\frac{P_{\text{ref}}}{P_{\text{forw}}} = \left| \frac{Z - 50\Omega}{Z + 50\Omega} \right|^2 \tag{3.1}$$

The forward and reflected power were measured with the bidirectional power meter as a function of $C_{\text{m,p}}$. For these measurements, the matching network was matched at 13.56 MHz and $C_{\text{m,p}}$ was varied, whereas $C_{\text{m,s}}$ was kept constant. The values of the stray impedances were determined by fitting the function to the measured values.

Then followed step 2: Connecting the load impedance. The settings of $C_{\text{m,s}}$ and $C_{\text{m,p}}$ in the matched situation with load were recorded, and from this the load impedance was determined. The load impedance was divided into two components: the needle itself and the discharge. The impedance of the needle was found when the plasma was turned off. It had a capacitive and a resistive component. The impedance of the discharge had only a resistive part. The transmission line that connected the matching network to the needle transformed the load impedance. This transformation is given in Equation 3.2 [15].

$$Z_{\text{load}} = Z_0 \frac{Z_{\text{needle+discharge}} + Z_0 j tan(\beta l)}{Z_0 + Z_{\text{needle+discharge}} j tan(\beta l)} \tag{3.2}$$

Z_0 is the impedance of the transmission lines and the internal impedance of the RF source, both non-imaginary and 50 Ω. β Is the phase constant: it is the imaginary part of the propagation constant. l Is the length of the coaxial cable from the matching box to the needle system, which was in our setup 0.25 m with a β of 0.43 rad m^{-1}.

3.2.3 Light emission

To analyze light emission, we performed spectroscopy measurements; the obtained data were used to determine the plasma composition. The helium flow rate was varied to investigate the influence of the flow velocity on the emission and thus the composition of the plasma.

For the spectroscopy, two types of spectrometers were used. The first was the JobinYvon H25, which had a good resolution (peaks 1 nm apart could be distinguished). For focusing, a quartz lens was used with a focal length of 0.25 m. The grating of the spectrometer had 1500 lines per mm. The image produced by the spectrometer was taken with an intensified charge-coupled device (iCCD) camera (Andor DH534) at a cooling temperature of -35 °C. The exposure time was set at 0.7 s, and the gate width at 2000 ns. The accumulation number we used was 100. The quantum efficiency of the CCD camera was greatly reduced for wavelengths above 800 nm, where the efficiency was at least a factor 10 lower than that in the range 300-500 nm.

For quicker but lower-resolution (peaks 5 nm apart could be distinguished) measurements, an Ocean Optics HR2000 was used. The fibre was 2 m long. Through the fibre the signal was greatly attenuated ($> 20\%$) for wavelengths below 300 nm and from 900 to 1000 nm. The numerical aperture of the fibre was 0.22, which equalled a whole acceptance angle of 24.8°. A collimating quartz lens was placed in front of the fibre to couple parallel beams into the fibre. The diameter of this lens was 5 mm, which enabled us to view the entire plasma at once.

Light intensity measurements were performed with a photodiode UV50 of UDT Sensors. The sensor had a sensitivity range of 200-1100 nm with a peak at 800 nm.

3.3 Result and discussion

3.3.1 Impedance measurements

In the previous section, we explained that, before impedance measurements could be done on the discharge, first the matching network needed to be known. To map the network, a short-circuit was used to close it. Then the reflection coefficient, which is the reflected power divided by the forward, was measured as a function of $C_{\mathrm{m,p}}$ (Figure 3.4). $C_{\mathrm{m,s}}$ was kept at a constant value (22.30 pF) during these measurements.

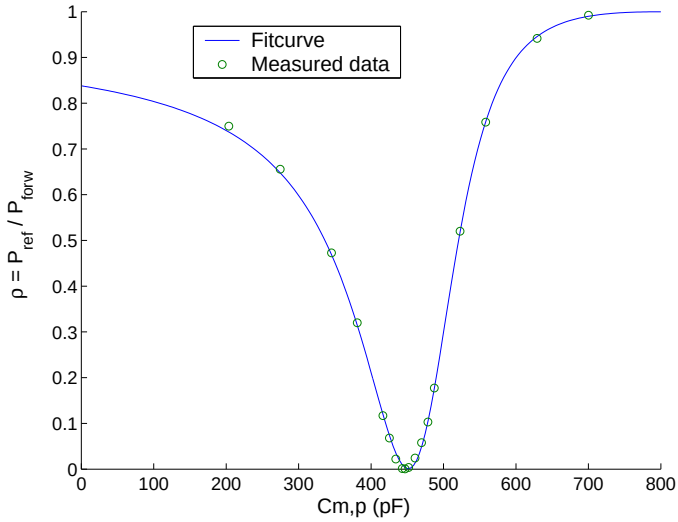

Figure 3.4: *The reflection coefficient in relation to $C_{\mathrm{m,p}}$ and the curve fit that is made to determine stray impedances.*

In the matched situation, the reflected power was about 50 μW, which was very small compared to the forward power of 1 W. The obtained data were used to make a model of the matching network and thus determine the stray impedance values (Table 3.1). This reflection coefficient calculated with the model fitted the measured coefficient well, with a dataset correlation of 0.9998.

Table 3.1: *Capacitance settings for matching network mapping and determined stray impedance values.*

Component	Value
$C_{\mathrm{m,p}}$	446.93 pF
$C_{\mathrm{m,s}}$	22.30 pF
C_{geo}	21.02 pF
R_{stray}	0.6728 Ω
L_{m}	3.018 μH
L_{stray}	14.6547 nH

Because the components of the matching network were now known, we could determine the plasma needle characteristics with a high precision. As was explained in section 3.2, the impedance of the plasma needle was divided into a resistive and capacitive component of the needle itself and a resistive component of the discharge. The resistance of the nee-

dle without discharge was 1.1 Ω, and its capacitance was 28.8 pF. The impedance of the discharge depends on external parameters like the forwarded power (Figure 3.5), and on the distance between the needle and the treated surface.

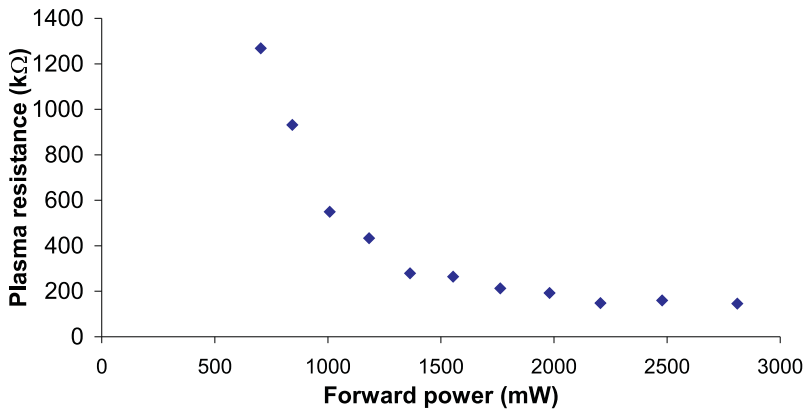

Figure 3.5: *Discharge impedance as function of forward power. The impedance ranges from 100 to 1200 kΩ.*

Without a nearby surface, the plasma impedance was calculated to be in the range 100-1200 kΩ. The resistance of the plasma decreased with increase in forward power. The power dissipated in the discharge ranged from tens of mW to a few hundred mW. The power efficiency increased from a few percent to 20%, when the forward power was increased from 700 mW to 3 W. We also observed that the size of plasma increased with increasing power (roughly from 1 to 4 mm in diameter).

Knowing the resistance of the discharge and the size of the glow, we can estimate the electron density, since the resistance of the plasma is mainly determined by elastic collisions of electrons with neutrals. For a weakly ionized plasma the conductivity σ in $\Omega^{-1}\mathrm{m}^{-1}$ depends mostly on the degree of ionization $n_\mathrm{e}/n_\mathrm{a}$, with n_e the electron density and n_a the neutral density. Equations 3.3 and 3.4 [16] can be used to estimate the electron density n_e.

$$\sigma = \frac{n_\mathrm{e} e^2}{m_\mathrm{e} \nu_\mathrm{ea}} \tag{3.3}$$

$$\nu_\mathrm{ea} = n_\mathrm{a} \sigma_\mathrm{ea} v_e \tag{3.4}$$

Firstly, we use Equation 3.4 to calculate the collision frequency ν_{ea}. The average speed of the electrons, v_{e} is taken to be 0.84x10^{6} m s^{-1}, because we can assume the average electron temperature to be 2 eV for an atmospheric helium plasma [17, 18]. At this speed, the cross-section σ_{ea} is 5x10^{-20} m^{2} for collisions between electrons and neutrals [16]. With the density of the gas at atmospheric pressure n_{a} = 2.5x10^{25} m^{-3}, the ν_{ea} was calculated to be about 1.6x10^{12} s^{-1}.
The conductivity in Equation 3.3 was calculated from the size of the plasma and the corresponding resistance. The size of the plasma was determined from the size of the glow, which was assumed to be spherical. The resulting electron density was found to be 10^{17} m^{-3}. The conductivity and thus the electron density varied as a function of the forward power, as shown in Figure 3.6. This figure indicated that, when the forwarded power exceeded 2000 mW, the plasma expanded in volume, but the electron density remained almost constant. So it seems that the chemical activity of the discharge remained the same while the glow increased in size.

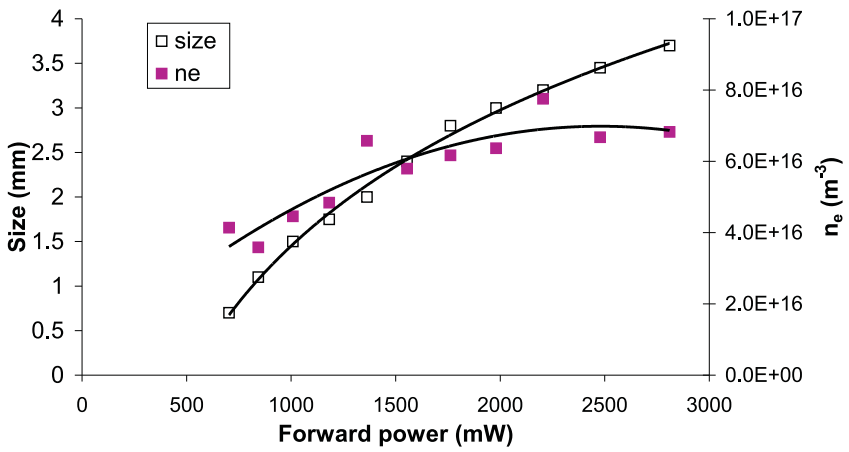

Figure 3.6: *Diameter of the plasma and the estimated electron density.*

The electron density of 10^{17} m^{-3} seems reasonable if we compare it with the electron density of another non-thermal RF plasma at atmospheric pressure with helium as feed gas: the atmospheric-pressure plasma jet (APPJ). The density for the α-mode discharge of the APPJ is 3x10^{17}m^{-3} [19], which is equivalent to the density we found for the plasma needle.

Using the model that was developed for the impedance calculations, we calculated the voltage at the connector of the transmission line to the plasma needle. Thus, the fall in voltage was calculated over both the resistance of the needle and the resistance of the

discharge. For this calculation, we used the forward power at the power meter to determine the start values V_0 and I_0. In a matched situation, the impedance of the system was non-imaginary and 50 Ω at the input of the matching network. The voltage at the load could then be determined from these start values, because all impedance components were known, including the transmission line from the matching network to the load (see Equation 3.2). It was not necessary to take into account the transmission line from the power meter to the matching network, because this line was terminated by 50 Ω in the matched situation and therefore it did not influence the amplitude of voltage.
The calculated voltage appeared to agree with the measured voltage (Figure 3.7).

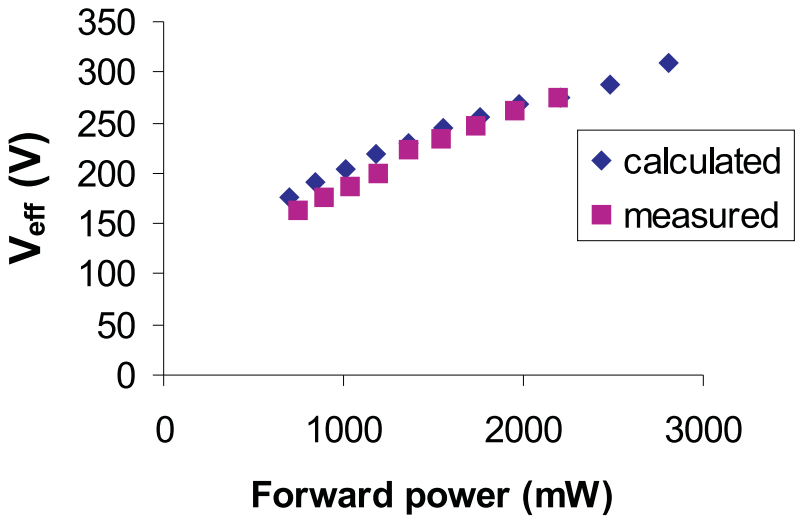

Figure 3.7: *Voltage at the connector of the plasma needle measured and calculated.*

The minimum voltage needed to sustain the plasma was just below 140 V. This is higher that in the old configuration, where it was as low as 90 V [1].

To ensure good reproducibility and high precision, it is important to learn how the plasma characteristics change during surface treatments. To this end, the needle voltage was measured when its tip was approaching a surface. The surfaces that were used during voltage measurements were: plastic (non-conducting), demineralized water (conductivity 2 μS cm^{-1}) and aluminium (conductivity 0.4 MS cm^{-1}) [20]. The conductivity of the water was closest to that of biological material (for most tissues in the range of mS cm^{-1})[21]. Only when the surface was (partly) conducting, the voltage decreased during approach. The first influence on the discharge could be noticed at a distance of 5 mm; from that point, the effect continuously increased. The size of the plasma was about 2 mm in diameter,

which means that the charged particles from the active plasma zone had to pass about 3 mm to reach the grounded surface. The voltage decrease was quite strong: a decline from 190 V to 150 V for the liquid and aluminium surfaces. When the aluminium surface was approached to about 1 mm, the voltage dropped to 125 V, and the plasma became arc-like in appearance. Upon the approaching the surfaces, the net power dissipated in the matching network and the plasma needle slightly increased. This relation can be used as an indicator of the distance from the treated surface. This is of importance in the treatment of biological tissues, where doses of plasma irradiation must be carefully controlled. For precise and well-reproducible treatment, the needle-to-surface distance should be kept constant.

3.3.2 Light emission

Light emission is monitored to detect possible UV emission and to determine the composition of the plasma. From the emission spectrum (Figure 3.8) the discharge composition can be studied by ascribing the emitted lines to specific excited atoms and molecules. We must keep in mind that only weak emission bands have been reported for ozone in scientific literature [22], so ozone is not likely to be detected.

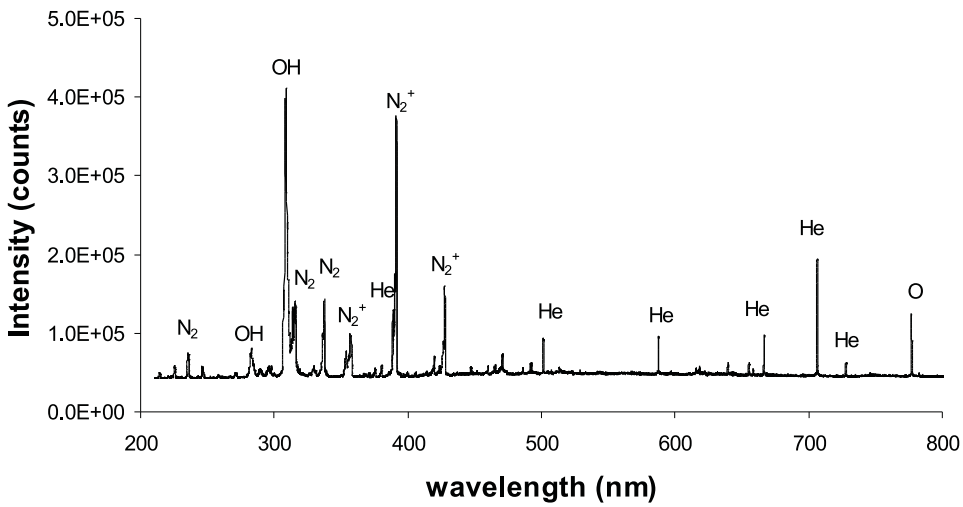

Figure 3.8: *Emission spectrum for plasma needle. Emission lines were ascribed to He, N_2, N_2^+, OH· and O·. Note that sensitivity drops notably for wavelengths greater than 750 nm.*

Emission lines could be ascribed to He, N_2, N_2^+, OH· and O·. The 3064 $\mathring{A}$ ($A^2\Sigma^+ \rightarrow X^2\Pi$

transition) emission of OH· is found generally when water vapor is present, as is the case in our open-air system. The first negative system of N_2^+ ($B^2\Sigma_u^+ \rightarrow X^2\Sigma_g^+$) can be observed, as was expected in the presence of excess helium [22]. For N_2 we see the second ($C^3\Pi \rightarrow B^3\Pi$) and fourth ($D^3\Sigma^+ \rightarrow B^3\Pi$) positive system. The second positive system appears readily in discharges containing nitrogen [22]. Interestingly, the intensity of the nitrogen lines was not dominant over the helium lines. This indicated that the discharge was mainly based on helium, and the blending of nitrogen was low.

For an atmospheric helium plasma, it is not possible to determine the electron temperature from the emission spectrum [17]. The relative densities of excited states, obtained from the spectra, can be used to make Saha plots [18], but these plots yield only the excitation temperature, which is not directly dependent on the electron temperature. This is because, in a non-equilibrium system, there is a drain of charged particles that leads to an overpopulation of the lower atomic states with respect to the Saha balance [18]. Electron temperature in such systems must be determined in another way, e.g. by means of Thomson scattering. The fact that helium is the lightest noble gas having high ionization potential results in high T_e and low n_e. As mentioned before, the typical electron temperature in atmospheric helium plasma is around 2 eV [17, 18].

Subsequently, we studied the relation between the applied voltage and the total (wavelength integrated) light emission, recorded by a photodiode. The total light emission was assumed to be an indicator for the size of the plasma. A sudden increase (jump) in light emission intensity was observed when the voltage and input power were raised above a certain threshold value (Figure 3.9).

This sudden increase in emission when voltage is raised above 160 V_rms could indicate a change in plasma mode, which is usually followed by a change in electron temperature. To study this behavior further, we analyzed spectra taken at point 1 and 2 in Figure 3.9 made with the Ocean Optics HR2000 (sensitivity between 200 and 600 nm). Going from 1 to 2, the total intensity of the spectrum increased by a factor of 6, whereas the intensity of the helium line at 588 nm increased by a factor of 12; the emission of the OH· and N_2^+ lines increased approximately at the same rate as the total intensity. The intensities of the N_2 lines decreased relative to the total intensity. This indicates that, in the low-voltage mode ($<$ 160 V) the plasma is sustained mainly by ionization of the impurities. This feature of the plasma needle can be understood, because the molecular impurities are relatively easy to excite and ionize, while efficient ionization of helium requires a certain threshold voltage.

Shi *et al* [23] described several modes of RF atmospheric plasmas that were similar to the alpha mode. In addition to the generally known alpha-mode, they introduced the nor-

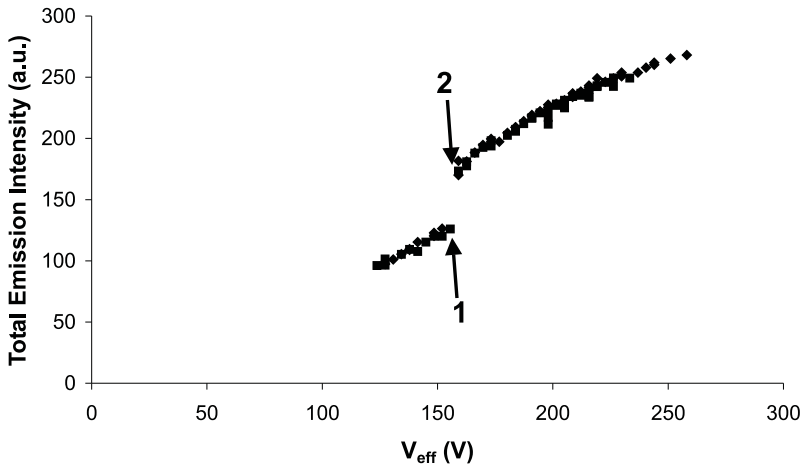

Figure 3.9: *At a certain voltage increase supplied to the needle, a jump in light emission was observed using a fotodiode. This could indicate a transition in plasma mode.*

mal glow mode and the recovery mode. These modes, similar to the alpha mode, had a diffuse and uniform appearance, and for both modes the ionized gas was close to room temperature. The two modes we observed in Figure 3.9 were both at low temperature and were most probably of the alpha-mode type. However, because the plasma needle has a unipolar configuration, we cannot directly compare the observed modes with those of Shi *et al*, and more research is needed to determine the exact plasma modes of the needle.

3.3.3 Influence of helium flow speed

The advantage of decreasing helium flow rate is that it is cost-saving, and it would be practical for use in small openings and for vulnerable tissues. However, due to the lower flow speed, more air will diffuse into the discharge and this will change its characteristics. The ionization potential of nitrogen is 15.58 eV, whereas it is 24.59 eV for helium, and therefore nitrogen will become the predominantly ionized gas. The disadvantage of a lower flow speed is an increase in gas temperature, because the heat loss by convection is lower. Furthermore, the heat conductivity of nitrogen is lower than that for helium (24x10^{-3} W m^{-1} K^{-1} versus 144x10^{-3} W m^{-1} K^{-1}).

To investigate the effect of the helium flow on the composition of the plasma, the flow was reduced from the standard 2 l min^{-1} to 0.5 l min^{-1} and the emission spectra were analyzed. This flow reduction meant that the flow speed varied from 1.4 to 0.35 m s^{-1}. At lower flow rates, the plasma became unstable. The power needed to sustain the plasma decreased

slightly from 3.8 W forward power to 3.7 W, with reflected power decreasing from 26 mW to 6 mW. At first sight this may seem illogical, because the supply of helium was lower and more impurity (molecules) was diffusing in, thereby causing a loss of electron energy due to excitation and dissociation of the molecules. However, the nitrogen molecules were easier to ionize due to their lower ionization potential.
The spectrometer used for these measurements has a sensitivity range of 200-600 nm, which means that some helium lines and the 777 nm atomic oxygen line were not included.

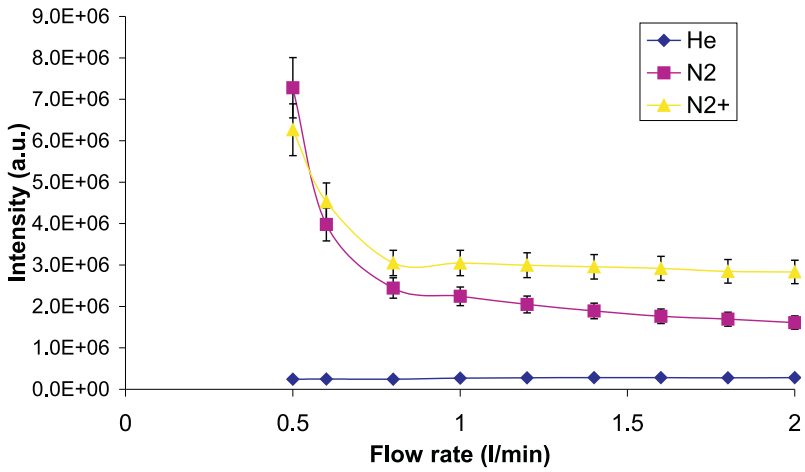

Figure 3.10: *Intensity dependence on the helium flow rate for He, N_2 and N_2^+. There is a large increase in emission for low flow speed, mainly for nitrogen lines.*

When the helium flow was turned down, the total spectrum intensity increased. This was mainly due to a substantial increase in N_2 emission (Figure 3.10). Because the strongest nitrogen lines were below 400 nm, the emission of UV light increased. Unfortunately, at low flow rates, nitrogen lines significantly interfered with the OH· lines and an increase in these lines could not be linked directly to a rise of OH radical density. Thus, we were unable to describe the behavior of the OH radicals. Our previous study using fluorescent probes [4] indicated that oxygen-radical density decreased when impurities such as oxygen or air were admixed with the helium. However, in those measurements [4], the concentration of molecular species was in the 0.1-1% range. Such amounts of oxygen led to a drastic reduction of plasma activity (e.g. decrease of electron density), which was expressed by suppression of helium line emission. This was not the case in the present experiment, because helium line emission remained constant even at low flow rates (Figure 3.10). Therefore we can tentatively conclude that the diffusion of air and water vapor into the plasma results in very low concentrations of nitrogen/oxygen molecules ($< 0.1\%$). At such low concentrations of air, reasonable densities of excited species can be reached, while

there is no unfavorable influence on the plasma. For optimal conditions of treatment, the concentration of reactive species should be maximized. This may be achieved by careful admission of low amounts of specific gases into the helium flow (in the 0.1% range) and also by reduction of helium flow rate, which leads to enhancement of the density of excited nitrogen species.

3.4 Conclusions

In this chapter, we described both optically and electrically the characteristics of the plasma needle in a new design. This design had recently been adjusted so that cell treatments need not have to be performed inside a box. A model was made to characterize the plasma needle impedance. Using this model, the discharge was found to be entirely resistive, ranging from 100 to 1200 kΩ. This allowed us to make an estimation of the electron density: 10^{17} m^{-3}. The electron density increased with increase in forward power until it saturated at about 2 W. At power levels above 2 W, the electron density remained relatively constant, whereas the size of the plasma increased.

Optical characterization was performed using emission spectroscopy. We found an abrupt increase of the emission intensity when the voltage at the needle was 160 V. This could indicate a transition into another plasma operation mode. In the low-voltage mode (140-160 V), the spectrum was dominated by N_2, N_2^+, OH· and O·, while at voltages higher than 160 V relatively more helium line emission was detected.
The presence of UV emission is an important factor in the treatment of biological materials, because of possible damage to cells. In our plasma, UV emission was found in the region between 250 and 400 nm, but the highest intensities were between 305 and 390 nm. At these wavelengths the damage to cells and tissues is limited [24].

The influence of the helium flow velocity was investigated for the purposes of cost saving and convenience of operation in small openings and on vulnerable tissues. A reduction of helium flow influenced the spectrum: nitrogen lines became much more prominent. This effect became significant when flow was reduced to below 0.8 l min^{-1}. A disadvantage of nitrogen admixture may be an increase in gas temperature due to the lower heat conductivity of N_2. The characterization of the needle allows a better control of the plasma source and helps to optimize plasma conditions in treatment of biological samples.

3.5 Acknowledgments

The authors thank Bart Broks for his useful comments. This research was supported by the Dutch Organization for Scientific Research (NWO).

References

[1] E. Stoffels, A. J. Flikweert, W. W. Stoffels, and G. M. W. Kroesen. Plasma needle: a non-destructive atmospheric plasma source for fine surface treatment of (bio)materials. *Plasma Sources Sci. Technol.*, 4:383–388, 2002.

[2] R. E. J Sladek, E. Stoffels, R. Walraven, P. J. A. Tielbeek, and R. Koolhoven. Plasma treatment of caries: a novel method in dentistry. *IEEE Trans. Plasma Sci.*, 32(4):1540–1543, 2004.

[3] I. E. Kieft, J. L. V. Broers, V. Caubet-Hilloutou, D. W. Slaaf, F. C. S. Ramaekers, and E. Stoffels. Electric discharge plasmas influence attachment of cultured CHO K1 cells. *Bioelectromagnetics*, 25:362–368, 2004.

[4] I. E. Kieft, J. J. B. N. v. Berkel, E. R. Kieft, and E. Stoffels. Radicals of plasma needle detected with fluorescent probe. *Plasma Processes Polym. , special issue after the 16th ISPC, Taormina*, pages 295–308, 2005.

[5] J. Janca, M. Klima, P. Slavicek, and I. Zajickova. HF plasma pencil - new source for plasma surface processing. *Surf. Coat. Technol.*, 116-119:547–551, 1999.

[6] J. Toshifuji, T. Katsumata, H. Takikawa, T. Sakakibara, and I. Shimizu. Cold arc-plasma jet under atmospheric pressure for surface modification. *Surf. Coat. Technol.*, 171(1-3):302–306, 2002.

[7] D. B. Ilic. Impedance measurement as a diagnostic for plasma reactors. *Rev. Sci. Instrum.*, 52(10):1542–1545, 1981.

[8] L. P. Bakker, G. M. W. Kroesen, and F. J. de Hoog. RF discharge impedance measurements using a new method to determine the stray impedances. *IEEE Trans. Plasma Sci.*, 27(3):759–765, 1999.

[9] K Kiyokawa, H Matsuoka, A Itou, K Hasegawa, and K Sugiyama. Decomposition of inorganic gases in an atmospheric pressure non-equilibrium plasma. *Surf. Coat. Technol.*, 112:25–28, 1999.

[10] E. A. H. Timmermans, J. Jonkers, I. A. J. Thomas, A. Rodero, M. C. Quintero, A. Sola, A. Gamero, and J. A. M. van der Mullen. The behavior of molecules in microwave-induced

plasmas studied by optical emission spectroscopy. 1. plasmas at atmospheric pressure. *Spectrochim. Acta B*, 53(11):1553–1566, 1998.

[11] Y-H Kim, Y-H Choi, J-H Kim, J-K Park, W-T Ju, K-H Paek, and Y-S Hwang. Characterisations of atmospheric pressure ejected plasma sources. *Surf. Coat. Technol.*, 174-175:535–540, 2003.

[12] E. Straface, P. Ulderico Giacomoni, and W. Malorni. Cultured cells as a model system for the study of UV-induced cytotoxicity. *J. Photochem. Photobiol. B*, 63(1-3):52–60, 2001.

[13] L. Proietti De Santis, C. Lorenti Garcia, A. S. Balajee, P. Latini, P. Pichierri, O. Nikaido, M. Stefanini, and F. Palitti. Transcription coupled repair efficiency determines the cell cycle progression and apoptosis after UV exposure in hamster cells. *DNA repair*, 1:209–223, 2002.

[14] Krishnaswamy Kannan and Sushil K. Jain. Oxidative stress and apoptosis. *Pathophysiology*, 7(3):153–163, 2000.

[15] J. C. Slater. *Microwave transmission.* Dover Publications, New York, 1959.

[16] Y. P. Raizer. *Gas discharge physics.* Springer, Berlin, 1991.

[17] J. Jonkers and J. A. M. Van der Mullen. The excitation temperature in (helium) plasmas. *J. Quant. Spectrosc. Radiat. Transfer*, 61(5):703–709, 1999.

[18] J. Jonkers. *Excitation and transport in small scale plasmas.* PhD thesis Eindhoven University of Technology, Eindhoven, 1998.

[19] J. Park, I. Henins, H. W. Herrmann, G. S. Selwyn, and R. F. Hicks. Discharge phenomena of an atmospheric pressure radio-frequency capacitive plasma source. *J. Appl. Phys.*, 89(1):20–28, 2001.

[20] Lide D.R. *Handbook of Chemistry and Physics.* CRC Press, Boca Raton, Fl, 2003.

[21] K. R. Foster. Thermal and nonthermal mechanisms of interaction of radio-frequency energy with biological systems. *IEEE Trans. Plasma Sci.*, 28(1):15–23, 2000.

[22] R. W. B. Pearse and A. G. Gaydon. *The identification of molecular spectra.* Chapman and Hall LTD, London, 1965.

[23] J. J. Shi, X. T. Deng, R Hall, J. D. Punnett, and M. G. Kong. Three modes in a radio frequency atmospheric pressure glow discharge. *J. Appl. Phys.*, 94(10):6303–6310, 2003.

[24] M. Laroussi and F. Leipold. Evaluation of the roles of reactive species, heat, and UV radiation in the inactivation of bacterial cells by air plasmas at atmospheric pressure. *Int. J. Mass Spectrom.*, 233(1-3):81–86, 2004.

Chapter 4

Radicals of plasma needle detected with fluorescent probe

Abstract
Non-thermal atmospheric plasmas can be used for fine treatment of heat-sensitive materials, including living cells and tissues. The newly developed "plasma needle" is capable of inducing sophisticated cell responses, which may become valuable in refined surgery. In our hypothesis, these effects are caused by interactions of plasma-produced radicals with the cell membrane and/or other cell components. Cells consist for the main part of water and are (especially *in vitro*) immersed in liquid. In this chapter we study the diffusion of radicals from the plasma into liquids.
Raman scattering experiments were performed to determine the gas composition in the plasma. A fluorescent probe (5-(and-6)-chloromethyl-2',7'- dichlorodihydro-fluorescein diacetate, acetyl ester by Molecular Probes® inc.) was used to detect reactive oxygen species in the liquid phase. This probe reacts with reactive oxygen radicals and the oxidation product displays fluorescence when irradiated with a laser. After plasma exposure, liquid samples were analyzed using a microplate fluorescence reader. In order to gain insight in the behavior of radicals under various plasma conditions, several parameters like plasma-to-liquid distance and plasma composition (O_2 content in the plasma) were varied. The absolute density in the liquid was estimated by calibration against NO radicals, produced by the NO releaser NOR-1. Furthermore, an estimation was made for the radical density in the gas phase. The usage of fluorescent probes allows a quantitative study of plasma radicals in liquids. The method is powerful and easy to use, and the obtained data are important to understand plasma effects on living cells.

This chapter was published as I.E.Kieft, J.J.B.N.van Berkel, E.R.Kieft, E. Stoffels, Radicals of plasma needle detected with fluorescent probe, *Plasma Processes Polym., special issue after the 16th ISPC, Tormina*, 295-308, 2005.

4.1 Introduction

Plasmas are widely used for industrial surface modification. In particular, atmospheric plasmas are becoming increasingly popular, because of their flexibility, convenience and low costs. Recently, non-thermal atmospheric plasmas have been developed for treatment (cleaning, sterilization) of heat-sensitive materials [1, 2]. In principle, such plasmas can be applied *in vivo* for disinfection or local removal of diseased tissues.
Chemically reactive species, and especially short-lived radicals are of major importance in any surface treatment. For example, the efficiency of bacterial decontamination is conditioned by reactive oxygen species (ROS), produced in the plasma [3]. According to Laroussi [2], free radicals are the most important sterilizing agent in atmospheric-pressure plasmas. Apart from bacteria, the responses of living cells and tissues are also dependent on the plasma chemistry. For specific cell treatment, a non-thermal microplasma ("plasma needle") has been developed [4]. *In vitro* experiments have already shown that the plasma needle can trigger complex cell reactions [5, 6]. Depending on plasma conditions, the treated cells can detach from each other and from the surface, or undergo apoptosis (programmed cell death). The mechanisms behind these responses are not yet completely understood, but we suspect that active radicals are responsible for the majority of the observed effects.
As in any medical therapy, plasma-produced species can play a double role. Moderate amounts of reactive oxygen species have a beneficial working, but an overdose leads to cell injury. Oxygen species react with and damage cell building blocks like lipids, proteins and DNA strands [7–9]. Montie *et al* [10] suggest that membrane lipids may be most vulnerable to reactive oxygen species attack, because of their location near the cell surface, and their sensitivity to oxidation. Severe oxidative stress causes cell injury and accidental cell death (necrosis), while mild oxidative stress leads to apoptosis [11]. A small imbalance in oxidant/antioxidant regulation can result in adaptation of the cells to the new environment. Adaptation of cells is realized through changes in the gene expression, so that the cells are capable of surviving in a hostile environment.

Regarding the importance of reactive oxygen species for cell condition, it is essential to study the diffusion of radicals from the plasma into the liquid phase. In this chapter we determined the densities of active species in a buffered solution that was exposed to the plasma. For these experiments we used the plasma needle: an RF discharge generated at the end of a metal pin. The main species in the plasma is helium. However, since it operates in open air at ambient pressure, some air admixture is always present. Thus, oxygen- and nitrogen-based active species like atomic oxygen, the metastable singlet state of molecular oxygen (O_2(a)), ozone, NO and NO_X are formed in the plasma. Due to air moisture, OH and HO_2 can be produced.

There are many methods to determine radical densities in the gas phase, e.g. laser induced fluorescence (LIF) [12], broad-band UV absorption spectroscopy [13] and the cavity ring-down technique [14, 15]. For radical detection in liquids laser-induced fluorescence in combination with fluorescent probes can be used: an easy and convenient method that is very popular in cell biology [16–19]. In this work we introduce LIF with a fluorescent probe as a new, powerful plasma diagnostics. This method is recommended for determining fluxes of radicals from atmospheric plasmas, concentrations of active species in plasma-treated fluids and gels, for dynamic studies of the plasma/liquid interface, and for many other applications.

4.2 Experimental

4.2.1 Plasma needle

The plasma was generated at the end of a sharp metal pin electrode (needle), to which 13.56 MHz radio frequency (RF) voltage was applied (Figure 4.1). The needle had a diameter of 0.3 mm and was about 10 cm long. It was inserted in a Perspex tube with inner diameter 0.8 cm. A helium flow of 2 l min^{-1}, regulated by a mass flow controller of Brooks series 5850E, was directed through the tube.

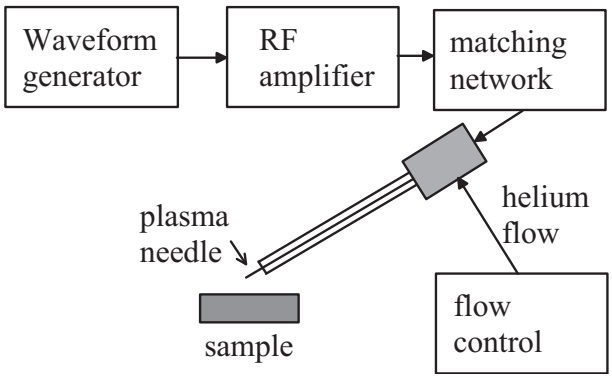

Figure 4.1: *A scheme of the setup. Radio-frequency voltage generated by a function generator is amplified, impedance-matched and applied to the hand-operated plasma needle (a metal pin). Helium is supplied to the needle by a Perspex tube.*

For the plasma generation a Hewlett Packard 33120A waveform generator and an Amplifier Research 75AP250RF RF amplifier were used. The power was monitored using a dual directional coupler and an Amplifier Research PM 2002 power meter. The power dissipated

in the plasma was below 100 mW. The effective voltage at the needle was about 200 V. The typical size of the plasma glow was below 1 mm. However, when the plasma was in contact with (water) surface, the glow expanded slightly so that the typical size of the treated spot was 1 mm^2.

The position of the needle in the Perspex tube could be varied by moving the tube along the axis of the needle (Figure 4.2). Normally, the tip of the needle and the end of the tube were at the same position, but the needle could also protrude from the tube up to 1 cm. In the latter case, more air was admixed in the plasma.

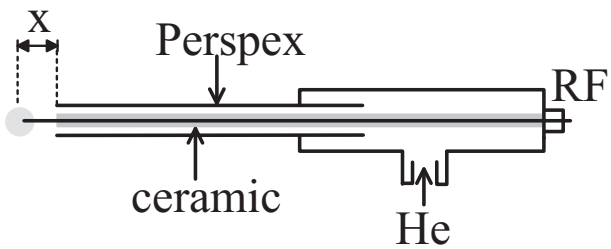

Figure 4.2: *A drawing of the plasma needle. The position of the needle to the end of the Perspex tube can be varied as is indicated in the figure by x.*

4.2.2 Raman scattering

Raman scattering experiments were performed to determine the gas composition. Raman scattering is an inelastic photon scattering on molecules. Typically, laser photons in the visible region are used for irradiation. Their interaction with the molecule induces a vibrational/rotational transition, so the scattered photons display a small wavelength shift corresponding to the energy of the transition. A Raman spectrum consists of lines that are fingerprints of various molecules (e.g. O_2, N_2 and H_2O in air) and it can be used to quantitatively determine the composition of gas mixtures. Here we determined the air content in our plasma by recording Raman spectra in helium/air flow, and comparing them to pure air spectra. First, the spectra were integrated over wavelength, then the helium/air flow values were divided by the pure air value. Measurements with and without plasma were performed to check the plasma influence on the gas composition.

We used the setup developed by Van de Sande [20]. The system was equipped with an Nd:YAG type laser (frequency doubled, $\lambda = 532$ nm, pulse length 7 ns, pulse repetition rate 10 Hz), focused with a 30-cm lens. Spectra were taken with an intensified charge coupled device (CCD) camera. Spectra were collected for 300 s per measurement. The

plasma needle was fixed vertically above a grounded metal plate (at the distance 2 mm). In the horizontal plane, the laser focal point was coincident with the needle tip, and in the vertical direction it was positioned at a distance of 1 mm below the tip. One-dimensional scans in the horizontal direction were taken.

4.2.3 Fluorescent probe

To detect reactive oxygen species that were formed in the plasma we used a molecular probe, called 5-(and-6)-chloromethyl-2',7'- dichlorodihydrofluorescein diacetate, acetyl ester (CM-H_2DCFDA). From the literature it is known that it can be used as an indicator of reactive oxygen species formation and oxidative stress [16]. Upon reaction with oxygen-containing reactive species, the probe is oxidized in such a way that a large multiple-conjugated double bond with a high degree of stability is formed (Figure 4.3). This double bond is also responsible for the fluorescent properties.

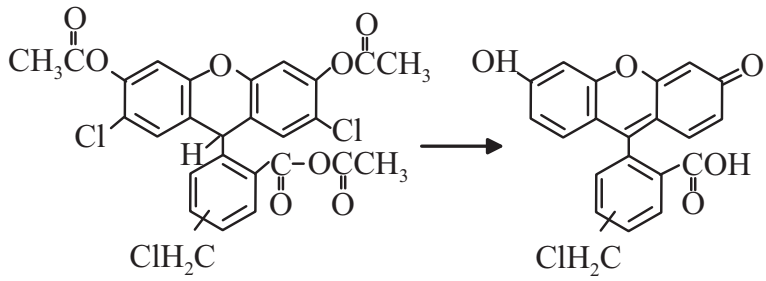

Figure 4.3: *The chemical structure of $CM - H_2DCFDA$ before (left) and after (right) reaction with reactive species. The acetate groups are removed by incubation in an alkaline solution.*

The probe was delivered by Molecular Probes®. It was guaranteed to react with at least the following reactive oxygen species: H_2O_2, OH·, HOO·, and $ONOO^-$. The package contained 50x10^{-6} g probe (8.653x10^{-8} mol). The content was dissolved in 100 μl dimethylsulfoxid (DMSO, > 99%, Merck). Then, 1 ml of 0.01 M solution of NaOH (99.99%, Aldrich Chem. Co.) was added to activate the probe. The solution was incubated for 30 min at room temperature and afterwards diluted to 10.81 ml with phosphate-buffered saline (PBS, Sigma-Aldrich Co.), resulting in a probe concentration of 8 μM. The PBS solution (pH 7.4 at room temperature) was a 0.01 M phosphate buffer with 0.0027 M potassium chloride, and 0.137 M sodium chloride. The probe is sensitive to light, so the solution was covered with aluminum foil and placed in a refrigerator. For the experiments a concentration of 1 μM was used.

The samples were prepared in 96-wells plates with a flat bottom of Nucleon Surface. After

plasma exposure, they were examined with a Microplate Fluorescence Reader FL600 of Bio-Tek. The oxidized CM-H_2DCFDA probe was irradiated by a quartz halogen lamp (P/N 6000556S) light source in combination with a 485/20X excitation filter (wavelength about 485 nm). Fluorescent emission was collected at about 530 nm using a 530/25M filter.

4.2.4 Calibration with NO radicals

To obtain quantitative data, the probe was calibrated using NO radicals, produced by NOR-1 (Sigma-Aldrich Co.), an NO releaser. From the work of Ueki *et al* [21] it is known that NOR-1 can be used as a standard for absolute measurements of low NO densities. They showed that NOR-1 releases a 1.4 excess of NO after 15 min of incubation, so [NO] = 1.4 [NOR-1]. The CM-H_2DCFDA probe may react directly with NO, or with its autoxidation derivatives like N_2O_3 or NO_2^- [17, 22].

The efficiency of the CM-H_2DCFDA probe to react with NO released by NOR-1 was tested by performing two experiments. In both experiments small amounts (10 to 100 μl) of the NO releaser NOR-1 in DMSO were dissolved in an Eppendorf tube containing 1 ml PBS with the CM-H_2DCFDA probe in varying concentrations. The tubes were incubated for 15 min at room temperature. Then 100 μl of the solutions were put in a 96-wells plate and data were collected with the microplate fluorescence reader.

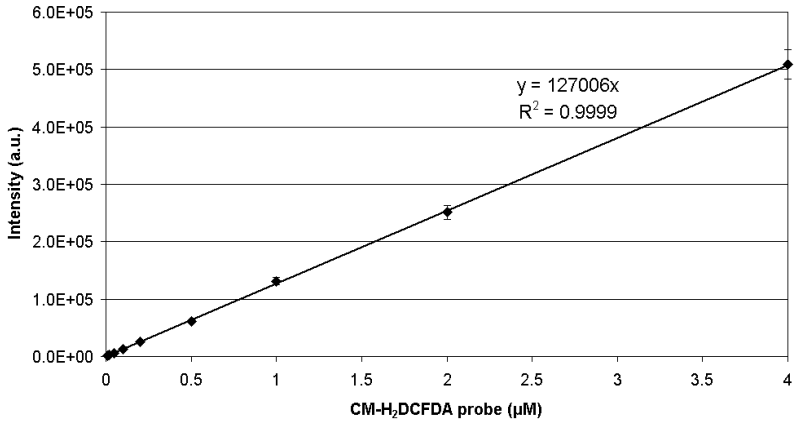

Figure 4.4: *Intensity of $CM - H_2DCFDA$ probe after reaction with an overload of NO (1 mM). The probe is maximally activated.*

In the first experiment (Figure 4.4) an excess of NO was administered to different concentrations of the probe. This yielded a linear curve (R^2 = 0.9999) for the maximum

intensity emitted by the probe, of which all molecules were activated. In the second experiment different concentrations of NO were added to the probe (concentration of 1 μM). The calibration curve (fluorescent intensity vs. NO concentration) showed that for NO concentrations below 10 μM the relation was linear (Figure 4.5). At higher concentrations the probe was slightly saturated, which caused the curve to flatten. We can now compare the two figures by looking, for example, at the intensity of the 1 μM probe (Figure 4.5) activated by addition of 5 μM NO; this gave 31 000 counts. The same intensity (31 000 counts) was reached by illumination of 0.25 μM fully activated probe. This means that about 5% of the NO molecules reacted with the probe.

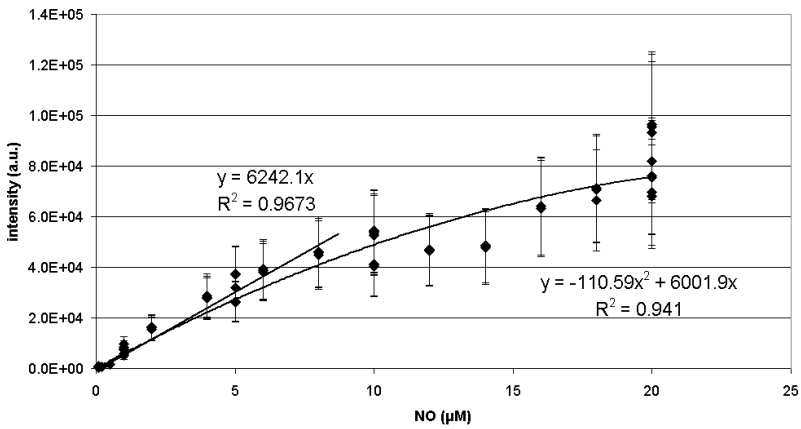

Figure 4.5: *Intensity of $CM - H_2DCFDA$ probe (concentration 1 μM) after reaction with NO from the NO-releaser. Figure shows two trend lines, the line fitted for concentration below 10 μM, and the polynomial curve fitted for all data points.*

The radicals from the plasma were taken to have the same reactivity in this setup towards the probe as NO radicals. Reaction rates of this specific probe with plasma radicals (reactive oxygen species) are not given in the literature. Rate constants for reactions of inorganic radicals with organic compounds in aqueous solutions range roughly from 10^6 to 10^{10} l mol^{-1} s^{-1} [23–25]. The reactions rates of OH and O are mostly one or two orders higher than the reaction rates of NO. The calibration with NO then serves as an upper limit for the radical concentration. The lower limit is set by Figure 4.4: In an ideal one-to-one reaction of radicals with probe molecules there need to be at least the number of radicals equal to the number of probe molecules to reach a certain fluorescence intensity. This minimum number of radicals can be derived from Figure 4.4 and is a factor 20 lower than the number derived from calibration to NO.

In our setup the probe is the only reactive organic molecule in the liquid (not including

reactions at the wall). It will efficiently capture any radical, independent of the actual reaction rate. The calibration against NO is thus valid in aqueous solutions with only inorganic species. In a real biological sample the situation may be somewhat different: the reactivity of the hydroxyl radical or atomic oxygen towards most organic compounds is higher than that of NO [23], while this of ozone is lower. This means that, e.g., cell damage inflicted by oxygen radicals is higher than the one caused by nitric oxide at the same concentration level. Thus, we must keep in mind that the concentration of ROS deduced from NO calibration is merely an indication for the "oxidizing activity" of the plasma.

4.2.5 Plasma treatment

400 μl of fresh probe solution was treated with the plasma. Unless mentioned otherwise, the samples were treated for 2 min, with a distance of the tip of the needle to the liquid surface of about 1 mm and the tip of needle at the same position as the end of the Perspex tube. After plasma treatment an antioxidant was added to the solution to prevent further oxidation of the probe by air. Vitamin C or L-Ascorbic acid is known to be a very efficient, water soluble antioxidant [26]. In the experiments 10 μl of 10 mM solution L-Ascorbic acid was used. The antioxidant was tested by incubation of the untreated probe solution of 1 μM in open air at room temperature. When ascorbic acid with a concentration of 100 μM was used, a small increase in fluorescence intensity of about 10% was observed after 40 min. When the concentration was increased to 1 mM, no increase of intensity could be detected within half an hour. The samples protected in this way could be kept in the refrigerator even up to 24 h, but we analyzed them immediately after plasma treatment. The samples were divided into 100 μl portions, and transferred to the plate reader for data collection. 100 μl of untreated probe solution was used for background subtraction.

4.3 Results and discussion

4.3.1 Raman scattering

Raman scattering measurements were performed to determine the admixture of molecular species in the helium gas flow. In the series presented below the Perspex tube surrounding the needle was pushed back (the distance x in Fig. 4.2 was varied), exposing the tip of the needle and thus allowing more air admixture. From the Raman spectra (Figure 4.6) it was established that the percentage of air in helium in the middle of the plasma (in the closest vicinity of the needle tip) was below 0.5%. It was actually below the detection limit of the method, so it was difficult to observe any changes when the needle became more

or less exposed. However, it can be seen that at the sides of the needle the air admixture increased up to 25% in the case of 5-mm distance between the tip of the electrode and the tube. The gradients of air concentration towards the middle also became higher, and therefore the influx of air into the active plasma zone was increased. Raman spectra that were recorded for the same helium flow but in presence of the plasma did not significantly differ from spectra taken without plasma.

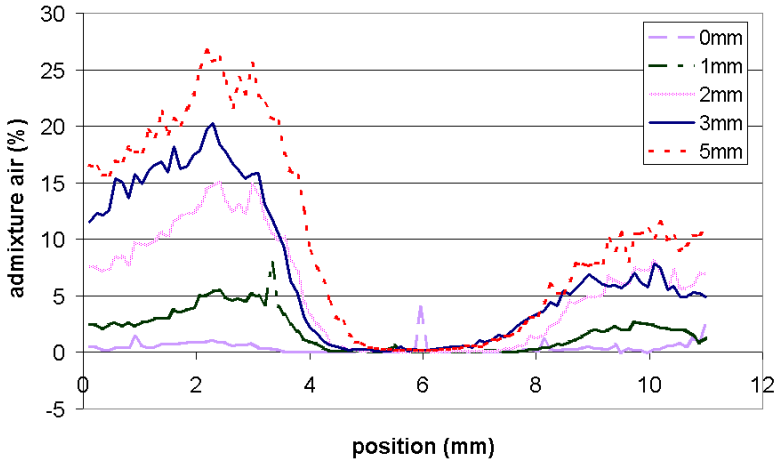

Figure 4.6: *Air admixture determined from Raman spectra of the helium flow from the Perspex tube without plasma. The horizontal position at 6 mm coincides with the tip of the needle; the laser is shot 1 mm below. Different curves correspond to the length of the exposed part of the plasma pin from the Perspex tube (x in Fig. 4.2). The sensitivity of the detection system decreases at peripheral positions due to alignment.*

Raman scattering measurements were performed in a configuration with a grounded metal plate opposite to the plasma needle. During plasma treatment of cells or tissues this plate was replaced by a biological sample. This could in principle have an influence on plasma chemistry and/or gas composition, due to, for example, different conductivity of the sample and the metal plate. However, such small differences cannot be visualized using the Raman scattering technique. The Raman data can be used to estimate air concentration/influx, but not to study the molecular composition of the plasma.

4.3.2 The fluorescent probe measurements

CM-H_2DCFDA was tested by applying the plasma to the probe solution, while the sample was scanned with a confocal laser scanning microscope (Figure 4.7). In this way a time

series was recorded, which allowed visualization of probe activation (fluorescence) within seconds after the onset of the plasma. Although the CM-H_2DCFDA probe is sensitive to light, the laser power was too low and irradiation time was too short to affect the fluorescence significantly.

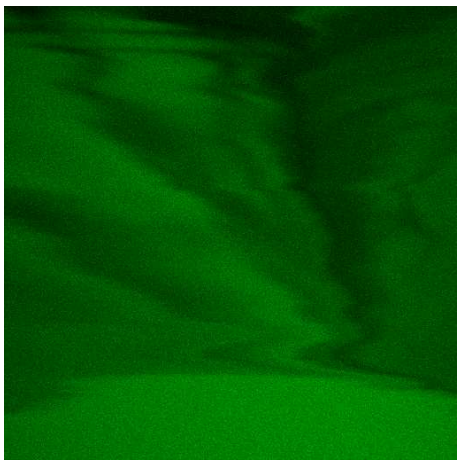

Figure 4.7: *Fluorescence emitted by $CM - H_2DCFDA$ probe during plasma treatment. Plasma was applied at the left hand side of the picture (size 0.92 x 0.92 mm). Bright color indicates higher fluorescence intensity.*

The real-time measurements revealed flow patterns in the solution, induced by the flow of helium from the plasma. These space- and time-varying fluorescent intensity patterns can be used to determine the dynamical behavior of radicals in the liquid. However, in this work we analyzed only the space-averaged intensities collected from a certain volume of liquid, treated by the plasma.

The radical concentration as a function of plasma treatment duration is depicted in Figure 4.8. As expected, a linear dependence up to 8 min was found. At longer treatment times the method was less reliable, because the probe might become saturated. From these data the number of radicals in the plasma was estimated. The radicals diffusing into 400 μl of liquid produced an oxidized probe solution after one minute of treatment that was comparable to 0.65 ± 0.2 μM NO. The number of radicals reaching the liquid was then 2.6x10^{12} s^{-1}. For the calculation of the radical density in the plasma using Equation 4.1 and 4.2 [27], we take the thermal velocity $v_{\mathrm{th}} = 300$ m s^{-1}, the surface through which radicals are transferred $A = 1$ mm^2 (the size of the plasma spot), gradient length $\lambda = 0.1$ mm (estimated plasma sheath thickness at the water surface) and mean free path $l_{\mathrm{fr}} = 10^{-5}$ m.

$$\Phi_{\mathrm{rad}} = n_{\mathrm{rad}} \cdot D \cdot A \cdot \lambda^{-1} \tag{4.1}$$

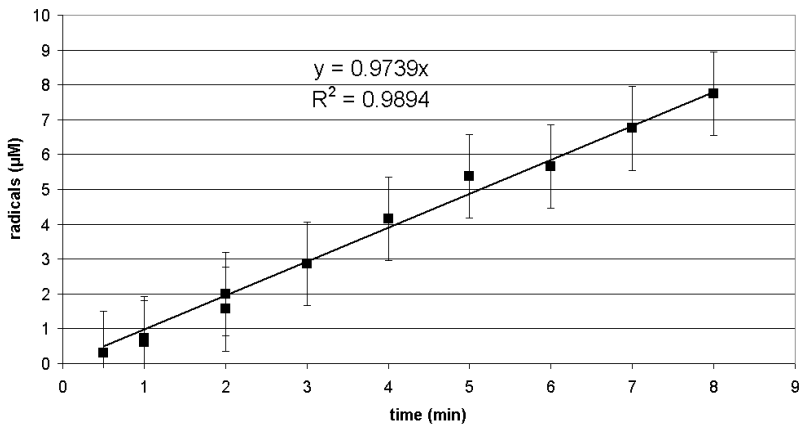

Figure 4.8: *The radical density in liquid, resulting from plasma treatment as a function of treatment time. The x-position was 0 mm, the needle-to-surface distance was 1 mm. The radical density was measured using the fluorescence from the CM-H_2DCFDA probe, and calibrated using a known NO concentration.*

$$D = \frac{1}{3} \cdot v_{\mathrm{th}} \cdot l_{\mathrm{fr}} \tag{4.2}$$

This estimation yields $n_{\mathrm{rad}} = 10^{19}$ m^{-3}, which is a reasonable value, noting that the admixture of air into the plasma was low (see the Raman scattering data).

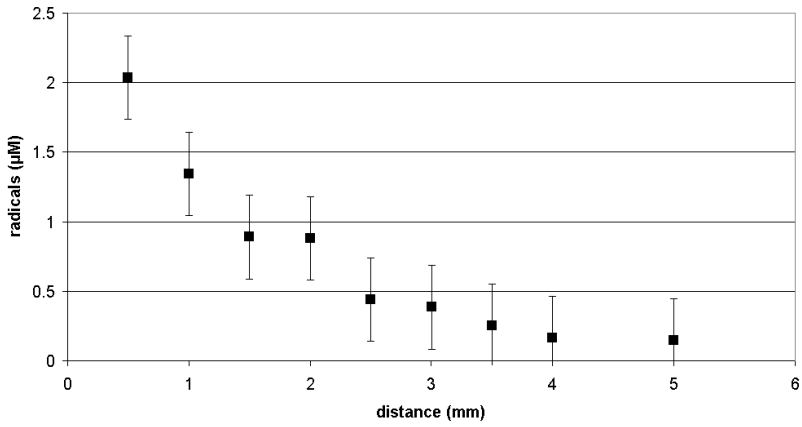

Figure 4.9: *The radical concentration as a function of distance from the tip of the needle to the surface of the liquid. The treatment time was 2 min, the x-position was 0 mm.*

In order to study the propagation of radicals in the gas phase (before they reach the fluid sample), we varied the distance between the tip of the needle and the surface of the liquid. A power fit of the data (the R^2 of the fit is 0.92) shows that the density decreased

with distance approximately as 1.2 power of 1/d, where d is the distance (Figure 9). This is weaker than the $1/d^2$, expected for homogeneous spatial expansion from the point-like source (glow). This means that at short distances the liquid preferentially absorbs the plasma species. Visually, we observed that at distances of about 1 mm the plasma was attracted to grounded objects, the glow expanded and a thin dark sheath at the object's surface was visible. As the needle was moved away, the glow remained confined in the closes vicinity of the pin. This occurred at distances larger than 2 mm.

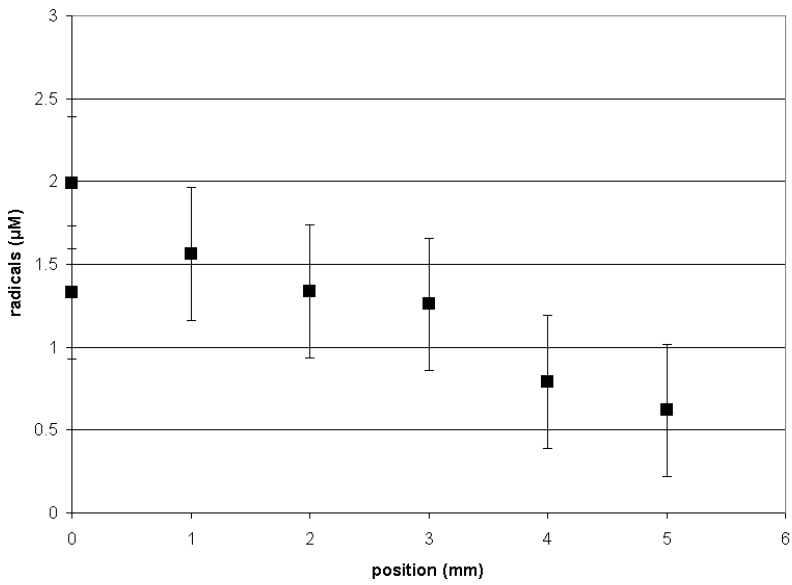

Figure 4.10: *The radical concentration as a function of the position of the tip of the needle with respect to the end of the Perspex tube (x-position in Figure 2). The treatment time was 2 min, the needle-to-surface distance was 1 mm.*

In another experiment we changed the plasma composition, to check its influence on the amount of produced radicals. First, we determined the radical densities for different positions of the tip of the needle with respect to the end of the Perspex tube (x-distance in Fig. 4.2). As observed during Raman scattering experiments, the longer the exposed part of the pin (outside the tube), the higher the air influx into the plasma. However, the number of radicals decreased as the needle was pushed further out of the tube (Figure 4.10), even though at the same time the influx of molecular species into helium increased. This can be explained by the unfavorable effect of oxygen and nitrogen on the plasma. Both of them cause dissipation of the electron energy due to vibrational and rotational excitation. Moreover, oxygen is electronegative, and its presence creates a sink for plasma electrons due to negative ion formation. This means that at the same power level, less energy is

available for the production of active radicals when air content in the plasma is high. This decrease of plasma activity is also evident from visual observation: the glow shrinks and the emission intensity decreases. This situation can be to some extent compensated by increasing the voltage (power), but then the glow-to-arc transition may take place and the plasma becomes difficult to control [4].

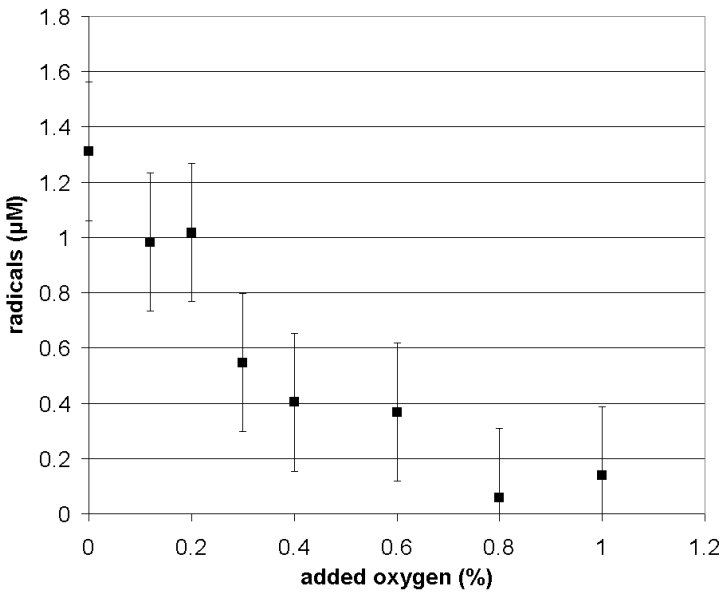

Figure 4.11: *The radical concentration as a function of oxygen admixture into helium flow. The treatment time was 2 min, the x-position was 0 mm, the needle-to-surface distance was 1 mm.*

In another experiment we measured the radical densities as a function of oxygen admixture in the plasma. From the Raman spectrum we deduced that the amount of oxygen at the position of the needle was normally well below 0.1%. By adding pure O_2 into the helium flow we observed that even an addition as small as 0.2% caused the plasma to shrink significantly; the color of plasma emission changed from pink to white. The radical density (Figure 4.11) also decreased as a function of oxygen admixture. As in the previous experiment (Figure 4.10), this can be explained by the influence of O_2 on the plasma: electron attachment causes depletion of plasma electrons and decrease of plasma activity.

At the present stage we cannot decide whether the concentration of radicals in the liquid is appropriate for the treatment of living tissues. This has to be defined in advanced *in vivo* experiments, and is also dependent on the desired effect of the therapy. In the biological studies on oxidative stress the exact concentrations are seldom mentioned. However, we can state that plasma does not produce dangerously high reactive oxygen species concen-

trations in the liquid phase. In fact, the amount of reactive oxygen species is comparable to that produced by the body itself, e.g. to fight bacterial infection or during increased metabolism. Radical concentrations found *in vivo* are in micromolar range. In high concentrations (0.5 mM) radicals may induce both necrotic and apoptotic cell death [28]. This is at least a factor 10 higher than the concentration that was found for plasma radicals. The inaccuracy in the calibration measurements for the radical concentrations is within the right proportions to draw the conclusion that the mild oxidative properties of the plasma may have a beneficial effect on the tissue (e.g. sterilizing or increasing the cell activity). This is in agreement with previous experiments on living cells, in which we established that plasma treatment usually did not kill the cells.

4.4 Conclusions

The use of a fluorescent probe for radical detection has proven to be a valuable method in plasma diagnostics. It can be used in any atmospheric and non-thermal plasma, and it gives information about the radical fluxes towards the surface. These data are useful in monitoring the plasma performance in surface processing (etching, cleaning, chemical and biological decontamination). In this work we tested this method using the plasma needle and a probe for detection of reactive oxygen species. The radicals from the plasma had sufficiently long lifetimes to reach the solution and bind with the probe. The radical flux into the liquid was 10^{12} s^{-1}; the radical density in the plasma was estimated to be 10^{19} m^{-3}. The radical density decreased with increasing distance from the needle. Addition of extra oxygen or air decreased the plasma activity and resulted in lower radical concentrations. For optimal reactivity, the plasma should be kept within 2 mm from the surface that is to be treated, and the air content should not be higher than 0.5%.

The reactive plasma species dissolve in the liquid and reach living cells that are cultured on the bottom of the wells-plate. The radicals generate oxidative stress that in principle is harmful, but at low radical concentrations the interactions with cells can have beneficial effects. The radical concentrations in liquid phase, generated by the plasma needle, are only in the order of μM, and we observe that under normal conditions plasma does not cause cell death.

References

[1] J. Park, I. Henins, H. W. Herrmann, G. S. Selwyn, and R. F. Hicks. Discharge phenomena of an atmospheric pressure radio-frequency capacitive plasma source. *J. Appl. Phys.*, 89(1):20–28, 2001.

[2] M. Laroussi. Nonthermal decontamination of biological media by atmospheric-pressure plasmas: review, analysis, and prospects. *IEEE Trans. Plasma Sci.*, 30(4):1409–1415, 2002.

[3] M. Moisan, J. Barbeau, S. Moreau, J. Pelletier, M. Tabrizian, and L. H. Yahia. Low-temperature sterilization using gas plasmas: a review of the experiments and an analysis of the inactivation mechanisms. *Int. J. Pharmac.*, 226(1-2):1–21, 2001.

[4] E. Stoffels, A. J. Flikweert, W. W. Stoffels, and G. M. W. Kroesen. Plasma needle: a non-destructive atmospheric plasma source for fine surface treatment of (bio)materials. *Plasma Sources Sci. Technol.*, 4:383–388, 2002.

[5] E. Stoffels, I. E. Kieft, and R. E. J Sladek. Superficial treatment of mammalian cells using plasma needle. *J. Phys. D: Appl. Phys.*, 36:2908–2913, 2003.

[6] I. E. Kieft, J. L. V. Broers, V. Caubet-Hilloutou, D. W. Slaaf, F. C. S. Ramaekers, and E. Stoffels. Electric discharge plasmas influence attachment of cultured CHO K1 cells. *Bioelectromagnetics*, 25:362–368, 2004.

[7] Thomas M. Buttke and Paul A. Sandstrom. Oxidative stress as a mediator of apoptosis. *Immunol. Today*, 15(1):7–10, 1994.

[8] K. M. Anderson, T. Seed, D. Ou, and J. E. Harris. Free radicals and reactive oxygen species in programmed cell death. *Med. Hypoth.*, 52(5):451–463, 1999.

[9] Barry Halliwell and John M. C. Gutteridge. *Free radicals in biology and medicine.* Oxford University Press, New York, 1999.

[10] T. C. Montie, K. Kelly-Wintenberg, and J. R. Roth. An overview of research using the one atmosphere uniform glow discharge plasma (OAUGDP) for sterilization of surfaces and materials. *IEEE Trans. Plasma Sci.*, 28(1):41–50, 2000.

[11] Simon H.-U., A. Haj-Yehia, and F. Levi-Schaffer. Role of reactive oxygen species (ROS) in apoptosis induction. *Apoptosis*, 5 (5):415–418, 2000.

[12] S. Hayashi, K. Kawashima, N. Ozawa, H. Tsuboi, T. Tatsumi, and M. Sekine. Studies of CF2 radical and O atom in oxygen/fluorocarbon plasmas by laser-induced fluorescence. *Sci. Tech. Adv. Mater.*, 2:555–561, 2001.

[13] J. P. Booth, G. Cunge, L. Biennier, D. Romanini, and A. Kachanov. Ultraviolet cavity ring-down spectroscopy of free radicals in etching plasmas. *Chem. Phys. Lett.*, 317:631–636, 2000.

[14] J. Benedikt, R. V. Woen, S. L. M. van Mensfoort, V. Perina, J. Hong, and M. C. M. van de Sanden. Plasma chemistry during the deposition of a-C:H films and its influence on film properties. *Diamond Relat. Mater.*, 12:90–97, 2003.

[15] J. P. M. Hoefnagels, A. A. E. Stevens, M. G. H. Boogaerts, W. M. M. Kessels, and M. C. M. van de Sanden. Time-resolved cavity ring-down spectroscopy study of the gas phase and surface loss rates of Si and SiH3 plasma radicals. *Chem. Phys. Lett.*, 360:189–193, 2002.

[16] C. P. LeBel, H. Ischiropoulos, and S. C. Bondy. Evaluation of the probe 2',7'-dicholorofluorescin as an indicator of reactive oxygen species formation and oxidative stress. *Chem. Res. Toxicol.*, 5:227–231, 1992.

[17] H. Kojima, Y Urano, K Kikuchi, T Higuchi, Y Hirata, and T Nagano. Fluorescent indicators for imaging nitric oxide production. *Angew. Chem. Int. Ed.*, 38(21):3209–3212, 1999.

[18] R. Cathcart, E. Schwiers, and B. N. Ames. Detection of picomole levels of hydroperoxides using a fluorescent dichlorofluorescein assay. *Anal. Biochem.*, 134:111–116, 1983.

[19] B. Li, P. L. Gutierrez, and N. V. Blough. Trace determination of hydroxyl radical in biological systems. *Anal. Chem.*, 69:4295–4302, 1997.

[20] M. J. van de Sande. *Laser scattering on low temperature plasmas.* PhD thesis, Eindhoven University of Technology, Eindhoven, 2002.

[21] Y Ueki, H Nakamura, K Matsumoto, T Tominaga, S Miyake, Y Kita, Y Katayama, S Fukuyama, Y Hirasawa, K Yoshida, and K Eguchi. NOR-1: a nitric oxide releasing agent for calibrating low levels of nitric oxide by the chemiluminescence method. *Blood Coag. Fibrinolysis*, 13(2):75–80, 2002.

[22] Peter C. Ford, David A. Wink, and David M. Stanbury. Autoxidation kinetics of aqueous nitric oxide. *FEBS Letters*, 326(1-3):1–3, 1993.

[23] P. Neta, R. E. Huie, and A. B. Ross. Rate constants for reactions of inorganic radicals in aqueous solution. *J. Phys. Chem. Ref. Data*, 17:1027–1284, 1988.

[24] N. C. Baird. Free radical reactions in aqueous solutions: examples from advanced oxidation processes for wastewater and from the chemistry in airborne water droplets. *J. Chem. Educ.*, 74(7):817–819, 1997.

[25] D. R. Grymonpre, A. K. Sharma, W. C. Finney, and B. R. Locke. The role of Fenton's reaction in aqueous phase pulsed streamer corona reactors. *Chem. Eng. J.*, 82:189–207, 2001.

[26] I Platzer and N. Getoff. Vitamin C acts as radiation-protecting agent. *Radiat. Phys. Chem.*, 51(1):73–76, 1998.

[27] T. I. Gombosi. *Gaskinetic theory.* Cambridge University Press, Cambridge, 1994.

[28] T Andoh, S. Y. Lee, and C. C. Chiueh. Preconditioning regulation of bcl-2 and p66shc by human NOS1 enhances tolerance to oxidative stress. *FASEB*, 14:2144–2146, 2000.

Chapter 5

Electric Discharge Plasmas Influence Attachment of Cultured Cells

Abstract
Non-thermal plasmas can be generated by electric discharges in gases. These plasmas are reactive media, capable of superficial treatment of various materials. A novel non-thermal atmospheric plasma source (plasma needle) has been developed and tested. Plasma appears at the end of a metal pin as a submillimetre glow.
We investigate the possibility to apply plasma needle directly to living tissues; the final goal is controlled cell treatment in microsurgery. To resolve plasma effects on cells, we study cultured Chinese hamster ovarian cells (CHO-K1) as a model system. When these are exposed to the plasma, instantaneous detachment of cells from the surface and loss of cell-cell interaction is observed. This occurs in the power range 0.1 - 0.2 W. Cell viability is assessed using propidium iodide (PI) and cell tracker green (CTG) fluorescent staining utilizing confocal laser scanning microscopy (CLSM). Detached cells remain alive. Use of higher doses (plasma power > 0.2 W) results in cell necrosis. In all cases, plasma-influenced cells are strictly localized in submillimetre areas, while no reaction in surrounding cells is observed. Due to its extreme precision, plasma treatment may be applicable in refined tissue modification.

This chapter is based on two publications: I.E.Kieft, J.L.V. Broers, V. Caubet-Hilloutou, D.W. Slaaf, F.C.S. Ramaekers, and E. Stoffels, Electric Discharge Plasmas Influence Attachment of Cultured CHO K1 cells, *Bioelectromagnetics*, 25:362-368, 2004 and I.E.Kieft , N.A. Dvinskikh, J.L.V. Broers, D.W. Slaaf, E. Stoffels, Effect of plasma needle on cultured cells, *Spie Proc.*, 5483:247-251, 2004.

5.1 Introduction

5.1.1 Plasma Application

Plasma is a partially ionized gas, containing electrons, positive/negative ions, radicals, and various excited atoms and molecules. Plasma generated by an electric discharge can be non-thermal: electrons present in this active medium are highly energetic, with typical temperatures above 10 000 K, while ions and neutral species remain at (almost) room temperature. Such a non-equilibrium situation is achieved when only electrons are electrically heated. This is common in high frequency driven discharges, e.g., in the radio frequency (MHz), or microwave (GHz) range, because in these systems only light and mobile electrons are able to follow rapidly oscillating electric fields. Energy transfer from electrons to heavy atoms and molecules is an inefficient process, so that the background gas remains relatively cold (< 1000 K). The best known example is a low pressure plasma, sustained in a vacuum reactor. Non-thermal discharges can be also obtained at atmospheric pressure [1]. When the size of the discharge is below 1 mm, energy leaks by thermal diffusion prevent gas heating. A combination of two physical principles: high frequency excitation and spatial constriction of the discharge, has recently resulted in the development of a novel non-thermal atmospheric plasma source, the "plasma needle" [2].
Due to their unique reactivity and chemical interactions with surfaces, non-thermal plasmas are capable of virtually any surface treatment. Plasma etching, thin layer deposition, cleaning, and activation of surfaces are well established techniques in material science. Recently, plasmas are also applied in biomedical technology, e.g., in plasma coating of artificial implants to increase their biocompatibility [3], surface micropatterning of scaffolds to achieve controlled cell adhesion [4], and bacterial decontamination of medical/surgical equipment [1, 5]. The effects of plasma treatment on microorganisms under lethal and sublethal doses have been studied by Laroussi *et al* [6].

For interactions with living tissues, the choice of an adequate plasma source is crucial. It must operate under atmospheric pressure, be electrically and chemically safe and may not cause any thermal damage to the living object. Most hitherto developed sources, although non-thermal, are still too hot or aggressive to be applied *in vivo*.

In this chapter, we shall demonstrate that the plasma needle is suitable for treatment of biological materials. Our aim is to introduce this source as a novel tool for high precision treatment of pathological tissues. Desired effects are controlled cell removal without inflammatory reaction and damage to the surrounding (healthy) tissue, and possibly inducing apoptosis. At present, we conduct a fundamental study to identify and elucidate various cell responses. First, we perform temperature measurements to establish that plasma

needle does not inflict thermal damage. Plasma-cell interactions are investigated using Chinese hamster ovarian cells (CHO-K1, ATCC number CCL-61). The specific apoptosis tests were performed on nonsmall cell lung cancer (NSCLC) cell line MR65 (Philips Universitats Klinik, Germany).These cells make a good model system for a study of basic cell responses to a medium, which up till now has been unknown to living objects.

5.2 Experimental methods

5.2.1 Principle of Plasma Operation

The discharge type was an atmospheric radio frequency (RF) glow. In case of RF excitation, an active plasma zone is created only at the powered electrode, i.e., the electrode to which RF voltage is applied. A bipolar (two electrode) configuration is not necessary. In our arrangement, the powered electrode was a metal wire. The (remote) surroundings, like the walls of the plasma box, act as the counter electrode (ground). In this type of discharges, voltage fall occurs in the closest vicinity of the powered electrode; in the outer plasma zones, which make contact with samples, only small rest electric fields are present. Plasma appears as a faint glow with less than 1 mm diameter, located at the tip of the powered electrode (see Figure 5.1). Depending on the desired chemical effect, various gases can be used, e.g., air, nitrogen, hydrogen and many others. However, it is recommended that the buffer gas be helium, because the operating voltages are lower than in other gases and the gas temperature is low due to high thermal conductivity of helium. Moreover, helium is inert and non-toxic. The latter feature allows keeping a good control of plasma chemistry, because active gases can be carefully dosed into the buffer gas.

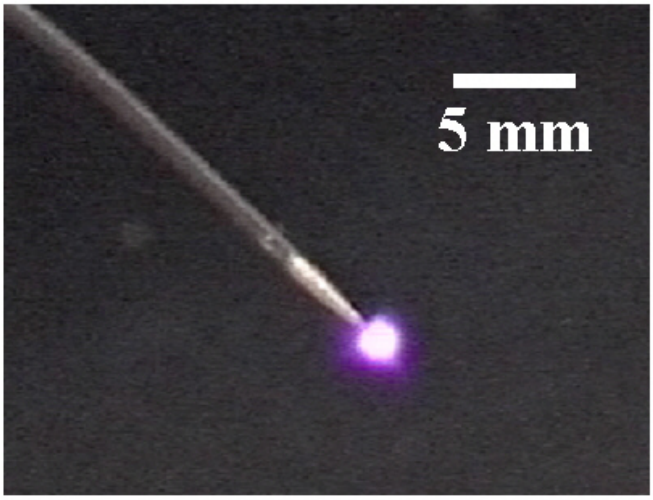

Figure 5.1: *Typical appearance of the plasma glow generated at the tip of a metal wire*

5.2.2 Electric Apparatus

Plasma was generated using a Hewlett Packard (Palo Alto, CA) 33120A waveform generator in combination with an Amplifier Research (Souderton, PA) 75AP250RF amplifier and a home-built λ-type matching network (see Figure 5.2). The powered electrode was a metal needle 5 cm long and 0.3 mm diameter; the discharge excitation frequency was about 10 MHz, and the peak-to-peak RF voltage was about 300 V. Both sine and square wave excitations could be applied; the latter had a somewhat lower ignition threshold voltage. Optimizing power dissipation in the plasma was performed either by varying capacitances in the matching network or by tuning the RF frequency to achieve resonance in this AC circuit. The latter method allowed for much finer tuning, because the circuit had a high quality factor (width of the resonance curve was in the kHz range) and the frequency of the waveform generator can be varied more accurately than the capacitances. The discharge power was monitored using an Amplifier Research PM 2002 power meter connected to an Amplifier Research dual directional coupler. The power input into the plasma was 0.1-0.3 W.

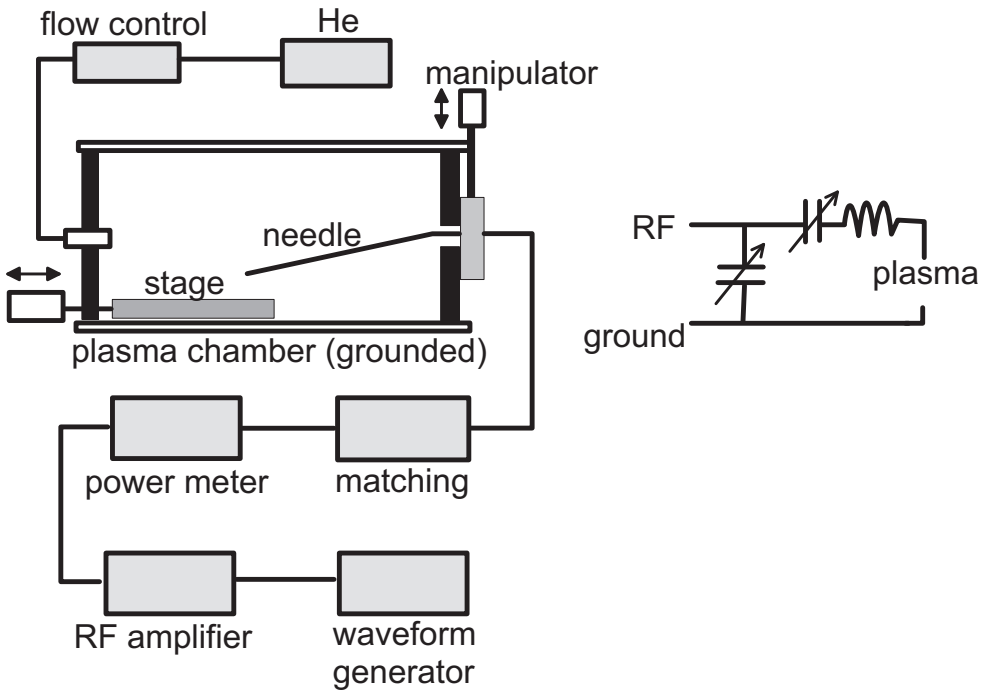

Figure 5.2: *Scheme of the experimental apparatus. The matching network is depicted at the right hand side. It consists of two variable capacitors (0-2 nF) and a coil (1.6 μH).*

5.2.3 Plasma Chamber

The plasma chamber was a 10x10 cm stainless steel box, closed by removable plastic covers (see Figure 5.3). The connection was not vacuum-tight. The plasma chamber was filled with gas (inlet is visible at the left hand side in Fig. 5.3) with a flow rate up to 2 l min^{-1}, controlled by a Brooks series 5850E mass flow controller (Brooks Instrument, Hatfield, PA). Air contamination due to leakage is in the sub percent range. Striving for higher purities was not of much use, because presence of air and water vapor is inevitable during treatment of the living cells. Samples for plasma treatment were placed on a moving stage, mounted at the bottom of the chamber. The samples could be moved up to 2 cm in the right-left direction. A similar manipulator was used to adjust the vertical distance between the needle and the sample. Both manipulators were operated externally with an accuracy of 0.01 mm.

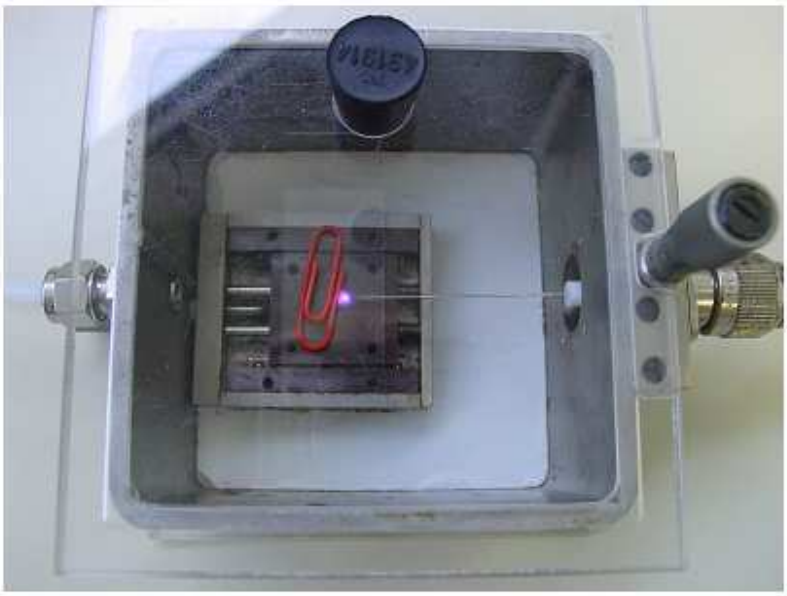

Figure 5.3: *Photograph of the plasma chamber from above. The plasma needle can be moved up and downwards. The samples are placed on the moving stage visible at the bottom.*

5.2.4 Cell Culture

CHO-K1 cells were cultured in flasks containing Ham's F-12 medium with stable L-glutamin (Bio Whittaker Europe, Verviers, Belgium) containing 9.0% of Fetal Bovine Serum (FBS, Biochrom AG, Berlin, Germany) and 0.45% of Gentamycin (10 mg ml^{-1}, Biochrom AG). The medium used for the NSCLC MR65 cells consisted of DMEM (ICN

Biomedicals) with 10% FBS, 1% L-glutamine and 0.005% Gentamycin.The cells were maintained in an incubator at 37 °C with 5% CO_2. To prepare samples for plasma treatment, the cells were trypsinized (0.05% Trypsin / 0.02% EDTA solution in PBS, Biochrom AG) and transferred onto sterilized object slides (26 x 10 x 1 mm) and placed in multiwell dishes. The cells were incubated in the multiwell dishes for 2 days prior to treatment.

5.2.5 Plasma Treatment

For the treatment the samples were taken out of the incubator for 15-30 min. No indication was found on control samples that cell were affected by this. Just before treatment, the sample was put in the helium-filled plasma box. To prevent drying out of the cells, the sample was covered with a layer of phosphate buffered saline (PBS). The plasma needle was brought close to the sample; visually the glow was just touching the surface of the PBS solution.
The treatment time was 1 min, during which the sample was moved by the manipulated stage over a distance of 1 cm. This produced a typical "track" of plasma-treated cells, which could be easily recognized under the microscope. Individual cells on this track were irradiated for 5 s. The total treatment time could not be varied in a broad range: it was limited by the (low) speed of the manipulator and by avoiding sample desiccation due to helium flow. The experiments were performed at least five times for a given condition. After exposure to the plasma, the samples were either immediately observed under the microscope (within 1-2 min) or returned to the incubator and observed several hours after treatment.

5.2.6 Visualization

Cells were studied with a light microscope and with a confocal laser scanning microscope (LSM 510 by Zeiss, Oberkochen, Germany). Trypan blue (0.5% in physiological saline, Biochrom AG) is a stain used to distinguish dead cells from living ones. The whole cytoplasm of a dead cell is colored blue, which is easily visualized by light microscopy.
For more detailed observations, propidium iodide (PI, 10 μg ml^{-1}, Molecular Probes, Eugene, OR) and cell tracker green (CTG, 10 μM, Molecular Probes) were used in combination with the CLSM. PI penetrates cells with permeable membranes and binds to DNA and RNA in the cell. It can be used to detect dead cells, or to reveal the structure of cell nuclei. The He-Ne laser of the CLSM (wavelength 543 nm) excited the PI. A long pass filter of 585 nm was used, and red fluorescence around 617 nm was monitored. CTG was used to detect living cells. When irradiated by an argon ion laser (wavelength 488 nm), CTG produces green fluorescence in the cytoplasm of viable cells. To monitor this fluorescence, we used a band pass filter of 505-530 nm. CTG is traceable for 36 h and is inherited by

daughter cells after cell division.
Typically, we used dual staining (CTG and PI) about 2 h after plasma treatment to distinguish between living and dead cells. For a study of long term viability after treatment, we applied CTG and observed the cells for a few hours up to 1 day. After the incubation, the cells were fixed with buffered 4% formaldehyde and permeabilized with 0.1% Triton (Tx-100). They were counterstained with PI and the structure of the nuclei was examined. This allowed detection of possible abnormalities induced by the treatment, e.g., apoptotic cells.

5.2.7 Apoptosis detection

If apoptosis is induced after plasma treatment, it can be detected 4 to 6 h after irradiation. For the detection, we have used M30 CytoDEATH (Roche diagnostics) in immunofluorescence. The M30 antibodies bound to the caspase cleavage products of cytokeratin 18. The antibodies were labeled with a fluorescent dye that was used for the detection. All incubations and washings were performed in a PBS buffer solution supplemented with 1% BSA and 0.01% Tween. After fixation of cells in ice-cold pure methanol at -20 °C for 30 min, aspecific antibody binding was blocked with incubation buffer for 10 min at 20 °C. After incubation with 100 μl M30 CytoDEATH antibody working solution for 60 min at 20 °C, cells were washed and incubated with rabbit anti mouse FITC (dilution 1:100, DAKO A/S, Glostrup DK) for 30 min at 20 °C. Cells were mounted and examined using a confocal laser scanning fluorescence microscope (MRC600, BioRad).

5.2.8 Temperature Measurements

To ensure that cells did not suffer from hyperthermia during treatment, the gas temperature in the plasma was measured using a NiCr-Ni thermocouple (Hasco z251/1, Ludenscheid, Germany) with a temperature range up to 400 °C and resolution of 0.1 °C. The thermocouple was fastened to the moving stage and the temperature was determined as function of the distance between the needle and thermocouple head, in both dry and wet environments. In the latter case, the thermocouple head was immersed in 0.4 ml PBS solution.

5.3 Results and discussion

5.3.1 Thermal Properties of the Plasma Needle

Since even slight heating may be fatal to cells, it is very important to keep a good control of gas temperature during plasma treatment. Figure 5.4 shows the temperature determined by a thermocouple placed at various distances from the tip of the plasma needle. Only slight temperature increase is observed at the distance of 2 mm, which is the normal working distance during cell treatment. In this situation, the sample is in direct contact with active plasma (glowing zone).

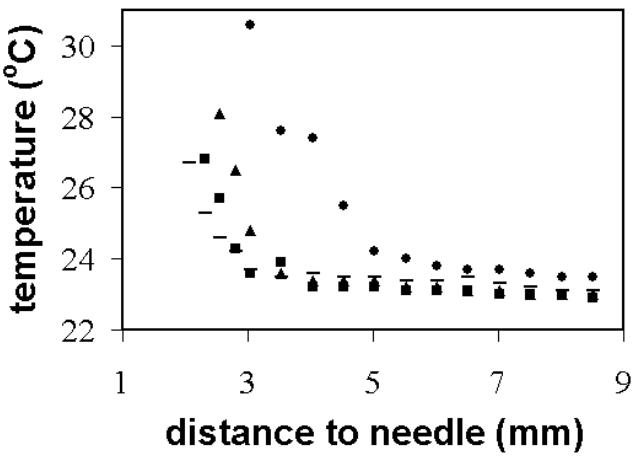

Figure 5.4: *The temperature determined by a thermocouple as a function of distance between the plasma needle and the surface for various conditions. Dry thermocouple: • 0.3 W plasma in helium, ■ 0.15 W in helium, ▲ 0.15 W in helium with 3% air. Thermocouple immersed in PBS: - 0.15 W in helium. Indicated plasma powers are initial values at 9 mm distance. Temperature increase is directly related to plasma power. In case the plasma is applied to a dry thermocouple, the temperature increase is slightly larger. The same is valid for air-contaminated plasma.*

The temperature recorded by the thermocouple is slightly higher when this metal device is dry. This is most likely due to lower heat capacity of the metal in comparison to water. During cell treatment, a sample containing cells is always covered by a thin film of PBS. This serves not only to prevent the cells from drying out, but also to create a smooth conducting surface, which is beneficial for plasma stability. Moreover, it can divert any static electricity (surface charging) created by the plasma away from cells and conduct it to the ground (metal moving stage).

As expected, gas heating is directly related to plasma power, so using higher powers in combination with short distances should be avoided. Plasma with 0.3 W power input, applied at the working distance of 2 mm, causes total necrosis in the treated area already after a few seconds of treatment.
We conclude that the thermocouple measurements show that heat generated by the plasma cannot cause damage to the cells when treatment is conducted under the following conditions: powers around 0.15 W or less, distances about 2 mm, and treatment time of about 5-10 s per cell.

5.3.2 Cell Responses

Treatment with the plasma needle induces cell responses in a restricted area. A typical "track" of the plasma left on the cell sample is merely 0.2 mm wide. This is the typical size of the influenced area, reproducible within 20%. It is also possible to create "plasma marks" of 100 μm size, as shown in Figure 5.5, but the treatment time must be very short (1 s per "spot") and the sample must be immediately brought out of the reach of the needle. In the present configuration it is difficult to control such fast movements.

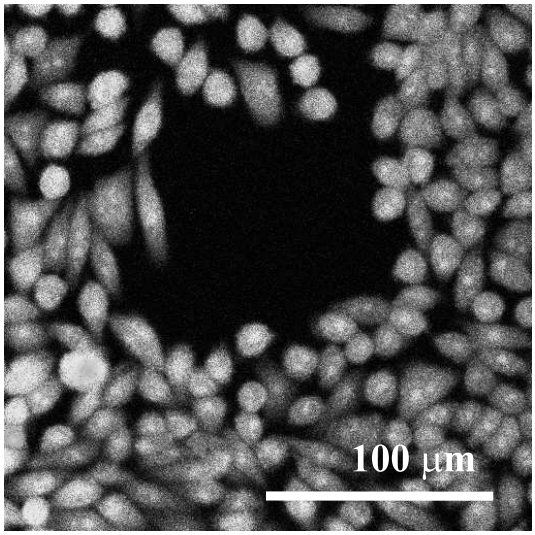

Figure 5.5: *Plasma-induced void with ca. 100 μm size on a sheet of cultured cells. This demonstrates high precision of plasma treatment. The cells have been treated with a very low-power (< 0.05 W) plasma, and after 2 h CTG has been applied. Prior to this observation (4 h after treatment), cells have been fixed with formaldehyde and treated with PI to reveal the internal structure, but no special features can be distinguished. The cells were alive after plasma treatment, but they did not reattach within 4 h. Objective lens Zeiss 40x, NA 0.95 corr, resolution 0.45 μm/pixel.*

There is clear threshold behaviour in cell responses. They occur only for a given range of parameters (e.g. plasma power), and within this range they are insensitive to parameter variation. All cells in the treated area are influenced in the same way, the borders between various regions are very sharp and no "mixing" of intact and altered cells is observed.
A typical image of the treated area is shown in Figure 5.6. In this case, a relatively high power plasma (0.2 W) was applied and a dual staining assay was performed 2 h after treatment. In Figure 5.6, three zones can be distinguished: in the top right of the picture a necrotic zone (PI positive cells exhibiting red fluorescence), in the middle a typical void, and in the lower left a cluster of normal and rounded cells, which are detached from the surrounding ones. Below, we shall describe these zones in more detail.

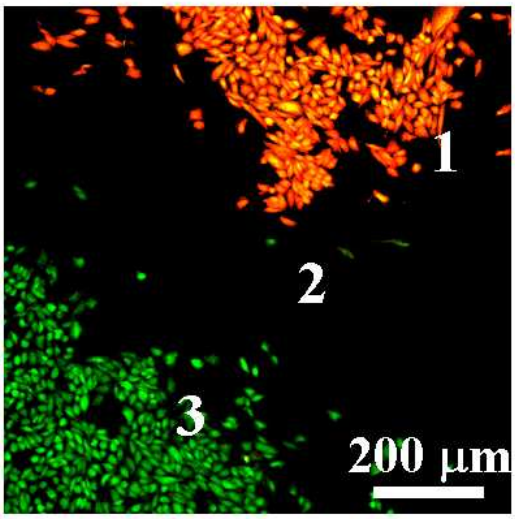

Figure 5.6: *Typical image of an area treated with a sufficiently high power to cause necrosis (ca. 0.2 W). Dual staining has been applied. The necrotic zone (indicated by 1), the void (indicated by 2) and the living cells (indicated by 3) are visible. A number of the living cells is detached; they form clusters and are stained green by CTG. Objective lens Zeiss 10x, NA 0.3, resolution 1.8 µm/pixel.*

The necrotic zone was closest to the plasma needle. Cells, which are not viable after plasma treatment, seem to preserve their shape and internal structure. However, they display an abnormal DNA distribution in their nucleus (see Figure 5.7). This type of cell death is not due to ordinary thermal damage, as verified by comparing with cells destroyed by heating. At present, we cannot decide whether this plasma induced necrosis is a useful method of disposing of unwanted cells in a tissue. Studying long term reactions of a tissue may supply an answer.
In this work, we attempt to observe and classify as many plasma induced cell responses as

possible, and therefore we mention necrosis as one of the options. However, cell necrosis is an a priori undesired effect and from now on we shall concentrate on other reactions.

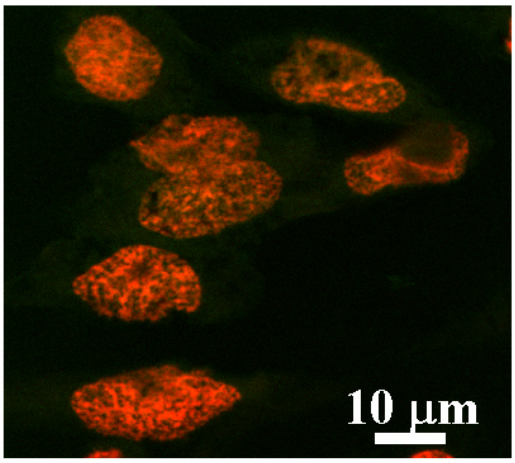

Figure 5.7: *Close-up of necrotic cells from Fig. 5.6. Objective lens Zeiss 40x, NA 0.95 corr, resolution 0.15 µm/pixel.*

As said before, cell necrosis occurs at powers higher than 0.2 W (threshold process). At lower powers necrotic zones like in Fig. 5.6 are absent in the treated sample. However, voids and rounded cells can be still observed. A global feature of plasma treatment is cell detachment, both from the bottom and from the surrounding cells. The first process is responsible for the formation of the void; the detached cells are floating in the liquid (PBS) and can be transferred to another Petri dish. The loss of cell-cell contact is reflected by rounding of cells. These cells are still attached to the bottom. Loss of cell contact appears even more readily than cell detachment from the surface. In some cases (about 20%) no voids, but areas filled with rounded cells, are present.
Cell viability after detachment was verified using CTG staining. Rounded cell were always stained green by CTG, like in the "clustered cells" zone visible in Fig. 5.6. The threshold power for cell detachment is about 0.1 W; all cells in the treated area are detached.

Long term behavior of detached cells deserves to be studied in detail. Information on cell condition and long term viability may allow us to manipulate cells with plasmas *in vitro* and possibly also in a living tissue. In our *in vitro* study we placed the treated CHO-K1 samples in cell culture medium and stored them in the incubator. Loose cells suspended in medium were collected separately.
Figure 5.8 shows the development of the CHO-K1 culture after plasma treatment. The viability of these cells is evident: only 1 h after exposure to plasma, cells start to move around and attach. The halos around the rounded cells disappear. After 4 h a sheet of cells

is formed and within 24 h confluence is attained, as in normal untreated samples. In case of fully detached cells, suspended in medium after treatment, reattachment is somewhat slower. Typically, cell-cell interaction is fully restored within 24 h.

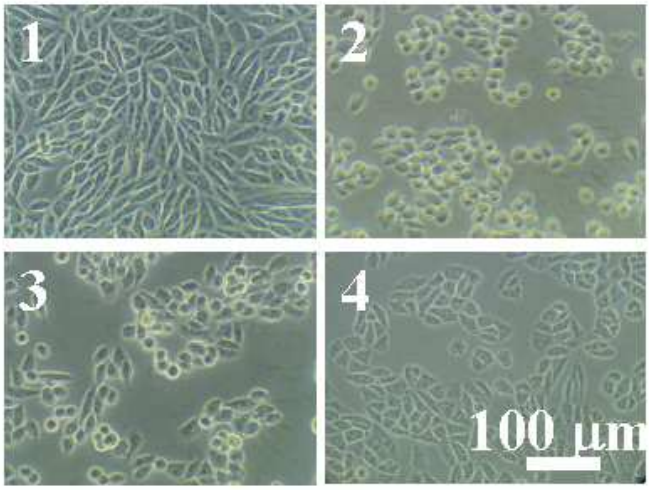

Figure 5.8: *Phase-contrast microscope photographs of cells treated with a 0.1 W plasma. Cells have been observed for several hours, and reattachment of detached cells has been established: 1 - before treatment, 2 - after 15 min, 3 - after 1 h, 4 - after 4 h. Objective lens Zeiss 10x, NA 0.25.*

At higher doses of plasma treatment, reattachment is inhibited. This occurs within the power range of 0.1 - 0.2 W, but at a total treatment time of 2 min (10 s per treated spot). Cells retain their rounded shape up to several days after treatment. Cell activities like proliferation continue, but at a slower rate than in normal cells. A typical treated area after 24 h is shown in Figure 5.9. Some cells are in advanced phase of cytokinesis. Before disposing of this sample the cells were stained with trypan blue, but no dead cells were found.

Under moderate conditions, plasma treatment leads predominantly to loss of contact between individual cells, and often cell detachment from the surface. The mechanism of this process is not yet completely clear however, it is expected to be of (plasma)chemical nature. The influence of other plasma-related factors was checked separately. The effect of UV radiation was studied by irradiating cells with excimer lamps described elsewhere [7]. Exposure to UV did not cause detachment, but necrosis appeared above a certain threshold of irradiance. RF electric fields applied to the needle in absence of discharge induced no reaction in cells, even at relatively high amplitudes (1000 V peak-to-peak) and distances shorter than 1 mm. Therefore we tentatively conclude that species emitted from the plasma are responsible for cell detachment. From all these species, including electrons,

ions and radicals, only the latter can penetrate under water and reach the cells.

Cell detachment can be a consequence of destruction (e.g. oxidation) of cell adhesion molecules (CAMs): cadherins and integrins. The first ones seem to be destroyed more readily: loss of cell contact is easier to induce than total cell detachment from the bottom. On the other hand, penetration of plasma species under water is limited. Densities of active particles may decrease drastically with depth, with a gradient length in the order of cell thickness. Integrins connect the cells to the bottom of the sample, so they cannot be reached by reactive species so easily as cadherins.

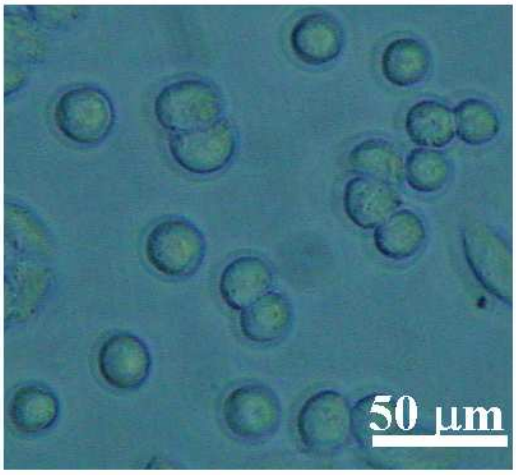

Figure 5.9: *In the case of a higher exposure time to the plasma, cell reattachment is inhibited even after 24 h. Objective lens Zeiss 20x, NA 0.3.*

CAMs in CHO-K1 are restored on a time scale of a few hours. This is also the typical observed time for cells to reattach and restore a sheet structure after plasma treatment. This supports the hypothesis of plasma induced damage to CAMs. Further studies will be carried out to identify specific chemical interactions that are responsible for this damage.

5.3.3 Apoptosis

Besides detachment of cells we observed that a small percentage of cells underwent apoptosis after plasma treatment. We used the M30 antibody method to detect apoptosis in our treated samples. Figure 5.10 shows the presence of three apoptotic cells (arrows) in an otherwise healthy cluster of cells. In the MR65 cells, there is always a small percentage of cells in a certain stage of programmed cell death. The number of apoptotic cells in the

treated samples was significantly higher than the natural number. A qualitative analysis was made with variation of treatment time. This revealed that shorter treatment times result in higher percentages of apoptotic cells.

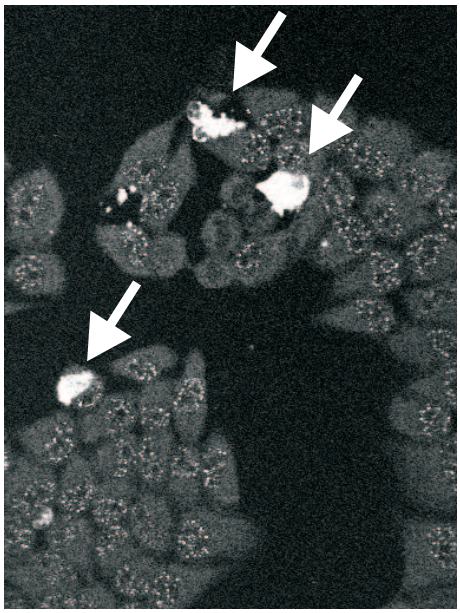

Figure 5.10: *Apoptosis detected with M30 in MR65 cells treated with plasma. (Objective 40x/1.3, 192x256 μm).*

While the amount of apoptotic cells may be slightly underestimated by this staining method, (detached cells are lost during staining), the number of apoptotic cells is relatively low if compared with apoptosis-inducing agents such as MG132 (data not shown).

These preliminary experiments show that the plasma needle can induce programmed cell death. A further optimization is expected to increase the percentage of apoptosis in the treated samples. Programmed cell death is quite critical and the right dose of plasma and reactive species needs to be supplied.

5.4 Conclusions

For the first time, interaction of an electrically generated plasma with single cells has been described. A CHO-K1 culture has been used as a model system to observe cell responses to a medium, which has not been applied to living objects before. We have verified that our newly constructed non-thermal atmospheric plasma source does not cause thermal nor

electric damage to the cells. Cell reactions induced by plasma treatment are of more sophisticated nature, such as cell detachment and apoptosis.
The percentage of cells that undergo apoptosis is expected to increase if the conditions are optimized.When the plasma power is in the range of 0.1 - 0.2 W, cell adhesion is affected. Cell detachment can be achieved with a high precision in an area as small as 0.1 mm diameter. Detached cells remain viable; they typically restore contacts with other cells and reattach to the bottom within a few hours. Based on this observation we conclude that plasma action is limited to cell exterior, so that only CAMs are destroyed.

A possible mechanism responsible for cell detachment may be damage of cadherins and integrins due to interactions with active radicals (oxygen and nitrogen species) emitted from the plasma. We suppose that the plasma conditions used for cell detachment have the least intrusive effect on the cells, since the treated cells do not seem to be altered in any other way. Of course, applying harsh conditions (plasma powers higher than 0.2 W) leads to severe damage and necrosis.

The final aim of this research is high precision, controlled cell manipulation in tissue. Tissue modification without necrosis would not lead to inflammation and unnecessary damage. Cell detachment is a promising method because it is easier to induce than apoptosis. The plasma effect on cell adhesion is potentially applicable in refined cell removal. Cell detachment in a living tissue will be investigated in the near future.

References

[1] M. Laroussi. Sterilization of contaminated matter with an atmospheric pressure plasma. *IEEE Trans. Plasma Sci.*, 24(3):1188–1191, 1996.

[2] E. Stoffels, A. J. Flikweert, W. W. Stoffels, and G. M. W. Kroesen. Plasma needle: a non-destructive atmospheric plasma source for fine surface treatment of (bio)materials. *Plasma Sources Sci. Technol.*, 4:383–388, 2002.

[3] C. P. Klein, P. Patka, J. G. Wolke, J. M. Blieck-Hogervorst, and K. de Groot. Long-term in vivo study of plasma-sprayed coatings on titanium alloys of tetracalcium phosphate, hydroxyapatite and alpha-tricalcium phosphate. *Biomaterials*, 15(2):146–150, 1994.

[4] A. Ohl and K. Schroder. Plasma-induced chemical micropatterning for cell culturing applications: a brief review. *Surf. Coat. Technol.*, 116-119:820–830, 1999.

[5] M. Moisan, J. Barbeau, S. Moreau, J. Pelletier, M. Tabrizian, and L. H. Yahia. Low-temperature sterilization using gas plasmas: a review of the experiments and an analysis of the inactivation mechanisms. *Int. J. Pharmac.*, 226(1-2):1–21, 2001.

[6] M. Laroussi, J. P. Richardson, and F. C. Dobbs. Effects of non-equilibrium atmospheric pressure plasmas on the heterotrophic pathways of bacteria and on their cell morphology. *Appl. Phys. Lett.*, 81(4):772–774, 2002.

[7] Victor F. Tarasenko, Mikhail I. Lomaev, Alexei N. Panchenko, Victor S. Skakun, and Eduard A. Sosnin. UV and VUV efficient excilamps. *Proc. SPIE*, 3343:732–741, 1998.

Chapter 6

Plasma treatment of mammalian vascular cells: a quantitative description

Abstract
For the first time, quantitative data was obtained on plasma treatment of living mammalian cells. The non-thermal atmospheric discharge produced by the plasma needle was used for treatment of mammalian endothelial and smooth muscle cells. The influence of several experimental parameters on cell detachment and necrosis was tested using cell viability assays. Interruption of cell adhesion (detachment) was the most important cell reaction to plasma treatment. Treatment times of 10 s were enough to detach cells in the cultured cell sheet. Under extreme conditions, cell necrosis occurred. Cell detachment without necrosis could be achieved at low voltages. It was shown that the thickness of the liquid layer covering the cells was the most important factor, which had more influence than treatment time or applied voltage. The results show no remarkable differences between the responses of the two cell types.

This chapter was published as I.E.Kieft, D. Darios, A.J.M. Roks, E.Stoffels, Plasma treatment of mammalian vascular cells: a quantitative description, *IEEE trans. plasma sci.*, 33(2):771-775, 2005.

6.1 Introduction

In biomedical technology, various plasmas have been extensively used for inactivation of bacteria [1, 2] and for surface modification of scaffolds to improve cell attachment [3, 4]. However, these plasmas were never applied directly to living mammalian cells and tissues. A special nonaggressive plasma source (the plasma needle) was developed for tissue treatment without causing cell necrosis and inflammation. The aim of plasma treatment is high-precision removal of pathological tissues without excessive damage to the body. Cell reactions after plasma treatment were first described by Kieft *et al* [5]. They found that the main effect of the treatment was the detachment of cells from each other and from their extracellular matrix. The detachment of cells starts within seconds after the treatment [6]. In this chapter, the dependence on the experimental plasma parameters was investigated.

The plasma needle is a non-thermal discharge at atmospheric pressure produced by radio-frequency (RF) excitation [7]. The size of the plasma is small (around one mm), and, therefore, it can be used with a high precision. The plasma acts on the surface with a minimum penetration depth. The mechanism of plasma treatment is still under debate. In case of bacteria, it is proposed that the main cause of deactivation is their poisoning and erosion by active radicals produced in the plasma [1]. It is thought that radicals are more important than ions or ultraviolet (UV) light. However, it is not certain whether mammalian cells respond similarly to these features, although both the radicals and UV radiation are known to interact with cells and tissues [8–10]. In particular, reactive oxygen species were identified to play a major role in the pathogenesis of cardiovascular diseases [11, 12]. Spectral analysis of the plasma needle showed that reactive oxygen species such as $O^{\cdot}$ and $^{\cdot}OH$ were present, and that UV was emitted [13]. Previous experiments with lamps showed that UV irradiation causes necrosis, but no cell detachment [14]. The reactions observed by Kieft *et al* [5] were most likely caused by radical interactions with the cell membrane.

Our goal is to optimize plasma treatment by varying experimental parameters, such as applied voltage, treatment time, and amount of liquid covering the cells. The incidence of necrosis should be minimized, while cell detachment should be achieved efficiently. The experiments were performed on two cell types: endothelial cells and vascular smooth muscle cells. These two cell types constitute the arterial walls, and their response to plasma treatment will provide us with information for possible future treatment of atherosclerotic lesions or postangioplasty restenosis. The critical parameter for the treatment appeared to be the thickness of the layer of cell culture medium covering the cells. This thickness provides directly the penetration depth of plasma species in the liquid. In future surgical applications, it will allow to accurately control the plasma dosage by screening the most

vulnerable tissue areas. This influenced the area that was reached by the plasma, as well as the presence of necrosis after treatment. An increase in plasma power merely caused an increase in necrosis percentage.

6.2 Experimental

6.2.1 Plasma Needle

The plasma needle is a non-thermal atmospheric RF glow discharge. It is easy to handle and small (the size of a pen). The RF signal (13.56 MHz) is generated by a waveform generator (Hewlett Packard 33120A) and amplified by an RF amplifier (Kalmus model 125C-CE). From the amplifier, the signal is directed to a home-built matching network. Figure 6.1 illustrates the plasma needle setup.

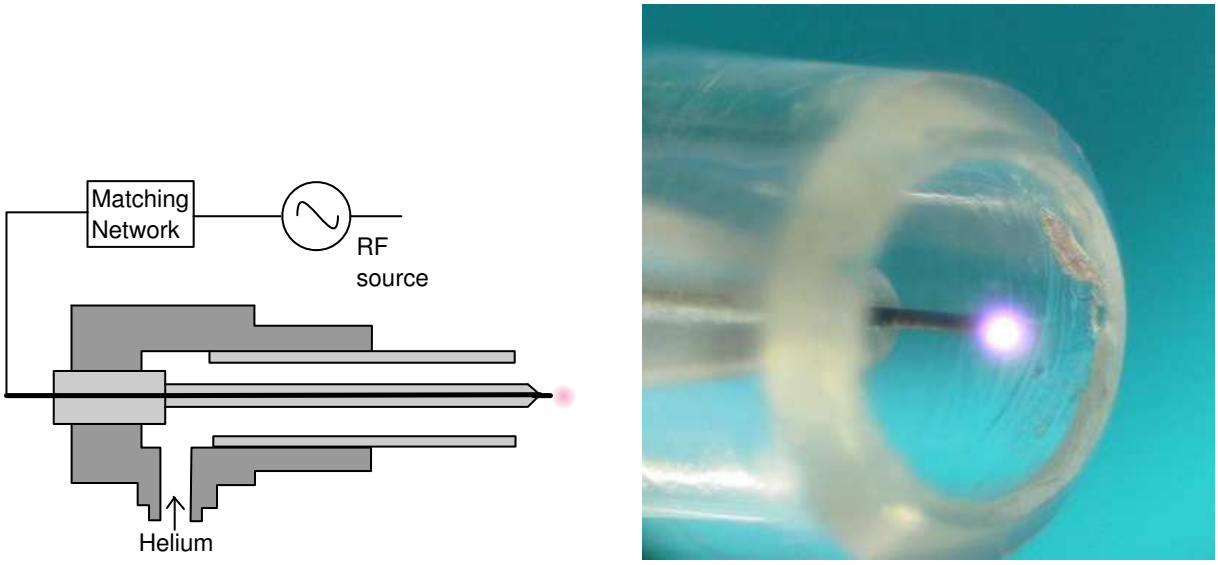

Figure 6.1: *(a) Schematic drawing of the current experimental setup. (b) Plasma glow generated at the end of the plasma needle.*

The plasma needle consisted of a metal alloy pin (0.3-mm diameter). The metal pin protruded from the stainless steel holder by 1.5 cm, while the total length of the needle was about 8 cm. It was insulated by glass in order to prevent a discharge from expanding along the entire pin. The latter was confined in a Perspex tube (5-mm inner diameter), which was filled with helium delivered at a flow rate of 2 l min^{-1}. Moving the Perspex tube relative to the fixed needle regulated the percentage of air in the vicinity of the needle tip.

In the work described here, the needle was protruding 8.5 mm out from the Perspex tube and the plasma appeared as a pink glow at the tip of the needle. The typical size of the plasma glow was 1-mm in diameter. Temperature measurements on the gas temperature of the plasma were reported in a previous paper [5]. It was shown that the gas temperature does not rise more than 10 ^{o} above room temperature (it is thus nog higher than 35-37 ^{o}C), so it does not affect cell viability.

6.2.2 Cells

Two cell types were used in the experiments that are prevalent in arterial walls: endothelial cells and smooth muscle cells. The specific cell types are Bovine aortic endothelial cells (BAEC) (Cell Applications Inc., San Diego, CA) and rat aortic smooth muscle cells (A7r5, ATCC, Manassas, VA). The cells are transferred every three or four days in a new flask with fresh culture medium and incubated at 37 ^{o}C with 5% CO_2. The culture medium is composed of: 500 ml Dulbecco's modified eagle medium (DMEM) with glucose 4.5 g l^{-1} and with L-glutamine (Biowhittaker, Cambrex, Verviers, Belgium); 50-ml fetal bovine serum (FBS by Biochrom AG, Berlin); 5-ml non-essential amino acids (100x) (Biochrom AG); 2.5-ml gentamycin (10 mg ml^{-1}) (Biochrom AG); and 10-ml HEPES-buffer (1M) (Biochrom AG). Both cell types are cultured in the same medium.

6.2.3 Stains

Fluorescent stains were used to visualize cell viability: cell tracker green (CTG) (10 μM, Molecular Probes, Eugene, OR) and propidium iodide (PI) (10 μg ml^{-1}, Molecular Probes). They show cell viability by coloring the live cells in green or dead cells in red respectively. The stains were used in combination with a fluorescence microscope (Axiovert 200M, Zeiss) and a microplate fluorescence reader FL600 (Biotek). Two filters were used on the fluorescence microscope: CTG was excited with 450-490 nm and emission was detected with a long-pass filter LP 515 nm; PI was excited with 510-560 nm and its emission was detected with an LP 590-nm filter. The plate reader was used to measure CTG emission using an excitation filter with a center wavelength of 485 nm and a bandwidth of 20 nm at one-half the maximum transmission; the center wavelength of the emission filter was 530 nm with a bandwidth of 25 nm.

6.2.4 Exposure procedures

The cell samples were prepared in 96-well plates. A haemocytometer in combination with Trypan blue was used to count the cells that were seeded in one well. In each well 10,000 cells were grown at 37 °C in 100-μl culture medium about 20 h before treatment. The treatment was performed at room temperature. Unless stated otherwise, after treatment cell samples were washed with phosphate buffered saline (PBS) and incubated with fresh medium for 3 h. Then, CTG and PI were applied and cells were again incubated for 30 min (at 37 °C). Control samples underwent exactly the same treatments except for the plasma exposure.
The wells in the 96-well plate had a diameter of 6.5 mm. This meant that the plasma treatment was not uniform over the well. This gave us the opportunity to test the reach of the plasma.
The height of the wells was 11.5 mm. Thus, the plasma needle tip was situated 3 mm above the cells, which were attached to the bottom of the plate.

6.3 Results

6.3.1 Penetration depth

The penetration depth of the plasma was tested by examining detachment and necrosis rates while varying the amounts of liquids that covered the cell samples. Detached cells left a circular void on the sample. An example of such a void is shown in Figure 6.2. The void is present in the lower right side of the picture; a few necrotic cells are still attached to the bottom. The picture was taken near the edge of the sample.

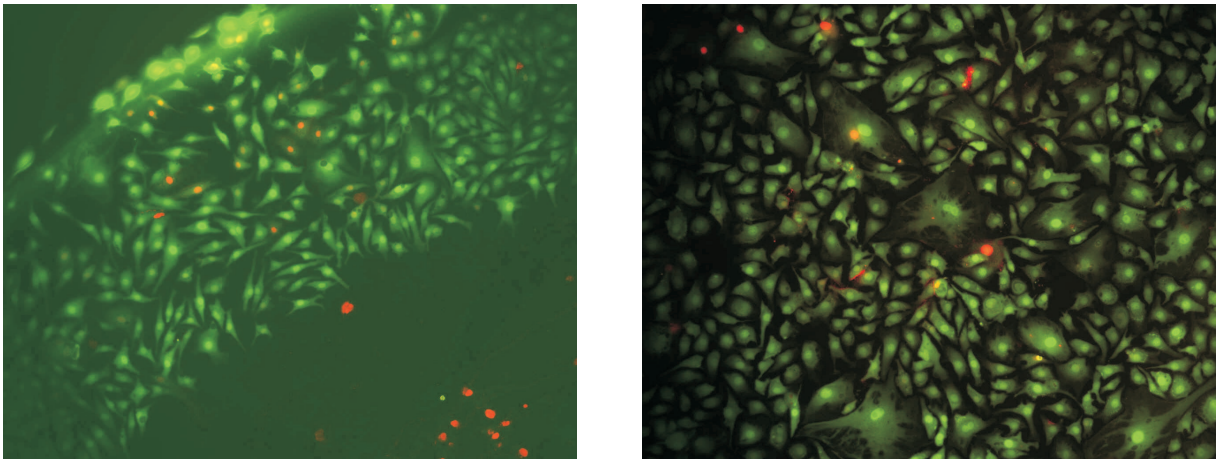

(a) (b)

Figure 6.2: *(a) Void introduced by plasma on BAEC cells by 30 s exposure with 10 μl. (b) Untreated sample. (Objective 10x/0.30 Ph1 Plan Neofluar; size 870x705 μm).*

The applied voltage in this experiment was 250 V_{rms} for 30 s. Different amounts of medium were added to the cells, resulting in varying thickness of the liquid layer. However, due the capillary forces, the entire surface of the well was not uniformly covered in case of 10 and 20 μl medium. Thus, an area in the center was covered with only a very thin liquid layer (<0.1 mm). For 10 μl, this area had a diameter of 3 mm; for 20 μl, this was 2 mm.

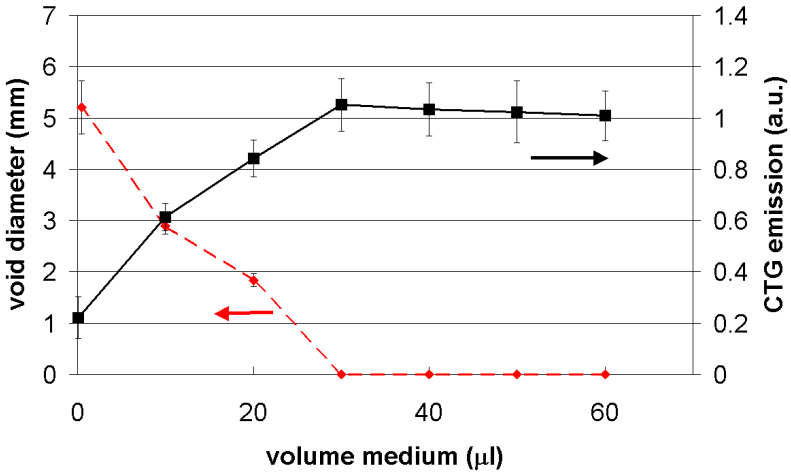

Figure 6.3: *CTG emission (squares) and void diameter (diamonds) for treated BAEC cells with varying amounts of liquid.*

For each medium volume, six samples were treated and the data were averaged (Fig. 6.3).

The void diameters were determined from the microscope photographs. If we compare the sizes of the voids to the sizes of the areas with only a thin layer of liquid during treatment, we can conclude that they are similar. Thus, the sizes of the voids in the cell cultures are mainly determined by the size of the thin liquid areas. Where the liquid layer is very thin, the cells easily detach. This indicates that the average penetration depth of the reactive plasma particles through the liquid is low: below 0.1 mm. However, one has to be careful while treating cells through very thin layers of culture medium, because other, undesirable effects may become important (dehydration and osmosis because of evaporation).

When no liquid was added to the cells, voids were induced with a diameter of over 5 mm. This is the radius that is reached by the plasma particles or UV light in the current configuration. However, if the thin liquid layer area was too large (and most likely the liquid layer too thin) there was a spot of necrotic cells in the center of the void. For the samples with 0 μl of added medium (note that some adhesive medium will have remained on the cells) this dead spot was 1-2 mm in diameter, for 10 μl this was 0-1 mm in diameter (see also Figure 6.2). The voids for 20 μl had no dead cells inside. It appears that the influence of the medium layer is important for the size of the hole that is introduced, but there is a risk of necrosis, possibly due to dehydration.

6.3.2 Effect of exposure time

Data obtained (not shown) on both A7r5 and BAEC cells show no time dependence for treatment times below 1 min when samples were treated with medium volumes ranging from 10-60 μl. Even for 10 s, voids were introduced in the cell layers for low amounts of medium. The voids induced for treatment times up to 60 s remained equal in size.
To check the effect of longer exposure times, BAEC cells were treated up to 9 min. The amount of the medium in these experiments was 40 μl, resulting in a height of 1.2 mm of liquid above the cells. Every 1.5 min 10 μl was added to keep the medium level constant.

Data were collected from three independent experiments. Note that the decrease in emission intensity in Fig. 6.4 cannot be caused by bleaching or quenching, since all samples were treated first and then measured simultaneously. The percentage of necrotic cells that remained in the well was below 10%. Thus, the decrease of the CTG intensity was due to cell detachment. We can conclude (Fig. 6.4) that for longer treatment times, the detachment of the cells proceeds linearly with time until eventually all cells detach. The plasma constituent responsible for cell detachment always penetrates the liquid, but for remote cells the dose is usually too low to induce an effect. This means that it is possible to increase the area of reach of the plasma, but the treatment time must be scaled up

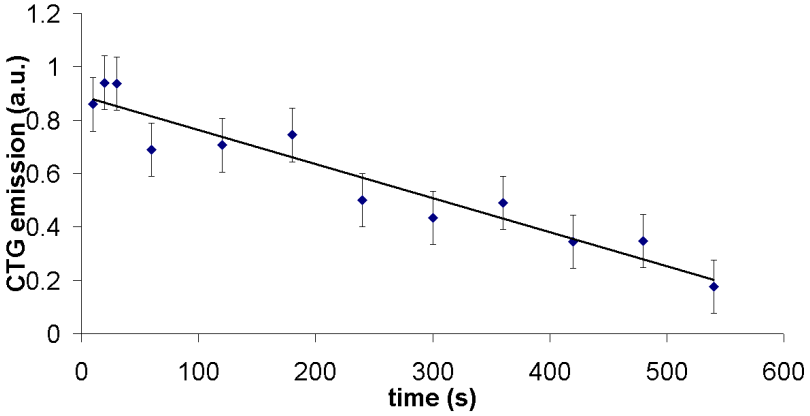

Figure 6.4: *CTG emission after treatment of BAEC cells with plasma. Emission data were scaled to untreated samples.*

accordingly.

6.3.3 Effect of applied voltage

When the voltage applied to the needle was increased, dissipated power and plasma size increased. With this in mind, one can expect that cell detachment and possibly also necrosis are enhanced. In the experiment, plasma was applied to 20 μl of medium for 30 s with increasing voltage from 226 V_{rms} to about 280 V_{rms}. The data points were averaged over six samples. Unlike the experiments discussed before, the fluorescent CTG stain was now applied before the treatment. The fluorescence emission intensity of the samples was scaled per individual sample by collecting data before and after the treatment.

As voltage increased, the CTG intensity decreased (Fig. 6.5). There are two reasons for this. First, there was a rise in the number of detached cells: not only in the central void but also cell density near this void appeared to be lowered. This effect was visually observed, but was not quantified. Second, the number of dead cells was increased; this is discussed in the following paragraph. Dead cells will still show some fluorescence, even though most of the cytosol containing the activated CTG will have leaked out of the membrane. Thus, the CTG fluorescence emission is an upper limit for the amount of living cells.

The sizes of the central voids were measured to be between 1.5-2 mm in diameter for all treated samples and did not change with increasing voltage. Again, this indicates the fact

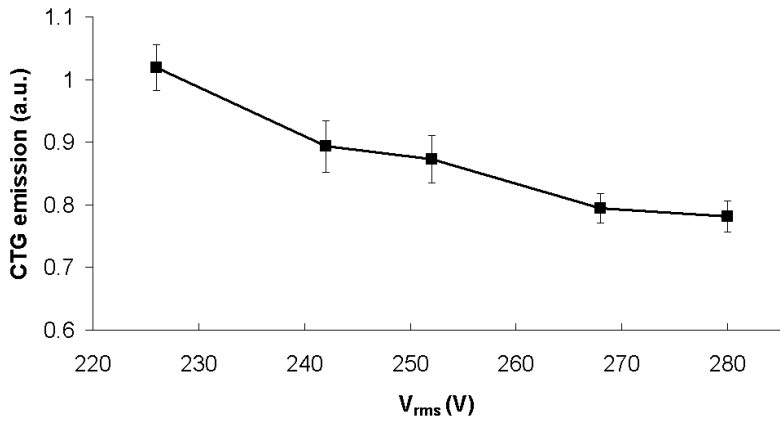

Figure 6.5: *CTG intensity as a function of applied voltage after 30 s of plasma treatment of A7r5 cells. The intensity was scaled to the intensity of the untreated samples.*

that the active plasma species have the most effect on the cells if the latter are covered with only a thin layer of culture medium. However, we must keep in mind that cell reactions may be affected by liquid evaporation.
On the other hand, the percentage of dead cells rapidly increased with increasing power (Fig. 6.6), up to 50% in particular spots. The increased necrosis may be due to dehydration, but also to membrane damage because of reactive oxygen species (ROS) attacking the cell surfaces.

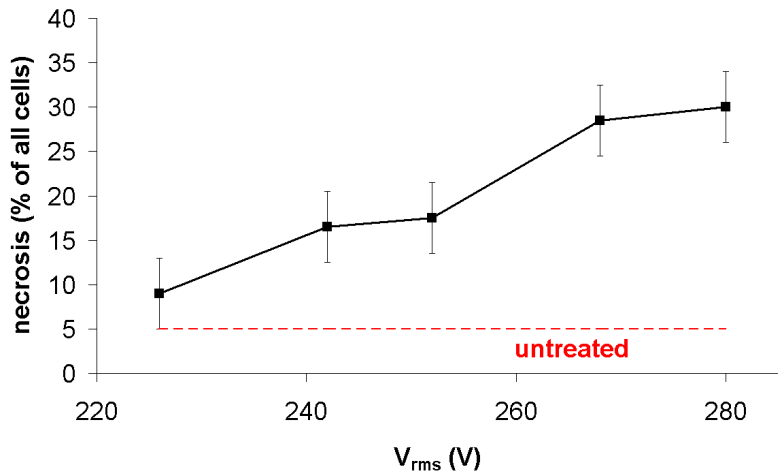

Figure 6.6: *Percentage of necrosis after treatment of A7r5 cells.*

In conclusion, we can say that the increase of power does not affect the cell detachment,

but does affect the viability of the cells. This is an unfavorable effect since we want to treat cells without inducing necrosis. In this view, for optimal plasma treatment, the voltage should be kept as low as possible to sustain mild plasma conditions.

6.4 Discussion

The chapter shows the influence of several experimental parameters on the detachment of cells. As was proposed in a previous paper [5], the reaction mechanism that causes the detachment may be the reactions of reactive species (e.g., radicals or ions) with the cell adhesion molecules (CAMs) of the cells. These adhesion molecules (integrins and cadherins) may be damaged, and, thus, attachment is lost and cells will start floating in the liquid. This idea is supported by the fact that detachment is reversible, and cell layers are reconstructed within 4 h. This is a typical time needed to repair the damaged CAMs.

However, the results from more recent experiments indicate that there may be another explanation. Cells do not detach instantaneously; the process of detachment starts a few seconds after the plasma treatment is terminated, and continues for up to 20 s [6]. Thus, the detachment may be a reaction initiated by a living cell upon the treatment. Indeed, when cells are accidentally killed (necrotic) due to e.g., high plasma power, they do not detach, but remain on the sample. Low doses of plasma species do not result in necrosis, but they may cause discomfort. A moderate damage to the cell's membrane or organelles can trigger an impulse to move away from the "dangerous" zone. Future flow cytometric assays will allow to unravel the nature of this damage and to evaluate its extent. At present, we can tentatively conclude that cell detachment does not affect cell viability in a drastic way, because both detached cells, floating in the medium, and cells remaining on the plate are capable of reattachment and further growth.

It is not yet clear which plasma property causes the detachment or damage to the cells. It has been checked that UV light alone (from narrow band UV lamps) causes in high doses cell necrosis, but it never induces cell detachment [14]. Thus, UV is probably not an important parameter in plasma-cell interactions. As the influence of temperature and electromagnetic field can be neglected [5], the remaining "suspected" species are electrons, ions, and radicals. The penetration depth of electrons and ions in the liquid is not sufficient to cause the observed effects directly; however, energetic ions in contact with the medium can create reactive radicals from water molecules. An experiment is planned, in which an external magnetic field that confines the ions will be applied. Reducing ion fluxes incident at the medium surface may reveal the importance of the ions.

6.5 Conclusions

Experiments with the plasma needle and cultured cells were performed to quantify the influence of experimental parameters on cell detachment and necrosis.
Exposure of mammalian cells to the plasma caused their detachment with only 10 s of treatment time. The size of the detached areas (plasma-induced voids) was mainly determined by the thickness of the medium layer that covered the cells. To be able to detach cells after short exposure times, this layer needed to be thin, preferably far below 1 mm. However, if the layer was too thin, necrosis occurred most likely due to dehydration. Thicker culture medium layers required a relatively long exposure time. Thus, in future medical treatment, a compromise must be made, so as to induce the desired reaction within an agreeable time and without dehydrating the tissue.
An increase in voltage applied to the needle increased the percentage of necrotic cells in the sample. There was no apparent difference found in the behavior of the endothelial cells compared to the smooth muscle cells after the plasma treatment.
The optimization of plasma parameters allows a plasma treatment with only small incidence of necrosis.

References

[1] M. Laroussi and F. Leipold. Evaluation of the roles of reactive species, heat, and UV radiation in the inactivation of bacterial cells by air plasmas at atmospheric pressure. *Int. J. Mass Spectrom.*, 233(1-3):81–86, 2004.

[2] M. Moisan, J. Barbeau, S. Moreau, J. Pelletier, M. Tabrizian, and L. H. Yahia. Low-temperature sterilization using gas plasmas: a review of the experiments and an analysis of the inactivation mechanisms. *Int. J. Pharmac.*, 226(1-2):1–21, 2001.

[3] D. E. MacDonald, F. Betts, M. Stranick, S. Doty, and A. L. Boskey. Physicochemical study of plasma-sprayed hydroxyapatite-coated implants in humans. *J. Biomed. Mater. Res.*, 54:480–490, 2001.

[4] K. Schroder, A. Meyer-Plath, D. Keller, W. Besch, G. Babucke, and A. Ohl. Plasma-induced surface functionalization of polymeric biomaterials in ammonia plasma. *Contrib. Plasma Phys.*, 41:562–572, 2001.

[5] I. E. Kieft, J. L. V. Broers, V. Caubet-Hilloutou, D. W. Slaaf, F. C. S. Ramaekers, and

E. Stoffels. Electric discharge plasmas influence attachment of cultured CHO K1 cells. *Bioelectromagnetics*, 25:362–368, 2004.

[6] I. E. Kieft, N. A. Dvinskikh, J. L. V. Broers, D. W. Slaaf, and E. Stoffels. Effect of plasma needle on cultured cells. *Proc. SPIE*, 5483:247–251, 2004.

[7] E. Stoffels, A. J. Flikweert, W. W. Stoffels, and G. M. W. Kroesen. Plasma needle: a non-destructive atmospheric plasma source for fine surface treatment of (bio)materials. *Plasma Sources Sci. Technol.*, 4:383–388, 2002.

[8] K. M. Anderson, T. Seed, D. Ou, and J. E. Harris. Free radicals and reactive oxygen species in programmed cell death. *Med. Hypoth.*, 52(5):451–463, 1999.

[9] Simon H.-U., A. Haj-Yehia, and F. Levi-Schaffer. Role of reactive oxygen species (ROS) in apoptosis induction. *Apoptosis*, 5 (5):415–418, 2000.

[10] E. Straface, P. Ulderico Giacomoni, and W. Malorni. Cultured cells as a model system for the study of UV-induced cytotoxicity. *J. Photochem. Photobiol. B*, 63(1-3):52–60, 2001.

[11] Y. Taniyama and K. K. Griendling. Reactive oxygen species in the vasculature, molecular and cellular mechanisms. *Hypertension*, 42:1075–1081, 2003.

[12] M. Yokoyama. Oxidant stress and atherosclerosis. *Curr. Opinion in Pharmacol.*, 4:110–115, 2004.

[13] I. E. Kieft, E. P. v. d. Laan, and E. Stoffels. Electrical and optical characterization of the plasma needle. *New J. Phys.*, 6:149, 2004.

[14] E. A. Sosnin, E. Stoffels, M. V. Erofeev, I. E. Kieft, and S. E. Kunts. The effects of UV irradiation and gas plasma treatment on living mammalian cells and bacteria: a comparative approach. *IEEE Trans. Plasma Sci.*, 32(4):1544–1550, 2004.

Chapter 7

A comparison of UV irradiation and gas plasma treatment of cells and bacteria

Abstract
Living mammalian cells and bacteria were exposed to irradiation from narrow-band UV lamps and treated with a non-thermal gas plasma (plasma needle). The model systems were: Chinese Hamster Ovary (CHO-K1) cells (fibroblasts) and Escherichia Coli bacteria. UV irradiation can lead to cell death (necrosis) in fibroblasts, but the doses that cause such damage are much higher than those needed to destroy Escherichia Coli. The usage of UV radiation in combination with active oxygen radicals lowers the UV dose sufficient to kill the cells. However, in any case the fibroblasts seem to be fairly resistant to UV radiation and/or radicals. Possibly, the lamps may be used for decontamination of infected wounds.

The most important active species in an atmospheric plasma are the radicals; the role of UV is less pronounced. Treatment of CHO-K1 cells with the plasma needle can lead to cell necrosis under extreme conditions, but moderate doses cause only a temporary interruption of cell adhesion. Plasma needle may be used for fine tissue treatment (e.g., controlled cell removal without inflammation) and also for bacterial decontamination.

This chapter was published as E.A. Sosnin, E. Stoffels, M.V. Erofeev, I.E. Kieft, S.E. Kunts, The effects of UV irradiation and gas plasma treatment on living mammalian cells and bacteria: a comparative approach, *IEEE Trans. Plasma Sci.*, 32:1544-1550, 2004.

7.1 Introduction

Non-thermal plasmas operate at room or slightly elevated temperatures. Treatment with such plasmas has been demonstrated to be a powerful method of inactivating microorganisms [1–5]. Plasma treatment has many advantages in comparison with other bacterial inactivation methods, such as dry heat or hot steam sterilization, irradiation by UV/gamma rays and other techniques [1]. Plasma decontamination is usually fast, efficient, and safe in terms of thermal, chemical or irradiation damage.

Non-thermal plasmas are easiest to generate under reduced pressures (less than 1 mbar) in specially designed vacuum reactors. In the last decennia, these plasmas found a broad spectrum of applications in material technology. The idea of employing low-pressure plasmas for bacterial inactivation was introduced long ago [2]. Primarily, it was assumed that the key agent in plasma sterilization is the chemistry (highly reactive unstable species - radicals). However, Soloshenko *et al* [3] showed that also the 160-220 nm UV radiation plays an important role in low-pressure plasma sterilization.

Nowadays, a general trend has arisen both in material processing and biotechnology: vacuum reactors are often being replaced by atmospheric plasma sources. There are already various principles and designs, which deliver plasmas operating at temperatures not higher than several tens of degrees. Examples include atmospheric jets [5], dielectric barrier discharges [6], and microplasmas [7]. These new developments allow treatment to materials, which can withstand neither high temperature nor low pressure (e.g., biological tissues). Anti-bacterial properties of atmospheric non-thermal plasmas are already well established [4, 5]. The inactivation of microorganisms proceeds faster than at low pressures; it is ascribed to radical interactions with the membrane, while the role of UV is less important [4].

In parallel to plasma sterilization, treatment with UV radiation alone is a subject of extensive investigations [8–14]. Effective bacterial inactivation was demonstrated for many kinds of bacteria and viruses; various sources were used and the wavelength dependence was determined [12–14]. Furthermore, the synergy of active oxygen radicals and UV was studied [15]. For this purpose, photosensitizers like H_2O_2 were used. This particular molecule produces OH, peroxy and hydroperoxy radicals upon irradiation. It was shown that the joint action of radicals and photons facilitates bacterial inactivation.

In the mentioned studies, UV and plasma treatment was performed *ex vivo*. One is reluctant to apply these media to living tissues because of the risk of cellular damage by UV [16] and radicals [17]. However, we have noticed that the lethal doses for bacteria are surprisingly low. Therefore, in this chapter, we investigate the possibility of *in vivo*

treatment, selective bacterial inactivation without harming the cells. For this purpose, one has to establish what doses of UV or plasma exposure can be applied without extensive tissue damage. We study the reaction of living mammalian cells to UV radiation, using narrow-band UV lamps (excilamps) and Chinese Hamster Ovary (CHO-K1) cells in culture as a model system. These cells are fibroblasts; a basal cell type, which is involved in many processes, e.g., wound repair. We compare the effects of UV radiation on cells with data on UV bacterial deactivation. Furthermore, the case when irradiated cells are immersed in a hydrogen peroxide solution (a photosensitizer) is considered.

Finally, we present some facts on *in vivo* treatment by means of a novel non-thermal plasma source (the plasma needle [7]). A fundamental study has been undertaken to identify all possible responses of living objects exposed to the plasma. This may lead to development of new techniques, like disinfection of tissues or removal of cells without inflammatory response, and on a longer time scale to new methods in the health care.

7.2 The Experimental Setup

7.2.1 Cell culture preparation

CHO-K1 cells were cultured in flasks containing Ham's F-12 medium with stable L-glutamin (Bio Whittaker, Europe) containing 9.0% of Fetal Bovine Serum (FBS, Biochrom AG) and 0.45% of Gentamycin (10 mg ml^{-1}, Biochrom AG). The cells were stored in an incubator at 37 °C with 5% CO_2. To prepare samples for UV treatment, the cells were trypsinized (0.05% Trypsin / 0.02% EDTA solution in PBS, Biochrom AG) and transferred into Petri dishes. For plasma treatment, the same procedure was followed, but the cells were transferred onto sterilized object glasses (26 x 10 x 1 mm, adapted to fit into the plasma chamber) and placed in multiwell dishes. The cells were incubated for 2 or 3 days, or until nearly confluent (see Figure 7.1).
Just before treatment, the medium was removed and the samples were rinsed twice with phosphate buffered saline (PBS). During irradiation or plasma exposure the cells were covered with a thin film of PBS (typically 0.3 mm) in order to prevent them from drying.

7.2.2 Bacterial sample preparation

A pure culture of Escherichia Coli, belonging to the main species of the enterobacteria group, was used. E. Coli is one of the most resistant species within enterobacteria group, so it is frequently used in a study of UV disinfection and sanitation, performed at the Scientific Research Institute of Balneology (Tomsk, Russia). The E. Coli was supplied by

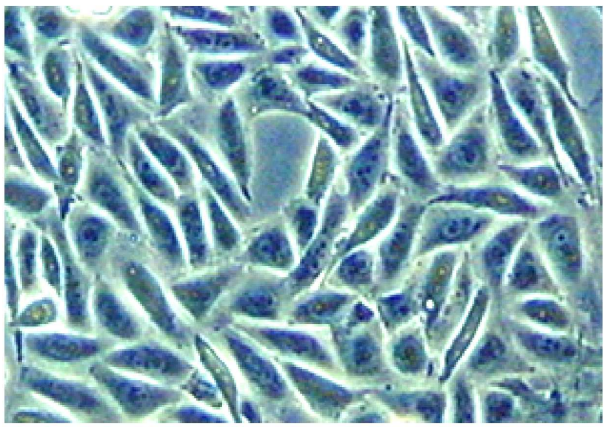

Figure 7.1: *CHO-K1 cells in culture, used for UV and plasma treatment. This is an untreated sample. The cells are about 30 μm long.*

the American National Academy, and had a series number K12 ATCC 25922.
The culture of E. Coli was supported on beef-extract agar (BEA) and kept at the temperature of 4°C. The optimal concentration of microbial dredge was found based on the method of multiple dilutions.

7.2.3 Ultraviolet radiation sources

Irradiation was performed using two low-pressure capacitive discharge UV lamps developed at Laboratory of Optical Radiation, High Current Electronics Institute, Siberian Branch of the Russian Academy of Science [18–22]. These lamps are confined in quartz tubes (38-mm inner diameter and 300-mm-long silica tube with 80% transparency at λ=200 nm).

The first of these lamps is a new excimer lamp, filled with Xe and Br_2 mixture (Type XeBr_LERA_5); the active radiating species is XeBr·. Excimer lamps (or so-called excilamps) are a subclass of electric discharge lamps emitting in UV or vacuum UV spectral ranges. Excilamps provide UV irradiance up to 10 mW cm^{-2} and their efficiency is typically 7%-30%. The main feature which distinguishes excilamps from other UV sources is that their spectra consist of narrow bands (the band halfwidth rarely exceeds 5-8 nm). The B→X band emission adds to as much as 80%-90% of the total radiation of excilamp. By varying the composition of the working mixture it is possible to select a required wavelength. Therefore, excilamps are suited to study wavelength-specific effects of UV radiation on various objects, including microorganisms. The XeBr-excilamp employed in our experiments produces a spectrum with an emission peak at $\lambda \sim 282$ nm and weak D→X and C→A bands. As confirmed in our previous experiments [14], XeBr-lamp is

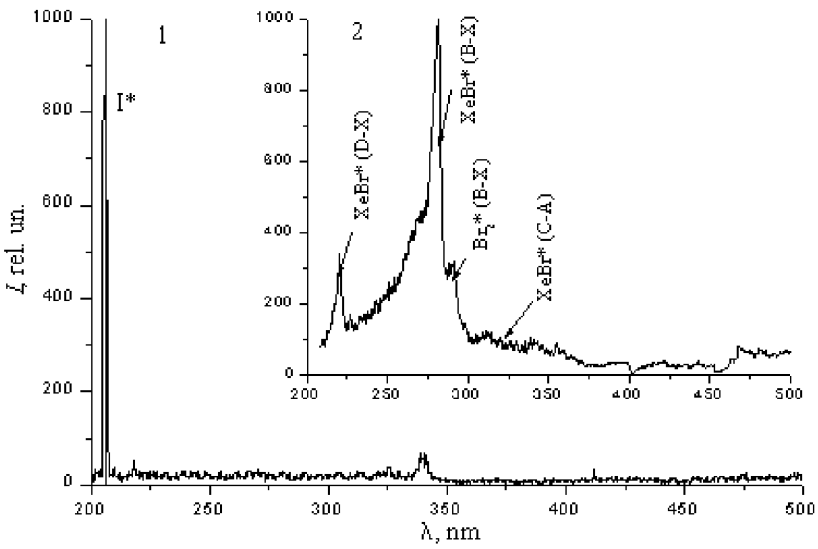

Figure 7.2: *Emission spectra (range 200-500 nm) from two different UV light sources: (1) iodine lamp and (2) XeBr-excilamp.*

most efficient in sterilization. This is because the inactivation of bacteria is mainly related to the DNA/RNA damage, and the maximum absorption of DNA and RNA occurs at the photon wavelength between 240 and 300 nm.

The second light source is a low-pressure lamp (Type I_LERA_5), filled with iodine vapor [19]. The Iodine lamp produces a spectrum with a narrow peak of I· emission at $\lambda \sim 206$ nm.

7.2.4 Low-temperature plasma

A small-size non-thermal plasma (plasma needle) has been developed for the purpose of studying plasma interactions with living species [7]. A plasma needle is an atmospheric glow initiated under helium atmosphere by applying radio-frequency (about 10 MHz) electric voltage to a sharp metal pin. The plasma operates under gentle conditions: the voltage needed to sustain the discharge is low (200-400 V peak-to-peak), and the electric power consumption is only 10-300 mW. The size of the glow is 0.1-1 mm.

It has been previously established that the gas temperature in the plasma is at most a few degrees above the room temperature. Also, energy fluxes from the plasma have been determined for different operation parameters, using a calibrated probe. The total energy flux (radiation, radical and ion contribution) ranges from 0 to 2 W cm^{-2}. The plasma can be applied to heat-sensitive materials or human skin (see Figure 7.3) without any thermal

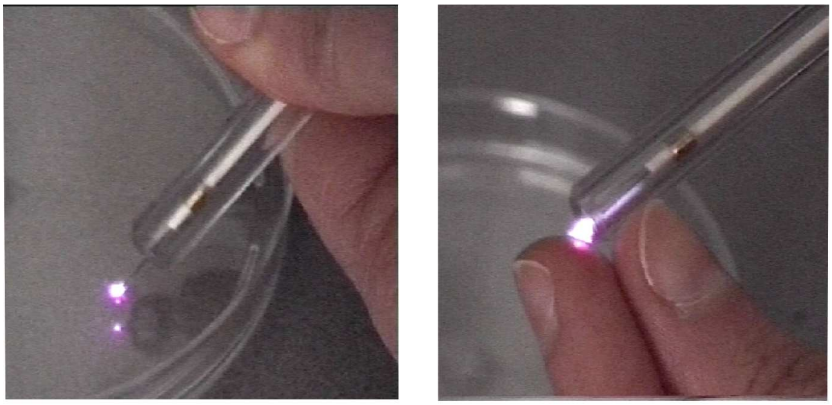

Figure 7.3: *Plasma needle: plasma is created at the tip of a sharp metal needle. (a) Treatment of cells in culture placed in a Petri dish (for precise positioning another setup was used, see Fig. 7.5). (b) The glow spreads over the surface of the tissue.*

damage or pain sensation. From spectral measurements, it follows that this plasma is a poor UV source[1]. Most of the emission (helium lines, nitrogen and oxygen bands) lies within the visible range. Some N_2 bands are detected between 300 and 400 nm, no emission can be found below 300 nm (see typical spectra in Figure 7.4).

Possibly, the plasma could emit radiation in the vacuum UV range ($<$ 100 nm, originating from the helium transitions), which we cannot detect using the present equipment. However, these short-wavelength photons cannot propagate outside the plasma; they are efficiently cut off by air and water (absorption coefficient in water is 10^7 m^{-1} at 100 nm).

The experimental arrangement for cell treatment is shown in Figure 7.5. The chamber was filled with helium at the flow rate of 2 l min^{-1}. Flat samples were placed on the bottom of the chamber, where an externally manipulated stage is installed. The distance between the sample surface and the needle tip was adjusted by means of another manipulator.

7.2.5 Sample treatment

For UV treatment, Petri dishes were placed at 5.5-cm distance from the UV lamp. At this distance, the heating effect of substrate was minimized, while the irradiance could be sufficiently high. The uniformity in the radiation dose over the surface of the sample was about 10%. UV radiation was dosed by varying the treatment time between 2 and 5 min,

[1]Later spectroscopic measurements were performed that showed higher emission in the range 300-400 nm, and revealed UV emission below 300 nm, see section 3.3.2

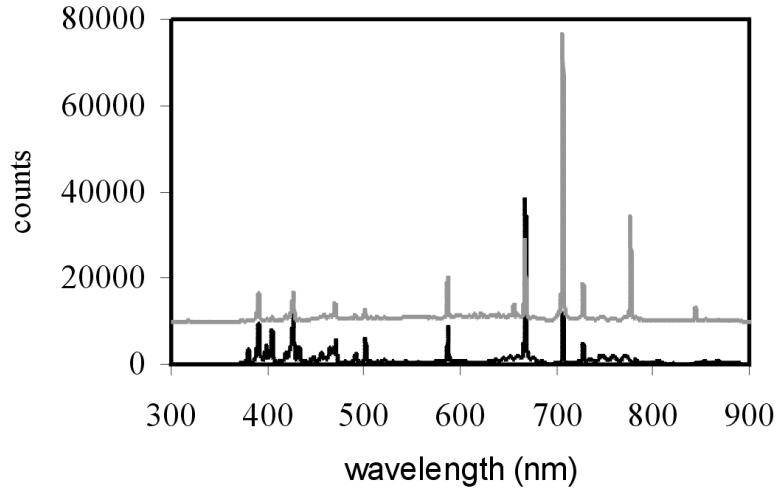

Figure 7.4: *Typical spectra of the plasma: in pure helium (gray line, given an offset of 10 000 counts) and in a mixture of 90% helium and 10% nitrogen (black line). In the latter case, atomic helium lines are suppressed and some N_2 bands emerge below 400 nm.*

while the lamp irradiance was kept constant at 4 mW cm^{-2} for the XeBr lamp and 3 mW cm^{-2} for the I-lamp. All experiments were repeated at least three times.

UV treatment of E. Coli bacteria was performed in Tomsk; Petri dishes with E. Coli cultures were irradiated from several seconds to several minutes at 5-cm distance and at different levels of UV irradiance (up to 10 mW cm^{-2}). Each exposure was repeated four to five times. For control, several dishes were left not irradiated. The number of survivors was determined by the method of bacterial inoculation in dense media (the Koch method of bacterial inoculation in agarized media in Petri dishes). The inoculations were cultivated at the temperature of 20 °C- 23 °C. After 72 h, the number of surviving microorganisms was determined.

During plasma treatment, the object glasses containing the CHO-K1 cells were placed on the moving stage at the bottom of the chamber. Plasma needle was brought at 1.5-mm distance to the sample; visually, the glow was just touching the surface of the PBS solution. Typical treatment time was 1 min, during which the sample was moved by the manipulator over a typical distance of 1 cm. This produces a typical "track" of plasma-treated cells, which can be easily recognized under the microscope. Individual cells on this track were irradiated for 1 to 10 s.

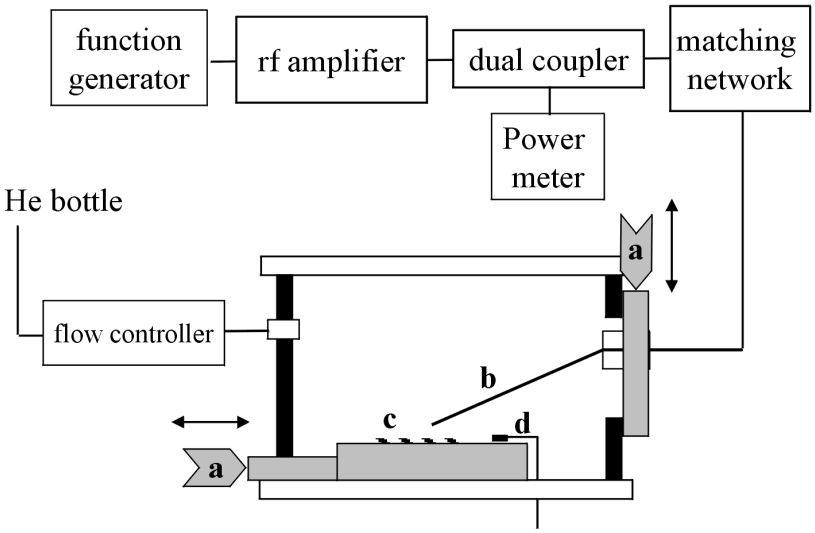

Figure 7.5: *Experimental arrangement for cell treatment with the plasma needle, rectangular metal/plastic box filled with helium. (a) Manipulators to move the sample and to adjust the needle - sample distance, (b) the needle, (c) the sample, and (d) a thermocouple to control the temperature.*

7.2.6 Observation

After treatment, the samples were observed under a light microscope. Trypan blue (0.5% in physiological saline, Biochrom) was applied in order to distinguish between dead and living cells. Trypan blue penetrates only the cells with membrane leakage (dead cells) and colors the whole cytoplasm blue; the living cells remain colorless. Dead and living cells were counted and the fraction of survivors was determined. The surviving fraction (SF) is defined by $N/N_0 \cdot 100\%$, where N_0 is the initial number of cells, and N the number of surviving cells. Mean values were calculated from numbers found in five different places of a Petri dish.

In some cases (mainly after plasma treatment), no trypan blue was applied, but the samples were incubated for several hours in order to study the long-term post-treatment phenomena.

7.3 Results and Discussion

As expected, high UV doses result in cell damage and death by necrosis (rupture of cell membranes). It can be seen in Figure 7.6, where a sample treated with the iodine lamp

at 0.6 J cm^{-2} and subsequently stained with trypan blue contains a mixture of dead and surviving cells. The dependence of the fraction of SF on the irradiation dose is displayed in Figure 7.7.

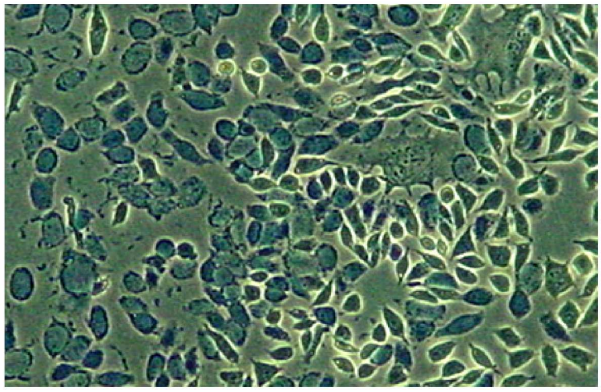

Figure 7.6: *A CHO-K1 sample irradiated by the iodine lamp at 0.6 J cm^{-2}. Most of the cells are necrotic.*

The most striking feature is the presence of a threshold. The process of inactivation begins only after some critical dose of radiation, which is about 0.5 J cm^{-2} for the iodine and 0.7 J cm^{-2} for the XeBr lamp. All cells within the irradiated area are dead when the dose exceeds 0.7 J cm^{-2} for iodine and 1 J cm^{-2} for XeBr lamp. The UV dose (threshold and lethal dose) is lower for UVC (I-lamp) than for UVB (XeBr lamp). This can be easily understood because absorption of UV radiation by lipids in cell membranes is highest for $\lambda <$ 230 nm [23] and the irradiated power of the iodine lamp lies mainly in this range (Fig. 7.2).

The presence of the threshold dose for cell deactivation (Fig. 7.7) makes these results significantly different from the ones obtained for deactivation of Escherichia Coli and other bacteria, widely reported in the literature [10–15]. For comparison, we include typical bacterial survival curves, resulting from the irradiation of E. Coli with XeBr and KrCl (λ = 222 nm) excilamps (both developed in the High Current Electronics Institute, Tomsk). These are given in Figure 7.8 and 7.9, respectively. First of all, one can immediately see that UV doses needed to deactivate E. Coli are much lower than the ones that cause necrosis in fibroblasts. Besides, already very low UV doses reduce the bacterial population by two decades. At higher doses, the killing rate is somewhat tempered, and the survival curves display exponential tails. Decontamination to 0.01% of the original population is achieved by UV doses, which are still too low to affect fibroblasts (at least not on the short term, or on a typical time scale of 2 days during which CHO-K1 cells can be maintained in the incubator). This shows that fibroblasts are extremely resistant to UV. Irradiation with UV lamps may become a method of selective bacterial decontamination of wounds

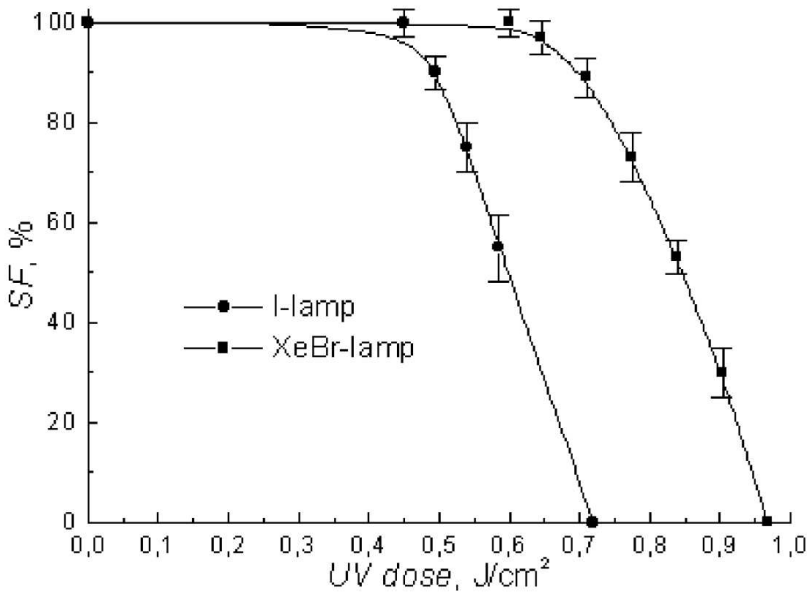

Figure 7.7: *The survival curve of CHO-K1 after treatment with UVB (block) and UVC (circle) radiation. Cells were irradiated at 37 °C.*

without killing the body cells that strive to repair the wound.

Note that the survival curve of fibroblasts (Fig. 7.7) does not have an exponential tail. This is most likely because the cell counting after irradiation was done after two-step flushing with PBS solution. In this way, small amounts of alive cells could be flushed away. Besides, we could not apply UV doses much higher than 1 J cm^{-2}, because of cell desiccation due to a too long treatment time or heat damage at a too short distance from the lamp.

In order to simulate the conditions characteristic for plasma treatment, it is necessary to supply active radicals simultaneously with UV irradiation. This can be performed using a photosensitizer, such as H_2O_2, which produces reactive oxygen species upon UV irradiation. Possibly, in the current experiment, the conditions were similar to those described by Soloshenko *et al* [3], who performed effective bacterial inactivation in a low-pressure plasma. However, it is difficult to compare the exact UV doses, because a low-pressure plasma emits also photons with a shorter wavelength (< 200 nm). These photons are normally lost by absorption in air at ambient pressure, but they can reach the surface when the sterilized object is surrounded by plasma under low-pressure conditions.

We used radiation with $\lambda = 206$ nm (I-lamp), which is not efficiently absorbed in air or water. A 3% aqueous H_2O_2 solution was applied to the CHO-K1 culture just before irra-

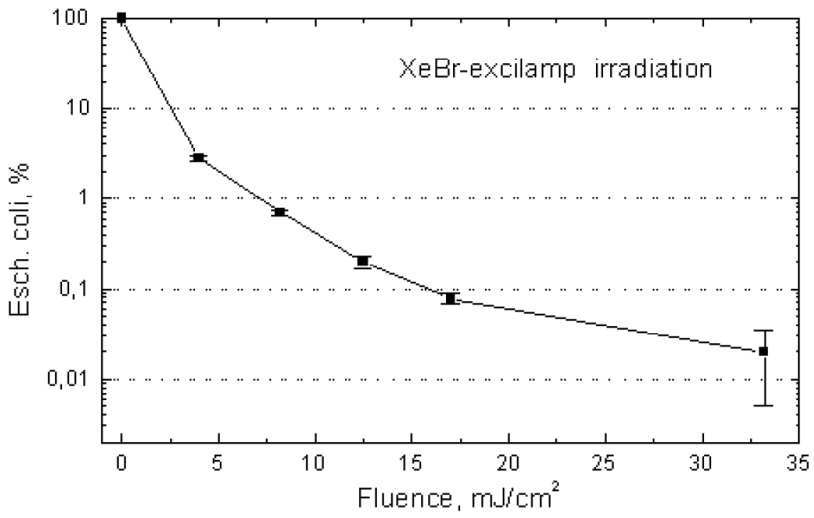

Figure 7.8: *The survival curve of Escherichia Coli irradiated with UVB (XeBr-excilamp).*

diation; the layer of fluid was about 1-mm thick. The H_2O_2 solution alone (without lamp irradiation) has also some toxic effects on cells, because small amounts of reactive oxygen species are released by decomposition of H_2O_2 by ambient light. However, the cells could survive in this environment for several minutes. The UV lamp in Figure 7.10 was applied to cell/H_2O_2 samples for up to 5 min. The last points, corresponding to long treatment times, may be influenced by natural toxicity of peroxide solution. However, when the UV was applied, we observed a major increase of the killing rate, even at short treatment times. Fig. 7.10 demonstrates that the usage of H_2O_2 together with UVC lowers the lethal radiation dose by a factor of two (compare with Fig. 7.7). Moreover, there is no threshold in the inactivation curve; the fraction of dead cells increases approximately linearly with increasing UV dose.

Similar studies of the effect of 1% H_2O_2 in combination with 254-nm radiation on bacteria were described by other authors [15]. They reported an efficient reduction of bacterial population; the UV doses needed to inactivate 99.99% of microorganisms were in some cases even ten times lower than in absence of a photosensitizer.

From the above results, it can be concluded that the effect of UV (alone or in combination with active radicals) on fibroblasts is by far not so drastic as on bacteria. The rate of killing cells is much lower than that for E. Coli (compare linear scales in Figs 7.7 and 7.10 with logarithmic scales in Figs 7.8 and 7.9), and the cells can withstand relatively large UV and radical doses. However, at present, we cannot decide on possible DNA damage in

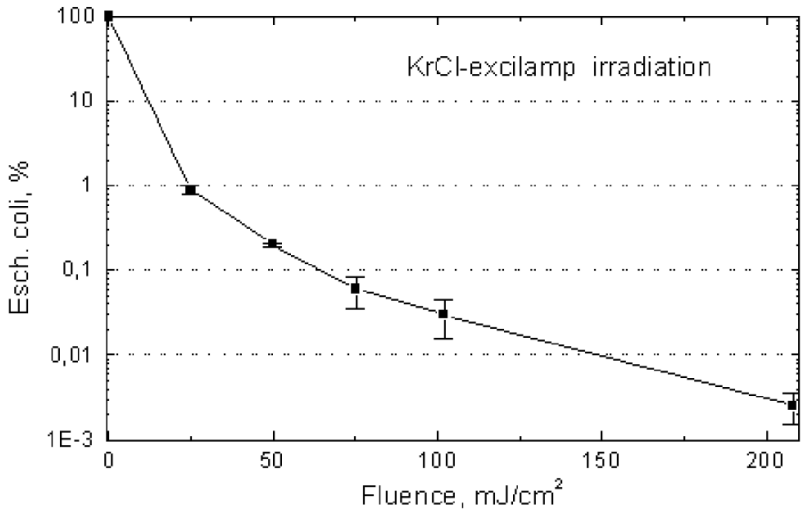

Figure 7.9: *The survival curve of Escherichia Coli after irradiation with a KrCl-excilamp (222 nm).*

cells, which have survived the UV treatment. For this purpose, cells should be observed for a long time, and CHO-K1 is not the most suitable cell line for such studies. Furthermore, at present, we cannot decide on the performance of UV lamps in *in vivo* disinfection. For this purpose, more tests must be performed on various kinds of bacteria. The bacterial spores must be investigated, because they may be more resistant to irradiation.

A UV lamp in combination with H_2O_2 may be compared to a low-pressure plasma [3], because the latter is a reasonable UV source (after all, the excilamps described here are also based on low-pressure plasmas). In case of the atmospheric plasma needle, the conditions are milder. As stated before, plasma needle is a poor UV emitter[2]. The plasma-related effects are rather of chemical nature (radicals). It is known that radicals alone are also capable of inactivating bacteria, though not as efficient as in combination with UV. Recently, bacterial inactivation with the plasma needle was performed on E. Coli [24]. The reduction of bacterial population by two decades (99%) was achieved within 1-2 min at the power level of about 10 mW. This dose does not cause any reaction in CHO-K1, which again confirms the particularly high sensitivity of E. Coli bacteria to UV/plasma treatment. Therefore we are confident that it is possible to find plasma conditions under which the bacteria are eliminated, but cells remain alive. When higher plasma doses are applied (>10 mW), interesting cell reactions are induced. We shall describe some general features of plasma interactions with CHO-K1 cells.

[2]see footnote on page 98

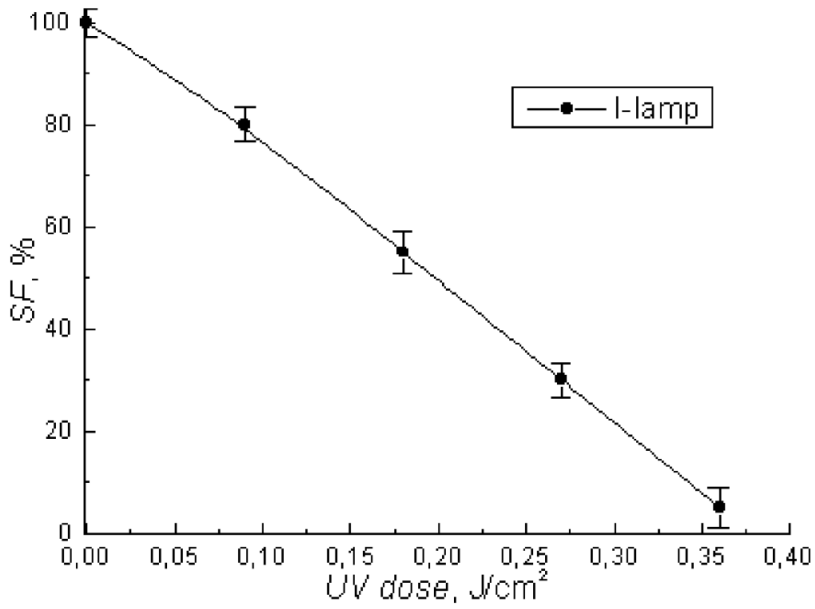

Figure 7.10: *The survival curve of CHO-K1 after irradiation with the iodine lamp in presence of 3% H_2O_2 aqueous solution. Cells were irradiated at 37 °C.*

Plasma treatment of living cells can have many consequences. Naturally, a high dose leads to cell death (necrosis). Typically, necrosis occurs when the plasma power is higher than 0.2 W and the exposure time is longer than 10 s (per treated spot). In terms of energy dose, this corresponds to 20 J cm^{-2}, which is very high. However, even upon such harsh treatment the cells are not disintegrated, but they retain their shape and internal structure (see Figure 7.11).

When the power and treatment time were substantially reduced (to 50 mW and 1 s per spot), no necrosis was observed. The cells remained negative to trypan blue. In Figure 7.12, it can be seen that the cells (partly) detach from the sample surface. Characteristic voids are created in the sheet of cells (Figure 7.12a). The partly detached cells assume a rounded shape (Fig. 7.12b).

Careful observation of treated samples showed that detachment is not an instantaneous reaction; it can occur within seconds or even up to 1 min after treatment. Viability of detached (rounded) cells was studied using assays described elsewhere [25]. Here, we can state that the interruption of cell adhesion is a temporary effect. The cells remain unharmed and after several (2 to 4) hours the attachment is restored. It seems that plasma treatment induces a temporary disturbance in the cell metabolism, which is expressed (among

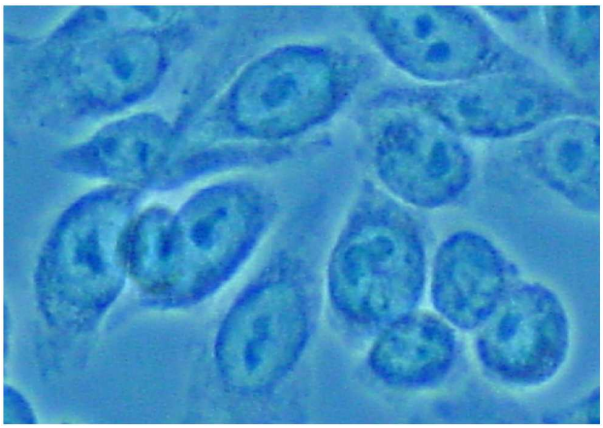

Figure 7.11: *Necrotic cells after treatment with the plasma needle at 0.3 W. These cells are stained with trypan blue (the membranes are damaged).*

others) by loss of adhesion. The reactive agent, responsible for this behavior has not been identified yet. It was checked that radio-frequency electric fields and static electricity do not induce such effects. Detachment is most likely caused by plasma species, which are in direct contact with the cell (under PBS solution). The role of active radicals cannot be ruled out. However, these are probably not the oxygen species created in photo-sensitized UV treatment with H_2O_2, because in the latter case no cell detachment was observed. In near future, we shall investigate whether positive ions from the plasma can trigger this specific cell reaction.
Cell detachment without severe damage is a refined way of cell manipulation. The loosened cells can be removed from a tissue, but as they are still alive, no inflammatory response should be induced. The area of plasma action is always well defined; the influenced cells are strictly localized and the borders between affected and unaffected zones are very sharp. This demonstrates the locality and precision of plasma treatment.

7.4 Conclusions

The effect of UVB and UVC radiation on Chinese Hamster Ovary (CHO-K1) cells in culture was studied. These cells are fibroblasts, a cell type that in important in tissue repair. The UV radiation was supplied by two novel lamps, which are characterized by narrow band spectrum with 80%-90% of the irradiated power lying in the UVB and UVC range, respectively. The UV dose that leads to necrosis in fibroblasts is more than ten times higher than the one needed for deactivation of E. Coli bacteria. The deactivation curve for CHO-K1 cells displays a rather high threshold of 0.5-0.7 J cm^{-2}; above this value, the

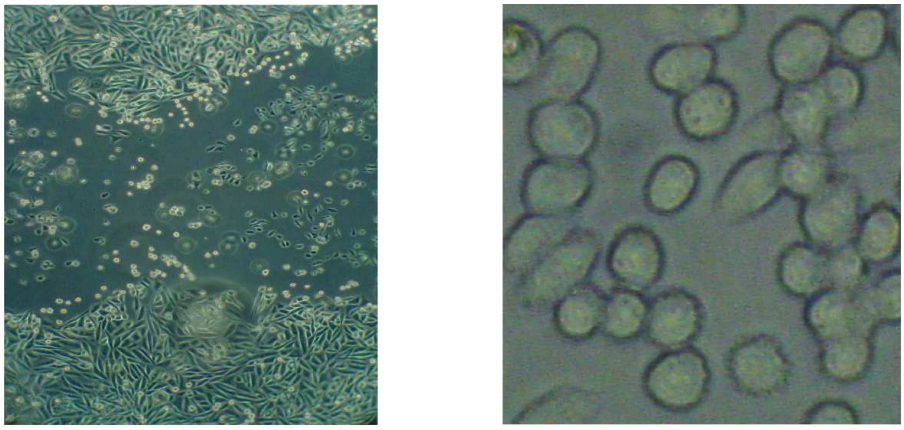

Figure 7.12: *: Treatment of CHO-K1 cells by the plasma needle at low power (50 mW) results in cell detachment. (a) A plasma-treated spot (track) in the sample, with a typical void resulting from cell detachment. (b) A close-up of the edge of the treated area: partly detached cells. When cell adhesion is interrupted, they assume a rounded shape (not spread over the surface like in Fig. 7.1). This situation is temporary; the contact between cells is restored within several hours.*

number of survivors decreases approximately linearly with increasing UV dose. The lethal UV doses (no survivors) for the fibroblasts are 1 J cm^{-2} for UVB and 0.7 J cm^{-2} for UVC radiation. In contrast, the threshold for inactivation of E. Coli (if existing) is extremely low, and the number of survivors decreases with increasing dose in a bi-exponential way.

When the photosensitizer (H_2O_2) was used together with the UV source, the cells were destroyed more readily than in case of UV irradiation alone; this is due to the joint action of UV and *in situ* formed active oxygen radical species. The threshold UV dose is drastically lowered, but the amount of survivors versus UV dose is still linear. The effects of UV and photosensitizer on E. Coli bacteria are much more drastic than on the cells.

Photosensitized UV treatment bears some resemblance to plasma treatment, but the UV emission from the lamp is usually more intense than plasma emission. We treated the fibroblast cells with a non-thermal plasma, which is an efficient source of radicals, but a poor source of UV. Under low-power conditions plasma treatment does not cause cell necrosis at all. However, an interesting cell reaction was observed; a temporary disturbance in cell adhesion. The loosened cells are viable and can be removed or rearranged on the substrate.

In the view of future *in vivo* applications, UV treatment may provide a method to decontaminate tissues. However, we realize that the presented results are valid for one kind of bacteria (E. Coli). Although E. Coli, as a Gram-negative type, is fairly resistant, there might be other species that are more difficult to eliminate; especially, the efficiency of

spore deactivation must be investigated. Therefore, additional studies are needed to assess the performance of UV decontamination. Plasma treatment offers possibilities of sophisticated tissue modification, like local removal or manipulation of cells without damage to the tissue. However, before the UV lamp and plasma techniques may be implemented, extensive studies of long-term effects of UV and plasma on living tissues must be performed. These studies should involve assays for possible DNA damage, and *in vivo* tests on animals.

7.5 Acknowledgment

The authors would like to thank D.V. Shitz and A.A. Lisenko for their assistance in this study.

References

[1] S. Lerouge, M. R. Wertheimer, and L. H. Yahia. Plasma sterilisation: a review of parameters, mechanisms, and limitations. *Plasmas Polym.*, 6:175–188, 2001.

[2] S. J. Fraser, R. B. Gillette, and R. L. Olson. Sterilizing process and apparatus utilizing gas plasma. *U. S. Patent 3*, 948:601, 1976.

[3] I. A. Soloshenko, V. V. Tsiolko, V. A. Khomich, A. I. Shchedrin, A. V. Ryabtsev, V. Yu Bazhenov, and I. L. Mikhno. Sterilization of medical products in low-pressure glow discharges. *Plasma Phys. Rep.*, 26:792–800, 2000.

[4] M. Laroussi. Nonthermal decontamination of biological media by atmospheric-pressure plasmas: review, analysis, and prospects. *IEEE Trans. Plasma Sci.*, 30(4):1409–1415, 2002.

[5] H. W. Herrmann, I. Henins, J Park, and G. S. Selwyn. Decontamination of chemical and biological warfare (CBW) agents using an atmospheric pressure plasma jet. *Phys. Plasmas*, 6(5):2284–2289, 1999.

[6] B. Gellert and U. Kogelschatz. Generation of excimer emission in dielectric barrier discharges. *J. Appl. Phys.*, B52:14–21, 1991.

[7] E. Stoffels, A. J. Flikweert, W. W. Stoffels, and G. M. W. Kroesen. Plasma needle: a non-destructive atmospheric plasma source for fine surface treatment of (bio)materials. *Plasma Sources Sci. Technol.*, 4:383–388, 2002.

[8] J. C. H. Chang, S. F. Ossoff, D. C. Lobe, M. H. Dorfman, C. M. Dumais, R. G. Qualls, and J. D. Johnson. UV inactivation of pathogenic and indicator micro-organisms. *Appl. Environ. Microbiol.*, 49:1361–1365, 1985.

[9] G. D. Harris, V. D. Adams, D. L. Sorensen, and M. S. Curtis. Ultraviolet inactivation of selected bacteria and viruses with photoreactivation of bacteria. *Wat. Res.*, 21:687–692, 1987.

[10] J. K. Race and M. Ewell. Examination of peak power dependece in the UV inactivation of bacterial spores. *Appl. Environ. Microbiol.*, 67:5830–5832, 2001.

[11] J. G. Anderson, N. J. Rowan, MacGregor S.J., R. A. Fouracre, and O. Farish. Inactivation of food-borne enteropathogenic bacteria and spoilage fungi using pulsed-light. *IEEE Trans. Plasma Sci.*, 28:83–87, 2000.

[12] S. A. Craik, D. Weldon, G. R. Finch, J. R. Bolton, and M. Belosevic. Inactivation of cryptosporidium parum oocysts using medium- and low-pressure ultraviolet radiation. *Wat. Res.*, 35:1387–1398, 2001.

[13] N. Giese and Darby J. Sensitivity of microorganisms to different wavelengths of UV light: implications on modelling of medium pressure UV systems. *Wat. Res.*, 34:4007–4013, 2000.

[14] E. A. Sosnin, L. V. Lavrent'eva, M. R. Yusupov, Y. V. Masterova, and V. F. Tarasenko. Inactivation of Escherichia coli using capacitive discharge excilamps. *Proc. 2nd Internat. Worksh. on Biol. Effects of Electromagn. Fields, Rhodos (Greece)*, pages 953–957, 2002.

[15] K. F. McDonald, R. D. Curry, R. E. Clevenger, B. J. Brazos, K. Unklesbay, A. Eisenstark, S. Baker, J. Golden, and R. Morgan. The development of photosensitized pulsed and continuous ultraviolet decontamination techniques for surface and solutions. *IEEE Trans. Plasma Sci.*, 28:89–96, 2000.

[16] J. E. Cleaver. Repair processes for photochemical damage in mammalian cells. *Adv. Rad. Biol.*, 4:1–75, 1974.

[17] V. Vallyathan, V. Castranova, and X. Shi. *Oxygen/nitrogen radicals: cell injury and disease.* Kluwer Acad. Publishers, Boston, 2002.

[18] E. A. Sosnin, M. V. Erofeev, V. F. Tarasenko, and D. V. Shitz. Capacitive discharge excilamps. *Instrum. Exper. Tech.*, 45:118–119, 2002.

[19] E. A. Sosnin, M. V. Erofeev, A. A. Lisenko, V. F. Tarasenko, and D. V. Shitz. Capacitive discharge excilamps performance investigations. *Optical J. (St. Petersburg)*, 69:77–80, 2002.

[20] M. V. Erofeev, E. A. Sosnin, V. F. Tarasenko, and D. V. Shitz. Efficient XeBr-excilamp excited by capacitive discharge. *Atmos. Oceanic Opt.*, 13:862–864, 2000.

[21] M. I. Lomaev, V. S. Skakun, E. A. Sosnin, and V. F. Tarasenko. Effective sealed-off excilamps excited by capacitive discharge. *Tech. Phys. Lett.*, 25:27–32, 1999.

[22] M. I. Lomaev, V. S. Skakun, E. A. Sosnin, and V. F. Tarasenko. Operating mixtures of HF capacitive discharge excilamps. *RU patent 2, 154*, page 323, 1998.

[23] Yu. A. Vladimirov and A. Ya. Potapenko. *Physics and chemistry of photobiological processes.* High School Publishing, Moscow, 1989.

[24] R. E. J Sladek, E. Stoffels, R. Walraven, P. J. A. Tielbeek, and R. Koolhoven. Plasma treatment of caries: a novel method in dentistry. *IEEE Trans. Plasma Sci.*, 32(4):1540–1543, 2004.

[25] E. Stoffels, I. E. Kieft, and R. E. J Sladek. Superficial treatment of mammalian cells using plasma needle. *J. Phys. D: Appl. Phys.*, 36:2908–2913, 2003.

Chapter 8

Plasma treatment of *ex vivo* arteries: preliminary results

Abstract
The plasma needle is a source to produce small non-thermal plasma at atmospheric pressure. The volume of the plasma is small (~ 1 mm^3) and it can thus be applied to induce various effects with precision.
Previous experiments have shown that cultured cells that were exposed to non-thermal plasma for tens of seconds, detach from their surface and contiguous cells, but remain viable. However, the environment of cells in culture differs substantially from cells in intact tissue. Therefore, pilot experiments have been performed to investigate the effect of plasma needle treatment on tissue. Carotid arteries of C57BL/6 and Swiss mice were treated and subsequently examined over their entire wall thickness using two-photon laser scanning microscopy (TPLSM).
Initially, arteries were treated in dry environment to ensure good reproducibility of plasma effects. However, cell damage was induced by dehydration. Furthermore, when higher plasma powers were used, the thickness of the arterial wall and elastin layers were affected, probably by heat. Experimental procedures were optimized and the influence of mounting procedures and tissue dehydration were investigated. In subsequent experiments, the artery was covered by a thin layer of liquid during treatment to prevent cell death by helium flow. The effects of plasma treatment appeared to be induced superficially and were not dependent on plasma power, when it was varied between 160 mW and 400 mW. After plasma treatment, most adventitia cells and only a few smooth muscle cells were necrotic. Further experiments have to be performed to elucidate the observed effects, and to distinguish between apoptosis and necrosis of cells.

Parts of this chapter were published as I.E. Kieft, K. Douma, R.T.A. Megens, M.A.M.J. van Zandvoort, D.W. Slaaf, E. Stoffels, Non-thermal plasma treatment of *ex vivo* arteries: preliminary results, *ICPIG 2005 proceedings*

8.1 Introduction

In the last decade, plasma applications in the biomedical field have been expanding. Examples of *ex vivo* applications include the sterilization of medical equipment and coating or surface modification of implants to achieve bio-compatibility [1]. An example of *in vivo* plasma application is argon plasma coagulation (APC) [2]. The latter application is based on high-power plasma that devitalizes the tissue by heat. In contrast, the plasma generated by the plasma needle [3] is essentially non-thermal. Therefore, the plasma needle has the potential to become a more refined surgical tool to locally influence cells and tissues.

Plasma treatment of cultured cells led to reversible cell detachment: cells remained alive and reattached within several hours [4, 5]. Furthermore, a small percentage of cells exhibited apoptosis. Necrosis was observed only when high powers were applied (> 200 mW). It is interesting to assess whether these effects also occur after treatment of tissues and to check whether these effects are dependent on plasma conditions. A tissue consists of an inhomogeneous cell population embedded in an extracellular matrix; the latter may influence cell reactions. We chose to treat arteries because the structure of arteries has been extensively described in scientific literature, especially with focus on atherosclerosis [6].
Injury models studied for better understanding of arterial functioning include damage caused by heating [7–10], beta particles (high energy electrons), gamma rays [11, 12], or oxidative stress [13–15]. Heating is known to cause denaturation of collagen and damage to smooth muscle and endothelial cells. Furthermore, it causes a decrease in diameter (shrinkage) of the artery. Ionizing radiation is used to prevent restenosis in atherosclerotic lesions treated with balloon angioplasty and stenting. The delivered radiation causes chromosomal damage in vascular fibroblasts, smooth muscle cells, and endothelial cells, which results in the loss of ability to proliferate [12]. Oxidative stress plays a role in formation of atherosclerotic lesions.
The plasma needle can induce thermal effects and/or cause oxidative stress. Primarily, plasma treatment of arteries may provide a new non-contact injury model that will help to understand mechanisms involved in atherosclerosis and arterial tissue repair. Possibly, when in the future the effect of plasma on cell proliferation rate and detachment is better understood, the needle may become a new tool for treatment of vascular lesions.

In this chapter we show first results of plasma treatment of arteries obtained using Two-Photon Laser Scanning Microscopy (TPLSM), a technique that combines good axial and lateral resolution with a large penetration depth [16]. It can be used to visualize cellular structures in intact arteries [17].
Murine arteries were chosen for this study since they are small (lumen diameter ~ 300 μm)

and contain only 2 to 3 layers of smooth muscle cells [6]. This allows good visualization of plasma effects. Furthermore, the genetic background of mice is well established, and genetically modified mice are often used as model for atherosclerosis. Initially, treatments were performed on dry arteries, without liquid coverage, taking a risk of dehydration. This was done because thickness of a liquid layer is difficult to measure, which would influence reproducibility. However, this treatment procedure caused a high amount of cell death, most likely due to dehydration. Thus, we decided to cover the artery with a thin liquid layer in subsequent experiments.

8.2 Experimental

8.2.1 Plasma treatment

The plasma needle consisted of a sharpened metal pin (diameter 0.3 mm) that was confined in a Perspex tube (Figure 8.1). Helium was supplied through the tube (2 l min^{-1}), which provided plasma operating in helium/air mixtures [3, 18].

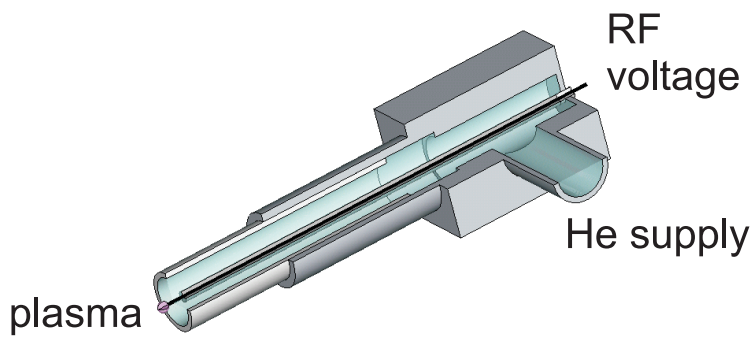

Figure 8.1: *Schematic drawing of the plasma needle.*

An RF signal (13.56 MHz) was generated by a waveform generator (Hewlett Packard 33120A) and amplified by an RF amplifier (Kalmus model 125C-CE). From the amplifier, the signal was directed to a home-built matching network. The resulting voltage at the tip of the needle was around 200 V_{rms}.
An Amplifier Research PM 2002 power meter with dual directional coupler was placed between source and matching network to measure forward and reflected power. Dissipated plasma power was determined using a subtraction method [19]: the difference in nominal

power with and without plasma at the same voltage was used to estimate dissipated plasma power. The value used for treatment will be indicated in the text.

8.2.2 Temperature measurements

Temperatures were roughly estimated using liquid crystal temperature strips (VWR). At the specific temperature, the color of the strip turned black. The strips had a working range of 37-65 °C in steps of 3 to 5 degrees centigrade. The needle was placed for 1 min above the strips with the tip of the needle at 1-mm distance from the strips.
Temperatures were measured both on dry strips and through a thin liquid layer.

8.2.3 Tissue preparation

Carotid arteries were obtained from C57BL/6 and Swiss mice. Mice were fed normal chow. They were killed using an overdose of CO_2, after which the arteries were excised and carefully cleaned from excessive connective tissue. For the experiments in dry environment the arteries were placed in hydroxyethyl piperazineethanesulfonic acid (HEPES) solution for one day before plasma treatment was performed. For experiments on influence of treatment procedures, arteries were dissected on the day of the experiment and placed in Hank's Buffered Saline Solution (HBSS). This buffer consisted of potassium chloride (5.36 mM), sodium chloride (136.89 mM), disodium phosphate (0.34 mM), potassium dihydrophosphate (0.44 mM), calcium chloride (2.50 mM), magnesium sulphate (1.09 mM), HEPES (15.00 mM) and glucose (5.56 mM).

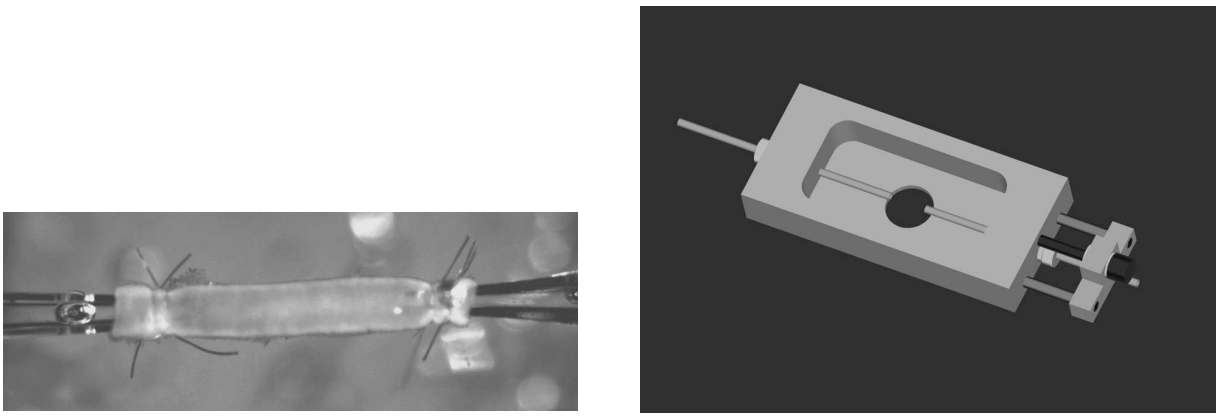

Figure 8.2: *Carotid artery mounted in a home-built perfusion chamber with inner dimension of 5 x 2.5 x 1 cm (IDEE, Maastricht). The average length of the artery segment is 3-4 mm.*

Arteries were mounted as shown in Figure 8.2. First they were tightened onto glass micropipettes and then pressurized. The transmural pressure was 40 mm Hg.

8.2.4 Plasma treatment

For good reproducibility of the experiments, treatment of the artery was started without coverage with liquid. A variation in the thickness of the medium layer results in a variation of active plasma species reaching the tissue. This affects the treatment, as was also found in Chapter 6. Plasma was applied at a distance of 1 mm to the outside of the artery using a micro-positioner. Standard treatment time was 60 s, unless stated otherwise.

Treatment of dry artery carries the risk of damage by dehydration. To assess and minimize damage by other factors than plasma, several experiments testing the experimental conditions were performed.
The dissection of the artery and its mounting in the perfusion chamber may cause damage, especially to the outer and most vulnerable layers. In the chamber, the artery was kept in HBSS for preservation and to prevent dehydration. Experiments have been performed to investigate the condition of the artery at this point, thus before plasma treatment.
If plasma treatment is to be performed on dry arteries, they suffered dehydration by air for at least 3 minutes. Experiments to check the effect of this dehydration were performed by removing the medium for 4 minutes. The influence of the helium flow was determined using exactly the same procedure as for plasma treatment, but without igniting the plasma. When plasma is applied to the artery, it is accompanied by a standard helium flow of 2 l min^{-1}. To investigate the influence of the helium flow, application times and flow velocity were varied.

8.2.5 Microscopy

The arteries were imaged using TPLSM. A Nikon E600FN upright microscope was incorporated in a BioRad 2100MP imaging system, using a Spectra Physics Tsunami Ti:Sapphire laser as excitation source. The latter was tuned and mode-locked at 800 nm or 850 nm. The latter was used for experiments using only PI labeling. A water-dipping objective lens 60X (NA= 1.0) was used.
Three photomultipliers detected fluorescence in different spectral ranges. Filters were used to select the wavelengths of interest. The data were imaged using a Kalman filter.

8.2.6 Staining procedure

Several assays were used to visualize distinct parts of the tissue. These will be indicated in the text. Samples were incubated with the probes for at least 30 minutes. All fluorochromes described are two-photon excitable.
To stain cell nuclei, SYTO 13 or SYTO 44 (both Molecular Probes, Leiden, The Netherlands) was used. Labeling concentration of SYTO 13 was 1 or 2 μM in either phosphate-buffered saline (PBS) or HBSS. Emission peak of SYTO 13 is at 510 nm. Instead of SYTO 13, sometimes SYTO 44 was used, which emits at a wavelength around 472 nm. SYTO 44 was applied in a concentration of 1.5 μM.
Usually arteries were co-stained, for example by combining SYTO 13 and Eosin (staining elastin with an emission peak at 545 nm). Labeling concentration for Eosin was 0.25 or 0.5 μM in PBS or HBSS.
To detect membrane leakage, Propidium Iodide (PI; Molecular Probes) was applied. PI penetrates membrane-damaged cells, binds to their RNA and DNA, and emits at a wavelength around 617 nm. It was applied in a concentration of 2 μg ml^{-1}.
As PI and SYTO both bind to DNA and RNA, a combined assay would result in competition between the two fluorochromes. Experiments were performed to visualize the result of the competition. To detect necrotic cells, it is important that cells initially stained with SYTO can still bind PI when damage is induced. In the experiment, the artery was stained with SYTO and PI and afterwards helium flow was applied with no liquid surrounding the artery. Then it was again incubated with PI for at least 30 minutes.

8.3 Results and discussion

8.3.1 Temperature measurements

Figure 8.3 displays temperatures measured at 1 mm from the needle tip after 1 minute of treatment. We were not able to measure temperatures below 37 °C and above 65 °C. Thus, when 65 °C is indicated in the figure, this means the temperature was at least 65 °C. Temperature was measured using both the standard 2.0 l min^{-1} and 0.5 l min^{-1}, because a lower flow rate could possibly lead to less damage of the artery.

Temperatures in the figure are valid for plasma treatment in dry environment. For a helium flow of 2 l min^{-1}, plasma powers up to 100 mW could be applied without risk of thermal damage as the temperature remained at 37 °C or below. When the flow rate was decreased to 0.5 l min^{-1}, temperature increased quickly with increasing power.

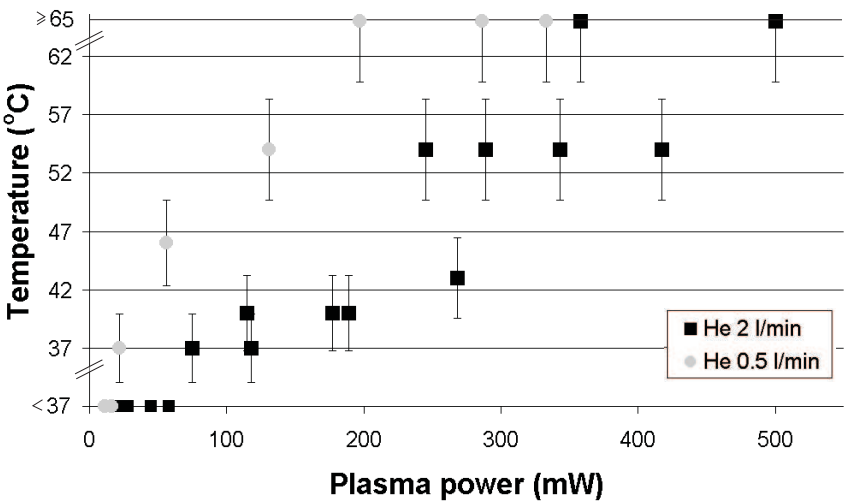

Figure 8.3: *Temperature in air at 1-mm distance from the needle using 2 l min^{-1} and 0.5 l min^{-1} helium flow. Error bars indicate accuracy of the strips. The exact temperature of points below 37 °C and of points at or above 65 °C could not be measured.*

The temperatures displayed in Fig. 8.3 may be higher than the temperature of an arterial sample at the end of plasma treatment. One reason is that before start of the treatment, samples are at room temperature. Furthermore, the thermal capacity of the liquid-filled vessels is larger than that of the strips. This means that more energy is required for an increase in temperature of the vessels than for the same increase in temperature of the strips.
To determine the temperature on the inside of the artery during treatment, an artery was sliced longitudinally and placed on top of the temperature strips with the adventitia facing the needle. The temperature was determined not to reach 40 °C when 400-mW plasma was applied, which means endothelial cells are hardly influenced by heat during plasma treatment in dry environment. Further experiments have to be performed to determine the exact temperature of the samples during treatment.

Furthermore, temperature was measured underneath a thin layer of water (about 0.5 mm) for treatment in a wet environment, and 37 °C was not exceeded for plasma powers up to 700 mW. However, the temperature will be strongly dependent on the thickness of the liquid layer, which could not be measured accurately.

8.3.2 Plasma irradiation of arteries in dry environment

The structure of the vessel wall can be divided into three regions. The first is the adventitia or the outermost connective tissue covering the vessel containing collagen and fibroblasts (amongst others). The second is the tunica media that consists of several layers of elastin and smooth muscle cells (SMC). The third layer consists of the internal elastic lamina (IEL) and vascular endothelium, which is in direct contact with blood [20]. Because the plasma was applied to the outside of the vessel, the highest dose of ultraviolet (UV) light and radicals was applied to the adventitia.

Treatment of arteries without medium covering them would improve reproducibility of plasma effects. A liquid layer covering the tissue may reduce UV light or radicals reaching the sample. Thickness of the layer could vary from one experiment to the other. Thus, initially experiments were performed without a liquid layer. In the next section the risk of dehydration will be assessed.

For low-power (below 100 mW) plasma experiments, damage was assessed using TPLSM with combined SYTO 13 and Eosin staining; no PI was applied to detect cell death. However, as will become clear in the next section, alsmost all fibroblasts and most SMC may have died by necrosis because of damage by helium flow.
In the treated sample, the cytoplasm was no longer visible around the nuclei of the adventitia cells. This effect may be caused by either leaking of the cell cytoplasm, or by changes in the morphology of the cell. Another possibility is that plasma influences the binding of SYTO 13. The sample was followed up to 4 h after treatment. The apparent effect did not change over this time period. Plasma treatment at low power does not affect the thickness of the wall, because it was found similar before and after treatment; no shrinkage occurred.

When higher plasma powers (450 mW) were applied, effects were enhanced and resembled the effects that were described for heat injury in literature. Collagen structure was damaged and wall thickness was reduced. Shrinking effect was comparable to that induced by heating. Under normal physiological conditions (80 mm Hg), shrinking starts at 75 °C, but in a condition of zero transmural pressure, it happens already at 60 °C [7]. Other effects were damage to SMC and endothelial cells. This was indicated by the uptake of Eosin by these cells, which does not occur in healthy, undamaged cells. Some cells exhibited blebbing, which is indicative of apoptotis.

It is known that elastin is not affected by heating [7]. However, in Figure 8.4 it seems that the elastin layers have condensed into 1 layer. Possibly this is due to dehydration. In all considered cases, the artery was subject to a certain transmural pressure. Since this

pressure did not drop after treatment, plasma treatment did not cause artery perforation.

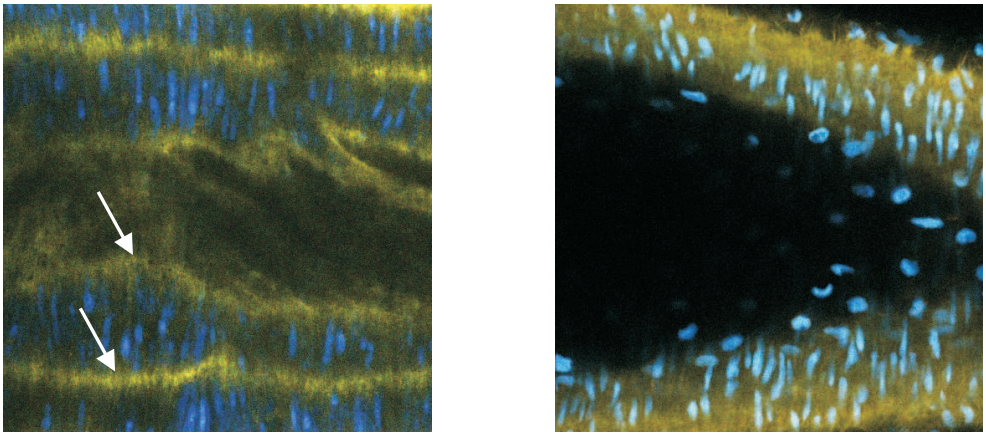

(a) (b)

Figure 8.4: *(a) Untreated carotid artery stained with Eosin and SYTO 44; arrows indicate elastin layers; (b) 1 min treatment time with 450 mW. Elastin layers containing the SMC appear more condensed. (Size 206x206 μm).*

8.3.3 Dehydration and helium flow

To minimize damage inflicted by other factors than plasma treatment, the influence of experimental procedure was tested. After mounting, some fibroblasts and endothelial cells showed an uptake of PI (see Figure 8.5). This means that their membranes were damaged and the cells were necrotic. This may be expected as adventitia and endothelium are the exposed layers and are thus more susceptible to damage. In 2 out of 7 cases, also some SMC were positively stained. This may be the result of pipettes touching the artery or of air bubbles that came into the lumen during dissection or mounting. It is advised to always check damage after mounting to distinguish this from damage induced by the plasma.
Experiments to check the effect of dehydration were performed by removing the medium for 4 minutes. In an average plasma treatment experiment, the artery was left dry for about 3 minutes. The result was that some fibroblasts and a few SMC were stained with PI. However, there was generally no significant increase in comparison to experiments after mounting only.

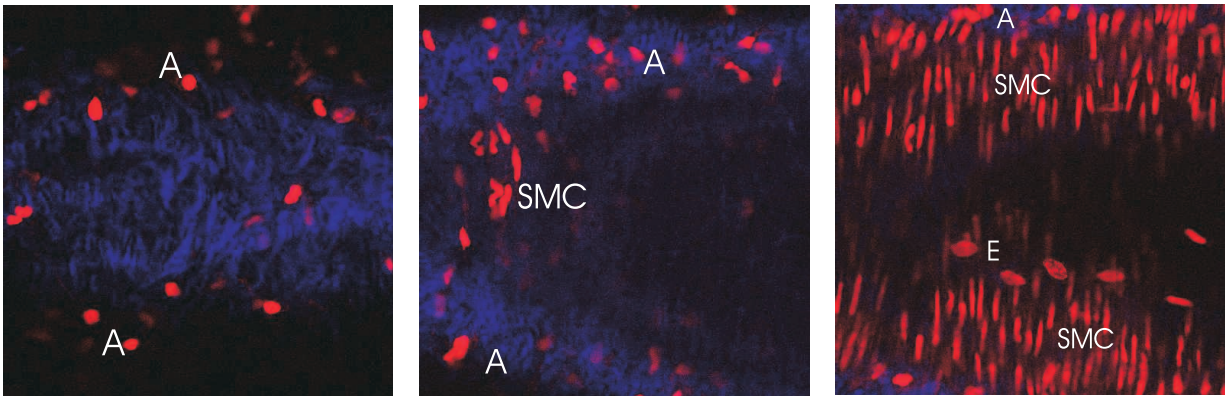

(a) (b) (c)

Figure 8.5: *(a) Damage due to mounting: some cells in adventitia (A) stained with PI, meaning some damage was induced. (b) Some SMC (middle left) are also stained after dehydration to air for 4 minutes. (c) Many cells in adventitia, SMC and endothelial (E) cells stained after a helium flow of 2 l min^{-1} for 1 minute. (Size 206x206 μm).*

Then the damage induced by helium flow was investigated. It appeared that when helium was applied as in standard plasma treatment, necrosis was induced in the entire sample: many SMC and endothelial cells died. Reduction of the treatment time to 10 s, and reduction of helium flow to 0.5 l min^{-1} still produced this effect. It was thus concluded that it was necessary to cover the artery by a thin layer of liquid during the treatment, to minimize damage.

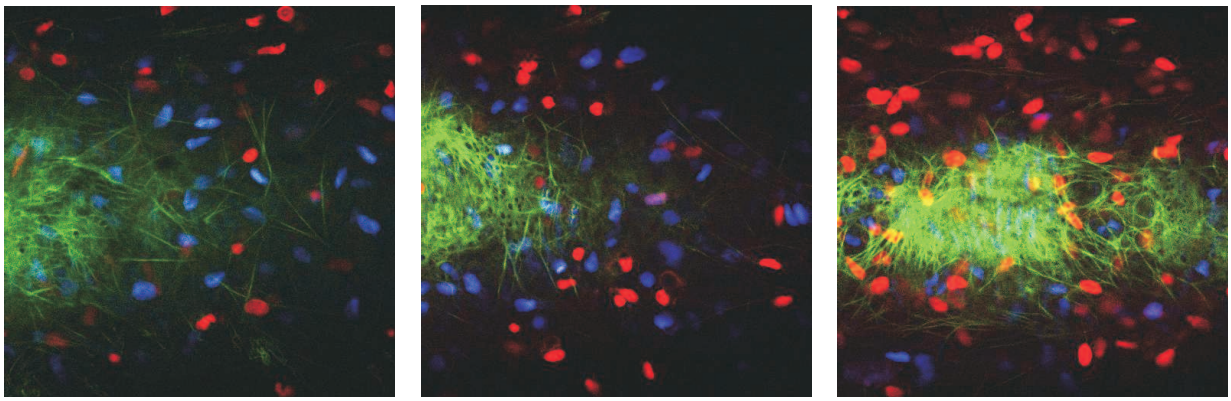

(a) (b) (c)

Figure 8.6: *(a) Adventitia after mounting. Artery was stained with PI (red), Eosin (green) and SYTO 13 (blue). (b) After mounting and helium flow (c) After plasma treatment (400 mW); most adventitia cells were dead. (Size 206x206 μm).*

An experiment with medium covering the artery when helium was applied showed that

necrosis was limited. No significant increase in damage to the adventitia and endothelium was observed compared to the damage after mounting (Figure 8.6).

8.3.4 Staining procedure

As described in Section 8.2.6, PI was used to detect necrosis. To obtain a good image of the various artery constituents and to assess if cells were viable or dead, a combined assay was used. Membrane-permeant SYTO 13 or SYTO 44 was used to detect DNA and RNA of all cells. When the cell membrane was (partially) disrupted, PI entered the cell and had to compete with the SYTO, because they both bind to DNA or RNA.
To test if PI can be used in combination with SYTO, cells were initially stained with SYTO only. Then the artery was dehydrated by helium flow of 2 l min^{-1} and afterwards incubated with PI. Cells that were stained positively with PI showed little or no SYTO fluorescence. This property makes the co-staining of PI and SYTO useful to detect cell death, because necrotic cells will always be stained with PI. One explanation of this is that the binding affinity of PI to DNA is stronger than of SYTO, and PI could thus replace the latter. A second explanation is occurrence of FRET (fluorescence resonance energy transfer, [21]) between SYTO and PI. When SYTO is excited it may transfer its energy to PI. Consequently, PI will give fluorescence, whereas SYTO will not. An experiment to resolve which is the right explanation is to measure fluorescence lifetimes of separate and mixed assays. If the lifetime of PI changes, this might be an indication of FRET.
To stain elastin, Eosin can be added to this combination. The emission peak of eosin is at a lower wavelength than that of PI. Thus, with the right filter settings, these two can be discerned.

8.3.5 Plasma irradiation of artery under thin liquid layer

First experiments with plasma treatment of an artery covered with a thin layer of liquid were performed using plasma powers of about 160 and 400 mW. The layer of liquid was 0.1 to 0.2 mm. This was estimated using the fact that the glass micropipettes (see Fig. 8.2) were attached to metal pipettes with a slightly larger radius (0.4 mm larger). The height of the liquid level was compared to this known size. Part of the cells in the adventitia was already damaged after mounting (Fig. 8.6), as was mentioned in Section 8.3.3.

For both the lower (160 mW) and higher power (400 mW) plasma treatments, apparent damage was limited to the adventitia: most adventitia cells, but only a few SMC were necrotic (see Fig. 8.6). When using relatively high plasma powers, plasma treatment

probably caused some heating effects, as the layer of liquid covering the artery was thin. However, no effects were observed below the adventitia, thus heating effects may be limited to this layer. Low-power plasma treatment did not lead to significantly less damage.
It seems that even at higher powers, plasma treatment can be used to induce superficial damage while layers underneath stay intact. However, long term effects have to be investigated.

8.4 Conclusions

We have shown that plasma treatment can induce controlled damage to vascular cells. The injury is inflicted in a non-contact way and may be used as a new injury model.
Experimental procedures were adjusted to minimize damage induced by other factors than plasma treatment. Damage induced by mounting and dehydration to air is limited to some cell death in the adventitia. However, direct helium flow along the artery should be avoided. Thus, during plasma irradiation, a thin layer of liquid should cover the artery.
Temperatures of plasma treatment were measured in air. For plasma powers below 100 mW with a helium flow rate of 2 l min^{-1}, temperatures remained below or at physiological temperature. However, at the start of plasma treatment, arterial samples are at room temperature and have an unknown thermal capacity. In future, experiments have to be performed to measure the temperature of samples during the treatment.
It appears that the effect of plasma treatment is limited to the adventitia when plasma power is below 400 mW and treatment time is less than 1 min. Application of lower (160 mW) and higher (400 mW) plasma powers induced comparable amounts of cell necrosis in the adventitia, and only little necrosis in the SMC. It seemed that the induced damage was not dependent on plasma power. A provisional conclusion is that, on average, active plasma species do not penetrate the arterial wall further than a few tens of micrometers. Future investigations should include variations in treatment time and observations of long term effects.
To distinguish viable and dead cells, SYTO 13 and PI can be used in a combined assay. Even if the cells are previously stained by SYTO, PI can enter the cell and emit fluorescence to indicate necrosis. In future experiments, apoptosis markers may be used to detect programmed cell death after irradiation.

References

[1] L Sun, C. C. Berndt, K. A. Gross, and A. Kucuk. Material fundamentals and clinical performance of plasma-sprayed hydroxyapatite coatings: A review. *J. Biomed. Mater. Res. (Appl. Biomater.)*, 58:570–592, 2001.

[2] K. E. Grund, T Straub, and G Farin. New haemostatic techniques: argon plasma coagulation. *Best. Pract. Res. Clin. Gastroenterol.*, 13:67–84, 1999.

[3] I. E. Kieft, E. P. v. d. Laan, and E. Stoffels. Electrical and optical characterization of the plasma needle. *New J. Phys.*, 6:149, 2004.

[4] I. E. Kieft, J. L. V. Broers, V. Caubet-Hilloutou, D. W. Slaaf, F. C. S. Ramaekers, and E. Stoffels. Electric discharge plasmas influence attachment of cultured CHO K1 cells. *Bioelectromagnetics*, 25:362–368, 2004.

[5] I. E. Kieft, D. Darios, A. J. M. Roks, and E. Stoffels. Plasma treatment of mammalian vascular cells: A quantitative description. *IEEE Trans. Plasma Sci.*, 33(2):771–775, 2005.

[6] P. Carmeliet, L. Moon, and D. Collen. Mouse models of angiogenesis, arterial stenosis, atherosclerosis and hemostasis. *Cardiovasc. Res.*, 39:8–33, 1998.

[7] W. Gorisch and K.-P. Boergen. Heat-induced contraction of blood vessels. *Lasers Surg. Med.*, 2:1–13, 1982.

[8] T. Kang, J. Resar, and J. D. Humphrey. Heat-induced changes in the mechanical behavior of passive coronary arteries. *ASME J. Biomech. Eng.*, 117:86–93, 1995.

[9] J.-H. Jun, J. L. Harris, J. D. Humphrey, and S. Rastegar. Effect of thermal damage and biaxial loading on the optical properties of a collagenous tissue. *ASME J. Biomech. Eng.*, 125:540–548, 2003.

[10] N. Sreeram, P. Townsend, and D. B. Morton. Radiofrequency thermal balloon angioplasty in an experimental model of peripheral arterial stenosis. *Int. J. Cardiol.*, 74:25–32, 2000.

[11] R. Waksman, K. A. Robinson, I. R. Crocker, M. B. Gravanis, S. J. Palmer, C. Wang, G. D. Cipolla, and S. B. King III. Intracoronary radiation before stent implantation inhibits neointima formation in stented porcine coronary arteries. *Circulation*, 92:1383–1386, 1995.

[12] M. Y. Salame, S. Verheye, I. R. Crocker, N. A. F. Chronos, K. A. Robinson, and S. B. King III. Intracoronary radiation therapy. *Eur. Heart J.*, 22:629–647, 2001.

[13] J. L. Witztum and D. Steinberg. The oxidative modification hypothesis of atherosclerosis: Does it hold for humans? *Trends Cardiovas. Med.*, 11:93–102, 2001.

[14] R. P. Patel, D. Moellering, J. Murphy-Ullrich, H. Jo, J. S. Beckman, and V. M. Darley-Usmar. Cell signaling by reactive nitrogen and oxygen species in atherosclerosis. *Free Radic. Biol. Med.*, 28(12):1780–1794, 2000.

[15] G. M. Chisolm and D. Steinberg. The oxidative modification hypothesis of atherogenesis: an overview. *Free Radic. Biol. Med.*, 28(12):1815–1826, 2000.

[16] W. Denk, J. H. Strickler, and W. W. Webb. Two-photon laser scanning fluorescence microscopy. *Science*, 248:73–76, 1990.

[17] M. v. Zandvoort, W. Engels, K. Douma, L. Beckers, M. oude Egbrink, M. Daemen, and D. W. Slaaf. Two-photon microscopy for imaging of the (atherosclerotic) vascular wall: A proof of concept study. *J. Vasc. Res.*, 41:54–63, 2004.

[18] I. E. Kieft, J. J. B. N. v. Berkel, E. R. Kieft, and E. Stoffels. Radicals of plasma needle detected with fluorescent probe. *Plasma Processes Polym. , special issue after the 16th ISPC, Taormina*, pages 295–308, 2005.

[19] C. M. Horwitz. Radio frequency sputtering - the significance of power input. *J. Vac. Sci. Technol. A*, 1(4):1795–1800, 1983.

[20] E. Rubin and J. L. Farber. *Pathology.* Lippincot-Raven Publishers, Philadelphia, 1999.

[21] W. R. Zipfel, R. M. Williams, and W. W. Webb. Nonlinear magic: multiphoton microscopy in the biosciences. *Nat. Biotechnol.*, 21(11):1369–1377, 2003.

Chapter 9

General discussion

9.1 Introduction

Goal of this work was to investigate possible biomedical applications of small low-power non-thermal atmospheric plasmas. With these plasmas we want to induce controlled reactions in cells. In industry, gas discharges are commonly used for surface modification (etching, cleaning and deposition). In the biomedical field (and in surgery in particular) plasmas are mainly applied *ex vivo*. Low-pressure plasmas (similar to the ones used for solid-state processing) are used to modify biological scaffolds; both low-pressure and atmospheric plasmas are applied in sterilization of surgical equipment, air, etc. For *in vivo* (surgical) applications, only high power plasmas are used [1] to thermally devitalize and dispose tissue parts. In this thesis, for the first time a non-thermal plasma has been applied to living biological samples, and the plasma-induced effects under the threshold of thermal damage have been studied.

For this study we used the plasma needle. This is a radio frequency (RF) plasma, operating in helium/air mixtures [2, 3]; the size of the active zone (plasma glow) is 1-2 mm. The plasma produces radicals and emits some ultraviolet (UV) radiation. These two factors may cause reactions in cells and tissues. Goal is to superficially induce local changes to cells in a non-thermal and non-contact way. Working area of this gas plasma can be small, i.e. operation on a chosen spot in tissue can be performed with precision. In the experiments, it was applied both to cultured cells (uniform population; easily accessible) and tissues to study the reactions. The main effect for cells in culture was detachment of cells without necrosis. Pilot experiments on tissues revealed that when low powers (about 100 mW) were used, penetration depth of the effects was limited to a few cell layers.

9.2 Plasma needle working range

The plasma needle operates in a unipolar configuration, i.e. it consists of one powered electrode and the (remote) surrounding as grounded electrode. In practice, this means that it is easy to apply to any surface, thus also to tissue. When one moves the needle close to tissue, the plasma is drawn towards it, and changes in shape. In this situation the voltage on the needle is lowered *(Chapter 3)*. At the same time, the electric field increases, the plasma becomes brighter and plasma power increases. The change in forward and reflected power upon approach of the sample may in future be used as an indicator of distance. The ideal distance to operate when treating a surface is less than 2 mm from the surface, because then the plasma is drawn towards the surface *(Chapter 4)*.
Even though the plasma is in principle non-thermal, we should be careful with applying it to living cells and tissues. Temperature should not exceed the physiological one by more

than a few degrees. The temperature of the plasma is, amongst others, dependent on plasma power and distance to the surface *(Chapter 5 and 8)*. At 1-mm distance, temperature in air is 37 °C or below for plasma powers under 100 mW. Use of high plasma powers (> 200 mW) resulted in necrosis in cell cultures, possibly due to heat *(Chapter 5)*. One should be careful when the distance becomes shorter than 1 mm, because plasma temperature is higher in the center of the plasma, which will result in an unwanted overheating of the sample.
When tissues are treated with plasma, their temperature may not rise to the plasma temperature that was measured in air. The samples normally start at room temperature and have a certain thermal capacity. Thus, it will take time for them to warm up. Exact temperatures of the tissue will have to be measured in future experiments.

Size of the plasma limits possible applications in two manners. First, for some applications, it might be useful to have a large plasma to treat larger surfaces faster. However, if we increase plasma size by simply increasing voltage and power, this leads to higher temperatures that can cause heat damage. A solution to this may be to construct a stack of needles in close range or an array of micro-plasma cells.
Second, for very local and high-precision treatment, the plasma should be even smaller. In this case, one is limited by plasma physical properties such as ionization and recombination rates. However, the limit is probably not reached yet. The point of the needle can be made sharper to increase the local electric field [4]. It is expected that the plasma will ignite at lower voltage and power, resulting in a smaller plasma. Furthermore, the material of the needle is important for miniaturization of the plasma. Currently we use an alloy containing tungsten, but a material with a lower work function leads to higher electron emission, which would allow to sustain a discharge at a lower voltage. A non-oxidizing material should be chosen because the needle is operating in humid air. A commonly used material is thoriated tungsten (W + ThO_2) [5].

To operate in small openings and on vulnerable tissues, helium flow should be limited to avoid pressure build-up and flow-induced desiccation. When flow is reduced, the admixture of air molecules increases. In the current configuration, admixture of air to helium is minimal (at most 1 %) for flow rates on the order of 2 l min^{-1} *(Chapter 4)*. In the emission spectrum, a reduction in helium flow from 2 to below 0.8 l min^{-1} results in an increase in intensity of the nitrogen lines *(Chapter 3)*. The influence of this admixture appears to be important. A numerical model by Brok *et al* [6] revealed that N_2^+ is the dominant ion even at small admixtures of nitrogen. They also conclude that the region of influence of the needle extends far from the region of the active plasma, which is a few hundred micrometers. The electrons and N_2^+ ions that are produced by Penning ionization of helium metastables can diffuse millimeters outward.

An extra advantage of helium reduction is that it saves costs, but a disadvantage is the uncontrolled increase of air admixture, and a decrease of convective cooling. The latter is important to keep plasma temperature low. Indeed, flow reduction results in a substantial temperature increase *(Chapter 8)*. A solution may be to change the design of the needle, its insulation and helium supply (e.g. by sustaining a high gas flow while recycling helium), so that admixture is suppressed and convection is maintained.

The working of the plasma is based on its chemical activity. The intensity of the latter is dependent on dissipated plasma power. We noticed before that dissipated power changes with distance, and that it is strongly related to temperature. Thus, for fundamental research, plasma power is an important parameter to measure. Power dissipated in the plasma (influx) cannot be measured directly, but is calculated by a subtraction method [7]. It ranges from tens of mW up to a few hundred mW *(Chapter 3)*.
For applications, however, the power outflux can be more important that the power influx. This is, because the outflux determines what actually reaches the sample surface. Power outflux measurements by Stoffels *et al* [8] show that 10 % of the plasma power outflux is transmitted through the medium between the needle and the surface as heat conduction and radiation (both visible and near UV/IR). The other 90 % is lost by heating of the medium (60 %) and (photo)chemical reactions (30 %). Total power outflux is around 0.1 W cm^{-2}.

For a satisfactory reproducibility of the experiments, it is important that the plasma is stable and reproducible. To achieve this, stability and efficiency of the power supply to the needle were improved by adapting the design of both the needle and the matching network *(Chapter 3)*. Electromagnetic radiation by the needle was reduced by shortening the part protruding from the metal case. This way, antenna behavior of the needle was reduced which also allowed to save power. The matching network was optimized to reduce power losses. Then, the electrical properties of the plasma were modeled and compared with experimental results determined from matching network parameters *(Chapter 3)*. The discharge resistance found was in the range 100-1200 kΩ. From this resistance, electron density was estimated to be 10^{17} m^{-3}. A Thomson scattering measurement was performed with the setup as built by Van de Sande [9], but electron density was below the detection limit of the specific experiment. This means that electron density was lower than 10^{18} m^{-3}. Longer measurements with higher laser power should make detection of the low density possible. Using a numerical model, Brok *et al* [6] calculated a density of 10^{17} m^{-3}.

9.3 Active plasma ingredient

When plasma was applied to cultured cells, a process was observed that appeared similar to a well known chemical effect. Cells detached after plasma treatment as they also detach after applying trypsine *(Chapter 5)*. Trypsine breaks down several types of proteins. When used on attached cultured cells, cell adhesion molecules are broken. These can be restored on a typical time scale of several hours. Trypsine is only used for research purposes because its action is neither specific nor local. After plasma-induced detachment, cell adhesion molecules could be restored as well.
Using our non-thermal atmospheric plasma, detachment voids up to 5 mm in diameter could be achieved at treatment times of 10 s *(Chapter 6)*. The induced void sizes were comparable to the deactivation areas induced on bacteria by Sladek and Stoffels [10]. The smallest void that was produced had a size of 100 μm diameter. This means that if the size of the plasma is further reduced, the precision of treatment might be increased to a few cells, or even to a single cell in low-density cell cultures.
Another effect of the plasma treatment was the induction of apoptosis in a small percentage of the cells. Optimization of treatment conditions, e.g., by addition of other gases to the helium buffer gas to produce specific radicals, might raise the percentage of apoptosis.

To optimize the efficiency of the plasma treatment, one has to know the cause of the reactions. We found several indications that plasma radicals (both neutrals and ions) are the main cause, and are more important than e.g., UV radiation.
Radicals are known, for example, to induce damage to DNA or to proteins, and to cause lipid peroxidation [11]. These effects are generally due to reactive oxygen species (ROS) or reactive nitrogen species (RNS), which include both neutral and ionized particles. When the level of ROS in or around cells is too high, this can lead to oxidative stress. The latter can result in either adaptation or (fatal) cell injury.
As mentioned above, ions are usually included in the broad definition of reactive species or radicals. However, it may be interesting to know the specific role of ions, because both positive and negative ions are known to deactivate bacteria or to inhibit their growth [12]. On the other hand, the density of ions in the plasma is probably one or two orders of magnitude lower than that of radicals *(Chapter 4)*. A method to clarify the role of charged particles would involve their magnetic confinement. The ions would be trapped in or near the plasma, so that they could not reach the tissue. Such tests are not within the scope of this thesis, but will be executed in near future.
Besides radicals, UV light also forms an important factor that may lead to cell injury. Experiments on bacterial cells with air plasmas at atmospheric pressure (emitting both UV light and radicals) [13] showed that highly reactive species like O, OH and NO_2 play the most crucial role in the destruction of microorganisms, hereby indicating UV light to

be of less importance.

Another indication of the low importance of UV light was found in our experiments. We observed that the liquid layer that covered the cells was an important parameter for the detachment area *(Chapter 6)*. When the liquid layer was thin, cells detached more easily. The UV light that was emitted by the plasma was in a range that was not absorbed by water. Thus, it is most likely that reactive species (neutral radicals and ions) are more important in the detaching.
Treatment of cells with UV light (no plasma) resulted in cell damage and eventually necrosis *(Chapter 7)*. No cell detachment was observed after UV radiation exposure alone. The CHO-K1 cells that were used for the experiments had a threshold value for the UV treatment of 0.5-0.7 J cm^{-2}, depending on the wavelength. Below this threshold value, no evident effects were observed. However, internal cell damage may be induced.
In contrast to eukaryotic cells, bacteria appeared to be much more sensitive to UV irradiation. It was found that the threshold for inactivation of E. Coli was extremely low or not existing, and that 99 % reduction of bacterial population was possible at an irradiation dosis lower than 0.05 J cm^{-2}. Since 99 % reduction is sufficient for tissue disinfection, it is not unthinkable that low-power UV sources could be used for *in vivo* treatment of infected sites.

A last indication that one "plasma ingredient" is dominant over the other was found by comparison of two publications. Moisan *et al* [14] employed a low-pressure plasma source, which emitted a substantial amount of high-energy photons. They characterized plasma inactivation of bacteria and spores by the existence of two or three distinct phases in the survival curve. The idea behind these phases is that there are different dominating inactivation processes at different exposure times. In the first phase, bacteria are destroyed very fast, because their DNA is broken by UV irradiation (up to about 1 min treatment time in their plasma setup). This is followed by a slower erosion of the microorganism through photodesorption and etching (again a few minutes). These two phases were not observed during treatment of bacteria with the plasma needle [10]. It is likely that the UV irradiated by the plasma needle is so low that the second mechanism is dominant from the start.

The reactivity of the different radicals varies [15] and they may react with different biological molecules [16]. Thus, it is important to know which radicals are formed in the plasma, or in the liquid as a reaction to species from the plasma. For specific applications, specific radicals may be needed. The radicals that are detected by optical emission spectroscopy in the plasma are OH and O *(Chapter 3)*; detection of ozone (O_3) was not possible. The latter may, for example, be measured by UV absorption [17, 18]. Another radical that is thought to be formed, but not detected by emission spectroscopy, is NO. However, studies on N and O containing plasmas state that significant amounts of NO are formed [19]. NO

has a central role in a wide variety of physiologic and pathophysiologic functions in tissues and organs. For example, it displays antitumor activity [20].
The amount of radicals formed by the plasma appeared to be determined by the mixture of air molecules into the helium buffer gas. Thus, it may be possible to increase the percentage of radicals by accurate admixing of small amounts of, e.g., oxygen. Addition of other gases may generate specific radicals [21].

For applications, it is not only important to know which radicals are formed, but also what fraction of them can reach the biological sample. For this purpose, measurements of radical densities in plasma-treated liquid samples were performed. In irradiated liquid, radicals from the ROS family were detected *(Chapter 4)*. Their density was found to be in the μM range, which is comparable to physiological concentrations. The detected species may be directly emitted by the plasma or formed in the liquid itself by reaction with, e.g., metastable atoms or ions from the plasma.
A last parameter that is important for applications, is how deep the active plasma ingredient penetrates the tissue. This penetration depth may be limited. An indication for this is that the thickness of a liquid layer covering cultured cells influences the rate of detachment *(Chapter 6)*. A second indication was found from first experiments *(Chapter 8)* on murine arteries. They were performed to verify damage after plasma treatment in the various layers. For powers between 160 and 400 mW with 1 minute treatment time, no dependency on plasma power was found for the effects, and damage was limited to the adventitia. A provisional conclusion was drawn that plasma reactive species cannot penetrate the tissue more than a few cell-layers.

9.4 Detachment mechanism

What is the mechanism that causes the detachment of the cells? In the previous section we described which plasma property is likely to cause the effects, but to understand the entire mechanism we need to know which parts of the cells are affected and how the cell responds.
At the moment, we developed two theories concerning the detachment: a passive and an active mechanism. The first is that the reactive plasma species break the cell adhesion molecules (CAMs) that connect the cells to each other and to the extracellular matrix. Consequently, cell morphology will change; they will puff up and because they are in a liquid solution they will start floating. The second theory is that the cells receive a certain alarming stimulus so that they start migrating towards a different and less dangerous area. The fact that dead cells are not detached after treatment supports the second theory.

Often when a cell is injured, gap junctions close, thereby isolating a damaged cell from its neighbors. This isolation process may result from a rise in calcium and a fall in pH in the cytosol of the damaged cell [22]. In future experiments, indicators for pH and calcium will be applied to investigate this possible reason for the disturbance in cell communication.

The question is then: do we see the same effect for cells in culture or in tissue? Cells in culture are of homogeneous type and reactions are not influenced by a complex extracellular matrix. Detachment of cells in a tissue would take more effort, as they are more strongly bound to the matrix. Even when detachment of cells in the tissue is present, it will be difficult to observe. The detached cells might still be enclosed by fibers of the matrix, so they will not float away. In principle though, it is possible to stain the adhesion molecules and detect if they are broken after the treatment.

9.5 Conclusion and future directions

In this work, we explored possible biomedical application of the plasma needle. We found that the small non-thermal atmospheric plasma is a well controllable and that it can be applied to locally influence cells and tissues. Possible applications are local cell removal and use of plasma treatment as an injury model.
It will be interesting to elaborately study specific effects at cellular level. Questions like "Are treated cells still communicating?" and "Can cells completely recover after treatment?" should be addressed. Furthermore, the influence of plasma on cellular proliferation rate should be investigated. Only pilot experiments were performed to assess the effects of plasma on tissue. Future studies should include detachment of cells from the extracellular matrix in tissues, induction of apoptosis and other processes.
To study plasma-cell interactions from a plasma-physical point of view, addition of gases to the helium to produce specific radicals, and magnetic confinement to clarify the role of the ions are of major interest.

References

[1] K. E. Grund, T Straub, and G Farin. New haemostatic techniques: argon plasma coagulation. *Best. Pract. Res. Clin. Gastroenterol.*, 13:67–84, 1999.

[2] E. Stoffels, A. J. Flikweert, W. W. Stoffels, and G. M. W. Kroesen. Plasma needle: a non-destructive atmospheric plasma source for fine surface treatment of (bio)materials. *Plasma Sources Sci. Technol.*, 4:383–388, 2002.

[3] I. E. Kieft, E. P. v. d. Laan, and E. Stoffels. Electrical and optical characterization of the plasma needle. *New J. Phys.*, 6:149, 2004.

[4] L. B. Loeb. *Electrical Coronas: Their Basic Physical Mechanisms.* Univ. of California Press, 1965.

[5] R. Ifflander. *Gas Discharge Lamps for Laser Excitation.* Schramberg, 2003.

[6] W. J. M. Brok, M. D. Bowden, J. Van Dijk, J. J. A. M. Van der Mullen, and G. M. W. Kroesen. Numerical description of discharge characteristics of the plasma needle. *J. Appl. Phys.*, 98(1):013302, 2005.

[7] C. M. Horwitz. Radio frequency sputtering - the significance of power input. *J. Vac. Sci. Technol. A*, 1(4):1795–1800, 1983.

[8] E. Stoffels, R. E. J Sladek, I. E. Kieft, H Kersten, and R. Wiese. Power outflux from the plasma: an important parameter in surface processing. *Plasma Phys. Control. Fusion*, 46:B167–B177, 2004.

[9] M. J. van de Sande. *Laser scattering on low temperature plasmas.* PhD thesis, Eindhoven University of Technology, Eindhoven, 2002.

[10] R. E. J Sladek and E. Stoffels. Deactivation of escherichia coli by the plasma needle. *J. Phys. D. : Appl. Phys.*, 38:1716–1721, 2005.

[11] Barry Halliwell and John M. C. Gutteridge. *Free radicals in biology and medicine.* Oxford University Press, New York, 1999.

[12] A. P. Krueger and E. J. Reed. Biological impact of small air ions. *Science*, 193:1209–1213, 1976.

[13] M. Laroussi and F. Leipold. Evaluation of the roles of reactive species, heat, and UV radiation in the inactivation of bacterial cells by air plasmas at atmospheric pressure. *Int. J. Mass Spectrom.*, 233(1-3):81–86, 2004.

[14] M. Moisan, J. Barbeau, S. Moreau, J. Pelletier, M. Tabrizian, and L. H. Yahia. Low-temperature sterilization using gas plasmas: a review of the experiments and an analysis of the inactivation mechanisms. *Int. J. Pharmac.*, 226(1-2):1–21, 2001.

[15] P. Neta, R. E. Huie, and A. B. Ross. Rate constants for reactions of inorganic radicals in aqueous solution. *J. Phys. Chem. Ref. Data*, 17:1027–1284, 1988.

[16] B. Halliwell and O. I. Aruoma. *DNA and free radicals.* Ellis Horwood Ltd., Chichester, 1993.

[17] W. F. L. M. Hoeben, E. M. van Veldhuizen, W. R. Rutgers, C. A. M. G. Cramers, and G. M. W. Kroesen. The degradation of aqueous phenol solutions by pulsed positive corona discharges. *Plasma Sources Sci. Technol.*, 9:361–369, 2000.

[18] K. H. Becker, U. Kogelschatz, K. H. Schoenbach, and R. J. Barker. *Non-equilibrium air plasmas at atmospheric pressure.* Institute of Physics Publishing, London, 2005.

[19] J. H. van Helden, G. Lombardi, R. Zijlmans, G. D. Stancu, J. Ropcke, D. C. Schram, and R. Engeln. Study of the formation of molecules in N and O containing plasmas. *ISPC conference proceedings, Toronto, extended abstract*, 2005.

[20] B. G. Bentz, R. L. Simmons, G. K. Haines III, and J. A. Radosevich. The yin and yang of nitric oxide: reflections on the physiology and pathophysiology of NO. *Head Neck*, 22:71–83, 2000.

[21] R. A. B. Zijlmans, G. Lombardi, J. Ropcke, R. Engeln, and D. C. Schram. NH3 destruction and NO formation in a recombining N2/H2 plasma as a result of adding O2. *17th symposium Plasma Physics and Radiation Technology, Lunteren, abstract*, page P51, 2005.

[22] R. A. Rhoades and G. A. Tanner. *Medical Physiology.* Lippincott Williams and Wilkins, Baltimore USA, 1995.

Summary

The plasma needle is a novel design of a radio-frequency discharge in helium/air mixtures at atmospheric pressure. The discharge contains neutral, excited and ionized particles, and emits ultraviolet (UV) light. It operates at low electric power and close to ambient temperature; it combines chemical activity with non-destructive character. Therefore it is expected that the plasma needle will be used in future in (micro) surgery, e.g. in wound healing and in controlled tissue removal through cell detachment or apoptosis, avoiding necrosis and inflammation reactions. Focus of this study is both on optimization of needle design and on assessment of effects of plasma activity on living cells. This work is a pioneering study of the effects of non-thermal plasma on biological samples.

The design of the plasma needle was adjusted in such a way that instead of operating in a closed reactor, now the treatments could be performed in open air. Thus, larger samples could be treated and handling times were reduced. Then, a characterization of the needle was performed using electrical as well as optical diagnostics *(Chapter 3)*. It was found that the needle operated at voltages of 140 V_{rms} and higher. A model was made to determine the resistance of the plasma and from this an estimation of the electron density could be made. The latter can be regarded as an indirect measure for plasma reactivity. Results from optical emission spectroscopy showed that reactive oxygen species, such as O· and OH·, were produced in the plasma. Furthermore, UV emission was detected. Both the radicals and the UV are known to interact with cells and tissues.
For applications, the amount of radicals that reach the sample or that are generated in the sample is important. For this reason, radicals were detected in liquid that was treated with plasma using a chemical technique *(Chapter 4)*. It involved a fluorescent probe: the probe was dissolved in liquid and after reaction with specific radicals it became fluorescent. Radical density in the liquid depended on plasma conditions, treatment time, and amount of liquid used, but it was always in the micromolar range. These concentrations were found to be comparable with physiological concentrations that were stated in literature.

Basic cell reactions after plasma treatment were determined by experiments on cultured Chinese hamster ovarian (CHO K1) cells *(Chapter 5)*. One of these reactions was cell

detachment: cells detached from their environment but remained alive after treatment. Other reactions included a small percentage of apoptosis and, when high plasma powers were used, necrosis. A comparison with the effect of UV light from UV lamps was made *(Chapter 7)*. The main effect of UV treatment was necrosis, but only above a certain threshold value. For mammalian cells, this threshold was reasonably high. Thus, the effects of plasma treatment could not be explained by the action of the UV light from the plasma.
Quantitative experiments were performed on cultured bovine aortic endothelial cells (BAEC) and rat smooth muscle cells (A7r5) *(Chapter 6)*. These two cell types constitute walls of blood vessels. It was shown that treatment times of less than one minute cause detachment of the cells if the layer thickness of the liquid that covered the cells was low (around 0.1 mm). This suggests that at short treatment times, the penetration depth of the plasma into the sample is limited. The percentage of necrotic cells was low after treatment. No difference was found in the detachment behavior of both cell types.

Finally, pilot experiments were performed on carotid arteries of C57BL/6 and Swiss mice *ex vivo (Chapter 8)*. They were studied using a two-photon laser scanning microscope (TPLSM). Cell nuclei, elastin bands, and collagen could be visualized. Preliminary results indicate that induced changes are not strongly dependent on applied energy if no heating effects are induced. Apparent effects were limited to the adventitia, probably due to a low penetration depth of active plasma species.

In conclusion, we can state that the plasma needle is a non-destructive tool that can be applied with precision. It has a superficial action and causes little damage to the tissue. The level of damage can be controlled to achieve a desired therapeutic effect. Both on cultured cells and on *ex vivo* arteries interesting effects were found that confirm the hypothesis that the plasma needle will have a future in surgery.

Samenvatting

Plasma's winnen de laatste jaren flink aan bekendheid vanwege de plasma tv-schermen die sterk in opkomst zijn. Veel mensen kennen plasma's ook van de TL-buizen die in de meeste kantoren voor het licht zorgen, hoewel niet iedereen zich zal realiseren dat het hier plasma's betreft. Wat de meesten waarschijnlijk niet weten is dat plasma's veel vaker voorkomen: maar liefst 99 % van het heelal bestaat uit geïoniseerd gas. Voorbeelden uit de natuur zijn: de zon, bliksem, vuur en het noorderlicht.

Maar wat is een plasma nu eigenlijk? Een plasma heeft veel overeenkomsten met een gas, het bevat namelijk vrij bewegende deeltjes. In een gas zijn dit atomen en moleculen. In een plasma komen daar geladen deeltjes bij, zoals ionen en elektronen. Plasma's zijn hierdoor in staat elektriciteit te geleiden. Andere eigenschappen zijn dat ze licht uitzenden en chemisch reactief zijn. Vooral dat laatste maakt dat plasma's vele toepassingen hebben gevonden in de industrie. Ze worden gebruikt voor het etsen van halfgeleidercomponenten, het deponeren van dunne lagen, het ontsmetten van medisch gereedschap en andere oppervlaktebewerkingen.
Ons project is erop gericht plasma toe te passen in het biomedische vakgebied. Het uiteindelijke doel is fijn-chirurgie waarbij cellen gecontroleerd verwijderd worden zonder dat een onstekingsreactie op gang wordt gebracht.

Plasma's kunnen worden gemaakt door het zodanig aanleggen van een elektrisch veld dat er een elektrische ontlading in een gas plaatsvindt. Door variatie in o.a. het soort gas, de gasdruk en de frequentie van de aangelegde spanning kunnen de eigenschappen van de ontlading sterk beïnvloed worden. Voor ons onderzoek gebruiken we de zogenoemde "plasmanaald". De werking van deze plasmanaald is gebaseerd op een radio-frequente (RF) ontlading in helium/lucht mengsels. De ontlading vindt plaats aan het einde van een scherpe metalen draad. In het eerste ontwerp was deze naald geplaatst in een afgesloten doos die werd gevuld met helium nadat het te behandelen voorwerp erin was geplaatst. Om behandeling van grotere voorwerpen mogelijk te maken en de doorlooptijd te verkorten is het ontwerp aangepast *(Chapter 3)*. De toevoer van het helium is parallel gemaakt aan de metalen draad waardoor het plasma in de lucht kan branden. De ontlading vindt plaats

vanaf een spanning van 140 V_{rms}.
In het geval van de plasmanaald zijn de eerder genoemde parameters zoals het soort gas en de frequentie zodanig gekozen dat een klein (orde 1 à 2 mm) niet-thermisch plasma ontstaat. Juist de combinatie van het niet-thermische karakter met de chemische reactiviteit maakt de plasmanaald potentieel toepasbaar voor verfijnde biomedische toepassingen. Het doel van het onderzoek in dit proefschrift is dan ook om meer inzicht te krijgen in deze mogelijke medische toepasbaarheid. Het focus ligt hierbij zowel op de optimalisatie van het ontwerp van de naald als op het in kaart brengen van de response van cellen na behandeling.

Om de effecten van het plasma goed te kunnen begrijpen is het noodzakelijk dat de samenstelling ervan bekend is. Met behulp van spectroscopie is het uitgezonden licht geanalyseerd *(Chapter 3)*. Hieruit is gebleken dat het grootste deel in het zichtbare gebied ligt, maar dat er ook UV licht uitgezonden wordt. Uit de specifieke golflengtes van het uitgezonden licht kan bepaald worden welke radicalen er o.a. in het plasma gevormd worden. Het blijkt dat er reactieve zuurstof deeltjes, zoals O· en OH·, worden gemaakt. Van zowel radicalen als van UV licht is bekend dat ze reacties veroorzaken in cellen.
Om radicalen in een vloeistof te meten is een andere methode toegepast *(Chapter 4)*. Hiervoor is een chemische techniek gebruikt, namelijk een fluorescente kleuring. Een chemische stof wordt hiervoor in een vloeistof opgelost. Vervolgens wordt deze vloeistof met het plasma bestraald en komen er radicalen in. Deze radicalen reageren met de chemische kleuring die fluorescerend wordt. Op deze manier is vastgesteld dat de concentratie van radicalen in de vloeistof in het micro-molaire bereik ligt.

De primaire celreacties op de gasontlading zijn onderzocht door experimenten op gekweekte cellen uit te voeren *(Chapter 5)*. Voor deze experimenten zijn cellen van de eierstokken van een Chinese hamster (CHO K1) cellen gebruikt. Het voornaamste effect bleek het loslaten van de cellen van hun buren en van de bodem waarop ze gekweekt waren. Verder ging een klein percentage van de cellen in apoptose. Dit is een geprogrammeerde celdood die in werking treedt als de cel onherstelbaar beschadigd is, maar nog wel enigszins metabolisch actief is. Als het plasma vermogen hoog is treedt ook necrose op. Dit is een vorm van celdood die vaak gevolgd wordt door een ontstekingsreactie.
Er is een vergelijking gemaakt met het effect van UV licht van UV lampen op cellen *(Chapter 7)*. Het belangrijkste effect van het UV was necrose, maar dit vond alleen plaats als de hoeveelheid licht boven een bepaalde drempelwaarde uitkwam. Voor de geteste diercellen was deze drempelwaarde relatief hoog t.o.v. bacteriën. Uit deze vergelijking blijkt dat de effecten van de plasma-behandeling niet verklaard kunnen worden door het uitgezonden UV licht.

Kwantitatieve experimenten zijn uitgevoerd op endotheelcellen van runderen (BAEC) en

spiercellen afkomstig van ratten (A7r5) *(Chapter 6)*. Deze twee celtypen vormen samen de wanden van bloedvaten. Een plasma behandeling van 10 seconden resulteert in het loslaten van cellen als de laagdikte van de vloeistof die de cellen bedekt klein is (rond de 0.1 mm). Dit wekt de suggestie dat voor korte behandeltijden de penetratie diepte van het actieve plasma "ingrediënt" in de vloeistof beperkt is. Het percentage necrose na de behandeling was laag. Er is geen verschil waargenomen in het gedrag van de twee bestudeerde celtypen.

Tenslotte zijn er proef experimenten uitgevoerd op carotide vaten van muizen *ex vivo* *(Chapter 8)*. Hiermee zijn de effecten op weefsels onderzocht. Dit is van belang omdat cellen in weefsels omgeven worden door een extracellulaire matrix die bestaat uit o.a. collagene en elastine vezels. De bloedvaten zijn bestudeerd met behulp van een twee foton laser scanning microscoop. Hiermee konden celkernen, elastine banden en collageen worden gevisualiseerd. De eerste resultaten geven aan dat de effecten niet sterk afhankelijk zijn van de toegevoerde energie, zolang er geen hitte effecten optreden. Er treedt celdood op, maar dit effect blijft beperkt tot de buitenste laag van het vaatje: de adventitia.

Een mogelijk toepassing van de plasmanaald is bijvoorbeeld het verwijderen of verplaatsen van cellen en weefsels zonder al te veel schade (voor bijv. huidziekten, kanker, stenoses, celbiologische manipulatie ten behoeve van gentherapie en celonderzoek). Verder zou de naald kunnen worden gebruikt voor het ontsmetten van levende organismen, omdat bacteriële infecties zorgen voor complicaties in wondgenezing, tandbederf etc.

We kunnen concluderen dat de plasmanaald een niet destructief instrument is dat met precisie kan worden toegepast. Het heeft een oppervlakkige werking en brengt weinig schade toe aan het weefsel. De hoeveelheid schade kan worden geregeld om het gewenste therapeutische effect te krijgen. Zowel op gekweekte cellen als op de *ex vivo* arteriën zijn interessante effecten gevonden die de hypothese bevestigen dat de plasmanaald een toekomst zal hebben in de chirurgie.

Publications

The publications associated with this thesis are:

Papers

- E Stoffels, I E Kieft, R E J Sladek, Superficial treatment of mammalian cells using plasma needle, *J. Phys. D.: Appl. Phys.* 36: 2908-2913, 2003
- I E Kieft, J L V Broers, V Caubet-Hilloutou, D W Slaaf, F C S Ramaekers, E Stoffels, Electric discharge plasmas influence attachment of cultured CHO K1 cells, *Bioelectromagnetics*, 25(5): 362-368, 2004
- E A Sosnin, E Stoffels, M V Erofeev, I E Kieft, S E Kunts, The effects of UV irradiation and gas plasma treatment on living mammalian cells and bacteria: a comparative approach, *IEEE Trans. Plasma Sci.*, 32(4): 1544-1550, 2004
- Eva Stoffels, Ingrid E. Kieft, Raymond E.J. Sladek, Ewout P. van der Laan, Dick W. Slaaf, Gas plasma treatment: a new approach to surgery?, *Crit. Rev. Biomed. Eng.*, 32(5-6): 427-460, 2004
- E. Stoffels, R.E.J. Sladek, I.E. Kieft, Gas Plasma Effects on Living Cells, *Physica Scripta*, T107: 79-82, 2004
- I.E.Kieft, E.P.v.d.Laan, E.Stoffels, Electrical and Optical Characterization of the Plasma Needle, *New J. Phys.*, 6: 149,2004
- E. Stoffels, R.E.J.Sladek, I.E.Kieft, H. Kersten, R. Wiese, Power outflux from the plasma: an important parameter in surface processing, *Plasma Phys. Control. Fusion*, 46: B167-B177, 2004
- I E Kieft, J J B N van Berkel, E R Kieft, E Stoffels, Radicals of plasma needle detected with fluorescent probe, *Plasma Processes Polym., special issue after the 16th ISPC, Taormina*, 295-308, 2005
- Ingrid E. Kieft, Delphine Darios, Anton J. M. Roks, and Eva Stoffels, Plasma treatment of mammalian vascular cells: a quantitative description, *IEEE Trans. Plasma Sci.*, 33(2):771-775, 2005
- I.E. Kieft, R.E.J. Sladek, E.P. van der Laan, E. Stoffels, Atmospheric plasma needle for biomedical applications, *PJAC*, accepted 2005

Conference proceedings

- I E Kieft, N A Dvinskikh, J L V Broers, D W Slaaf, E Stoffels, Effect of plasma needle on cultured cells, *SPIE proc.*, 5483: 247-251, 2004
- R.E.J. Sladek, I.E.Kieft, E. Stoffels, The plasma needle and its biomedical applications, *Proc. CAPPSA*, Ghent 2004
- E. Stoffels, I.E.Kieft, R.E.J.Sladek, E.P.van der Laan, Towards plasma surgery: interactions of cold plasmas with living cells, *Proc. GD2004 conf.*, Toulouse, 1049-1052, 2004
- I.E. Kieft, K. Douma, R.T.A. Megens, M.A.M.J. van Zandvoort, D.W. Slaaf, E. Stoffels, Non-thermal plasma treatment of *ex vivo* arteries: preliminary results, *Proc. ICPIG 2005 conf.*, Eindhoven, p51, 2005
- M. Erofeev, I.E. Kieft, E. Stoffels, Effects of KrBr and XeBr UV lamp irradiation on 3T3 cells, *Proc. ICPIG 2005 conf.*, Eindhoven, p52, 2005

Conference abstracts

- ALW/FOM/VvBBMT-Meeting On Molecular and Cellular Biophysic, 7-8 Oct, 2002, Lunteren, The Netherlands, E. Stoffels, I.E. Kieft, and V. Caubet, "Plasma needle" - novel treatment of tissues using electric discharges
- 5th Euregional Welt-PP, Workshop on the Exploration of Low Temperature Plasma Physics, 28-29 Nov, 2002, Rolduc, Kerkrade, The Netherlands
  - I.E.Kieft, E. Stoffels, V. Caubet-Hilloutou, J.L.V. Broers, F.C.S. Ramaekers, D.W. Slaaf, Micro-discharge treatment of CHO K1 cells (Oral presentation)
  - M.V. Erofeev, I.E. Kieft, E. Stoffels, The influence of UV radiation on cells in culture (Poster presentation)
  - R. Walraven, I.E. Kieft, E. Stoffels, R.E.J. Sladek, P.J.A. Tielbeek, Investigation of possibilities for plasma treatment of dental caries (Poster presentation)
- APP Spring meeting Biomedical Aspects of Plasma Physics, Feb 23th - 26th 2004, Bad Honnef, Germany
  - I.E.Kieft, E. Stoffels, V. Caubet-Hilloutou, J.L.V. Broers, F.C.S. Ramaekers, D.W. Slaaf, Micro-discharge treatment of CHO K1 cells (Oral presentation)
  - E. Stoffels, I.E. Kieft, R.E.J. Sladek, J.-C. Cigal, C.Y.M.Maurice, Plasma treatment of biological objects
- Plasma Physics and Short Time-Scale Physics Spring Meeting, DPG, 24-28 Mar, 2003, Aachen, Germany, Ingrid Kieft, Eva Stoffels, Veronique Caubet-Hilloutou, Jos Broers, Frans Ramaekers, Dick Slaaf, Plasma needle treatment of cultured cells (Oral presentation)

- 2003 ASME Summer Bioengineering Conference, 25-29 June, 2003, Miami, USA, Ingrid E. Kieft, Eva Stoffels, Veronique Caubet-Hilloutou, Jos L.V. Broers, Frans C.S. Ramaekers, Dick W. Slaaf, Cell Detachment using Electric Discharge Plasmas (Poster presentation)
- AMPL-2003 Atomic and Molecular Pulsed Lasers, 15-19 Sep, Tomsk, Russia, I.E. Kieft, J.L.V. Broers, D.W. Slaaf, F.C.S. Ramaekers, E. Stoffels, Micro-Discharge Treatment of Cultured Cells (Oral presentation)
- 6th Euregional Welt-PP, Workshop on the Exploration of Low Temperature Plasma Physics, 27-28 Nov, 2003, Rolduc, Kerkrade, The Netherlands I.E. Kieft, J.J.B.N. v. Berkel, E. Stoffels, D.W. Slaaf, Use of a fluorescent probe to detect radicals formed by the plasma needle (Poster presentation)
- CAPPSA, International Workshop on Cold Atmospheric Pressure Plasmas: Sources and Applications, 14-16 Jan, 2004, Ghent, Belgium
  - I.E. Kieft, R.E.J. Sladek, E. Stoffels, The plasma needle: A non-thermal atmospheric plasma for treatment of biological tissue (Poster presentation)
  - R.E.J. Sladek, I.E. Kieft, and E. Stoffels, The plasma needle and its biomedical applications
- 16th NNV/CPS - symposium for Plasma Physics and Radiation Technology, 16-17 Mar, 2004, Lunteren, I.E. Kieft, E. van der Laan, D. Slaaf, E. Stoffels, Electrical and optical characterization of the plasma needle (Poster presentation)
- International Workshop High-Intensity Physical Factors in Medicine, Biology, Agriculture and Ecology, Sarov, Russia, 26-28 Apr, 2004, R.E.J. Sladek, I.E. Kieft, E. Stoffels, The plasma needle and its biomedical applications
- 21st Symposium on Plasma Physics and Technology, Praha, Czech Republic, 14-17 Jun, 2004, E. Stoffels, I.E. Kieft, R.E.J. Sladek, E.P van der Laan, Medical Applications of Non-thermal Plasmas
- Chemia Plazmy 2004, Slok k/Bechatowa, Poland, 16-19 Jun, 2004, E. Stoffels, I.E. Kieft, R.E.J. Sladek, and E.P. van der Laan, A non-thermal atmospheric plasma source for disinfection and medical treatment of living cells and tissue
- 31st European Physical Society Conference on Plasma Physics, London, UK, 28 Jun -2 Jul, 2004, E. Stoffels, I.E. Kieft, R.E.J. Sladek, E.P. van der Laan, Plasma treatment of living cells and tissues
- The 31st IEEE International Conference on Plasma Science, (ICOPS2004), Baltimore, Maryland, USA, 28 Jun-1 Jul, 2004 E. Stoffels, I.E. Kieft, R.E.J. Sladek, E.P. van der Laan, D. Bronneberg, J.L.V. Broers, Plasma Interactions with Living Cells
- XVth International Conference on Gas Discharges and their Applications, Toulouse, France, 5-10 Sep, 2004, E. Stoffels, I.E. Kieft, R.E.J. Sladek, E.P. van der Laan, Towards plasma surgery: interactions of cold plasmas with living cells

- 2nd International Workshop on Microplasmas: Symposium on Environmental Biological and Medical Applications of Microplasmas 4-8 Oct, 2004, Jersey City, New Jersey, USA, I.E. Kieft, E.P. v.d. Laan, D. Darios, E. Stoffels, Quantitative analysis of cell treatment with a plasma needle (Oral presentation)
- 7th Euregional Welt-PP, Workshop on the Exploration of Low Temperature Plasma Physics, 25-26 Nov, 2004, Rolduc, Kerkrade, The Netherlands, I.E. Kieft, D. Darios, A.J.M. Roks, E. Stoffels, Plasma treatment of mammalian vascular cells (Oral presentation)
- 17th NNV/CPS - symposium for Plasma Physics and Radiation Technology, 1-2 Mar, 2005, Lunteren, I.E. Kieft, W. Engels, D.W. Slaaf, E. Stoffels, Plasma treatment of the vascular wall: preliminary results (Poster presentation)

Dankwoord

Een proefschrift schrijf je nooit alleen. Het is een resultaat van een samenwerking met vele enthousiaste mensen. Een aantal van hen wil ik hier in het bijzonder noemen. Om te beginnen natuurlijk Eva Stoffels. Jij kwam als mijn directe begeleider altijd met veel nieuwe ideeën en jouw optimisme zorgde voor een goede sfeer binnen ons team. Dankjewel voor je hulp en ondersteuning.
Mijn eerste promotor, Dick Slaaf, lette zowel op de details als op het grote geheel. Dankjewel hiervoor Dick, vooral ook voor je grote steun aan het hele project.
A number of trainee students helped me with my experiments. Verónique Caubet-Hilloutou, Natasha Dvinskikh, Joep van Berkel, Paul Claassen, Delphine Darios and Leonie Paulis thank you for your effort! I really enjoyed working with you and discussing about the strategy to follow.

De volgende mensen wil ik in het bijzonder bedanken voor de bijdrage die ze hebben geleverd:

Gerrit Kroesen, mijn tweede promotor, voor je hulp en steun aan het project.

I want to thank the members of my core committee prof. Schoenbach, prof. Steinbuch and prof. Ramaekers for reading my thesis and for making useful suggestions.

Remco Megens, Kim Douma, Wim Engels en Marc van Zandvoort wil ik bedanken voor een hele fijne samenwerking in Maastricht op de Biofysica afdeling. Ondanks de drukke bezetting van de twee foton microscoop bleven jullie heel enthousiast en behulpzaam.

Jos Broers van de afdeling Moleculair Celbiologie in Maastricht. Jos, jij hebt mij, een natuurkundige, op weg geholpen in de biomedische technieken en terminologie. Je hebt hier vast veel geduld voor nodig gehad, maar ik heb er veel van geleerd!

Anton Roks van de afdeling Klinische Farmacologie in Groningen, voor je ideeën over de cel-behandelingen.

Ewout van der Laan, als afstudeerder aan de plasmanaald en in het bijzonder het matching network heb je ons een enorme stap vooruit geholpen!

Wouter Brok. Toen jij de plasmanaald ging modelleren hebben we regelmatig discussies gehad over de werking. Dit heeft mij heel erg geholpen en ik vind het dan ook fijn dat je hier zoveel tijd voor nam.

Erik Kieft. Als je zusje heb ik altijd veel steun van je gehad, maar hier wil ik je toch in het bijzonder noemen vanwege je hulp met de Raman scattering metingen.

Mikhail Erofeev. You came twice from Tomsk to do measurements here. You helped to compare effects of cell irradiation by UV lamps to effects of irradiation by plasma. I enjoyed the cooperation and I think we learnt a lot from each other.

Mark Bowden and Lukas Grabowski. Your help with spectroscopy measurements was greatly appreciated!

Huib Schouten, Evert Ridderhof, Charlotte Groothuis en Loek Baede. Als technici in onze groep zijn jullie onmisbaar!

Rina Boom dankjewel voor het oplossen van allerlei papierwerk problemen en natuurlijk voor de gezellige gesprekken.

Christa Dam en vele anderen in het Cell and Tissue Engineering lab voor hun behulpzaamheid.

Ruben Wiese. Thank you for coming especially from Greifswald to measure the power outflux of our plasma needle.

Lutz Baars-Hibbe and Christian Schräder from Braunschweig. When you were in Eindhoven, you kindly offered to measure the needle with your V/I probe.

Many thanks go to the people of the EPG group. I think this is a great group; I always had a good time during lunches and coffee breaks! Special thanks go to Raymond Sladek, Gabriela (Gabby) Paeva and Tanja Briels. As roommates we supported each other and had a lot if discussions, but also a lot of fun!

Als laatste wil ik Jimi, mijn familie en goede vrienden bedanken voor hun luisterend oor en steun. Dankjewel!

Curriculum Vitae

July 8, 1978	Born in Wageningen, The Netherlands
1990-1996	Gymnasium at Christelijk Lyceum Veenendaal
1996-2002	Applied Physics, Eindhoven University of Technology
	Traineeship in the group Low Temperature Physics (prof. dr. A.T.A.M. de Waele) *Ontwerp van een pulsbuis zonder regenerator*
	Traineeship at the Micro Analytical Research Centre (Assoc. prof. D.N. Jamieson PhD), University of Melbourne, Australia *PIXE cluster analysis of ancient ceramics from North Syria*
	Graduation project in the group Applications of Ion Beams, (prof. dr. M.J.A. de Voigt) *Production of [^{15}O]O_2 for PEP analysis of ammonia oxidation on Pt sponge*
1997	Propedeuse Applied Mathematics, Eindhoven University of Technology
1998-1999	Chair of the student union of Applied Physics SVTN J.D. van der Waals, Eindhoven University of Technology
2001	Certificate of Technical Management, Eindhoven University of Technology
2002-2005	Ph.D. project, Eindhoven University of Technology
	Department of Biomedical Engineering, group Elementary Processes in Gasdischarges *Plasma needle: exploring biomedical applications of non-thermal plasmas*